8-2016

Impact of luminance and spatial parameters on the generation of the human pattern electroretinogram.

Kate A. Godwin
University of Louisville

IMPACT OF LUMINANCE AND SPATIAL PARAMETERS ON THE GENERATION OF THE HUMAN PATTERN ELECTRORETINOGRAM

By

Kate A. Godwin
B.S., Berry College, 2011
M.S., University of Louisville, 2013

A Dissertation
Submitted to the Faculty of the
College of Arts and Sciences of the University of Louisville
In Partial Fulfillment of the Requirements
For the Degree of

Doctor of Philosophy
In Experimental Psychology

Department of Psychological and Brain Sciences
University of Louisville
Louisville, Kentucky

August 2016

IMPACT OF LUMINANCE AND SPATIAL PARAMETERS ON THE GENERATION

OF THE HUMAN PATTERN ELECTRORETINOGRAM

By

Kate A. Godwin
B.S., Berry College, 2011
M.S., University of Louisville, 2013

A Dissertation Approved on

June 22, 2016

by the following Dissertation Committee:

_____
Paul DeMarco

_____
Heywood Petry

_____
Pavel Zahorik

_____
Zijiang He

_____
Maureen McCall

ACKNOWLEDGMENTS

First and foremost, I would like to extend my deepest gratitude to my faculty mentor and dissertation committee chair, Dr. Paul DeMarco. None of my graduate work (including the present dissertation) would have been possible without his guidance, patience, and constant example of both the personal and professional qualities that exemplify a successful academic. I also wish to thank the other members of my dissertation committee, Dr. Zijiang He, Dr. Maureen McCall, Dr. Heywood Petry, and Dr. Pavel Zahorik for the valuable time and feedback they contributed. Further, I would like to thank the ophthalmologists who collaborated on this work, Dr. Judith Mohay-Ambrus, Dr. Joern Soltau, and Dr. Brett Mueller, who were pivotal in applying this research to the glaucoma population. This particular effort was also aided by the entire staff of the Kentucky Lions Eye Center, to whom I am also indebted. Dr. Jonathan Nussdorf acted as an additional resource for understanding this patient population, and I am appreciative of the time and expertise he offered in planning the design of the third experiment. I am also grateful for the assistance of Dr. Thomas Roussel, who so graciously offered his time and knowledge to improve the programs written for these experiments and decrease the electrical noise of the recording area. Further, I wish to thank both past and current lab mates, Pan Shi and Eleanor O'Keefe, for their support, encouragement, and friendship. Finally, I would also like to extend my thanks to all participants of this study for making this research possible.

ABSTRACT

IMPACT OF LUMINANCE AND SPATIAL PARAMETERS ON THE GENERATION OF THE HUMAN PATTERN ELECTRORETINOGRAM

Kate Godwin

June 22, 2015

The current project assessed some of the key hypotheses behind the generation of the pattern electroretinogram (PERG) response. The first of these hypotheses states that the PERG response is the result of linear cancellation of simultaneous increment and decrement retinal responses, as generated by the retinal ON- and OFF-pathways. To test this theory, Experiment 1 evaluated the possibility of simulating the PERG by summing the ERG responses elicited by increment and decrement flashes. Results from this experiment showed that it was indeed possible to simulate the PERG from these flash responses, but that a single set of modeling parameters was only sufficient for simulating the steady-state PERG response.

The second hypothesis evaluated a theory that the retinal ganglion cells (RGCs) which generate the PERG response should be sensitive to spatial scaling of the PERG stimulus, and that an optimal spatial stimulus can be constructed based on the density of RGCs as a function of eccentricity. Experiment 2 assessed the validity of this claim by comparing the spatial tuning seen from uniform checkerboard stimuli to gratings that were spatially scaled to mimic the continuous change RGC receptive field size. Although spatial tuning was found in response to uniform checkerboard stimuli, it was not found in

response to scaled grating stimuli. It appeared that luminance-based components of the PERG response may be driving the spatial tuning observed based on which PERG components showed this pattern.

Finally, the third experiment tested the validity of the results from Experiment 1 in a population of glaucoma patients. Both the N95 and steady-state amplitudes from simulations could be modeled in both patients and age-similar controls. While the PERG response and the simulated PERG both appear to track perimetric data, the sample size in the present study is likely too small to address the predictive validity of the PERG modeling as a tool for tracking disease progression. Based on the findings across these three experiments, it is clear that the components which contribute to the generation of the PERG are more complex than previously thought, and future studies will be required to further elucidate these mechanisms.

TABLE OF CONTENTS

LIST OF TABLES

TABLE PAGE

LIST OF FIGURES

FIGURE PAGE

CHAPTER I

INTRODUCTION

Overview of Retinal Physiology

When light enters the eye, it first traverses various layers of ocular media and then falls on a layer of nerve tissue in the back of the eye known as the retina. The most distal layer of the retina is the retinal pigment epithelium (RPE), which primarily serves to supply nutrients to other retinal cells and absorb stray light that is not captured by the outer segments of the photoreceptors. Following the RPE is the photoreceptor layer,

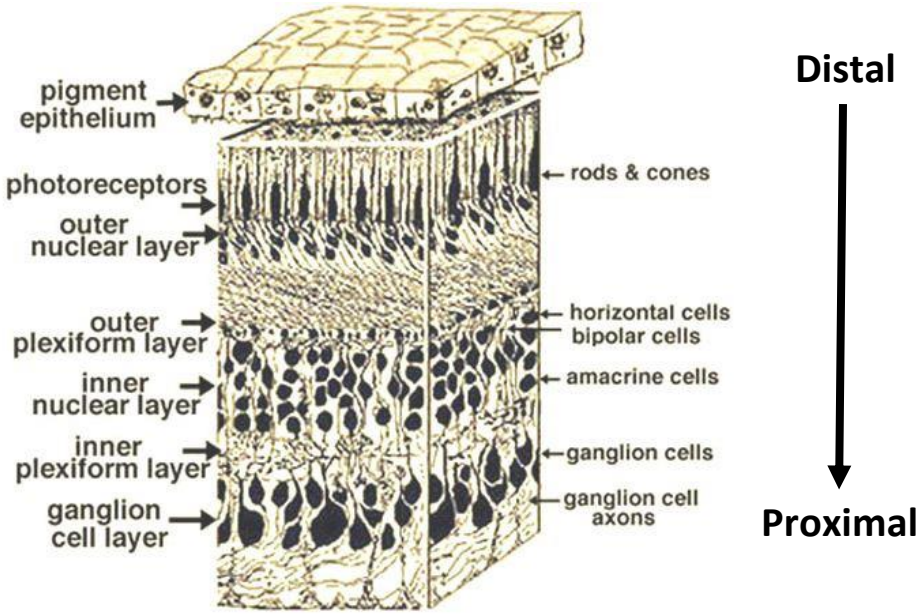

Figure 1. Layers of the Retina. The retina is composed of numerous layers (listed on the left side of the figure), with each nuclear layer consisting of cell bodies (listed on the right side of the figure) and each plexiform layer consisting of connections between cells of the surrounding nuclear layers. A further discussion of the processes that take place in each layer is described in the text. Modified from http://webvision.med.utah.edu.

which contains the outer segments of the rods and cones. Beyond the photoreceptor layer lies the five main layers (see Figure 1) which are as follows, in order from most distal to most proximal: outer nuclear layer (ONL), outer plexiform layer (OPL), inner nuclear layer (INL), inner plexiform layer (IPL), and retinal ganglion cell layer (RGCL). The RGCL and each of the nuclear layers contain cell bodies, while each of the plexiform layers serves as a connection site between cells in the surrounding layers. Axons of the RGC bodies also form their own layer, known as the retinal nerve fiber layer (RNFL); these axons exit the eye at the optic disk to relay visual information from the retina to the cortex.

The path of a photon can serve to explain each of these layers' cellular composition and function. When a photon traverses the cornea and ocular media to reach the retina, it must first travel to the most distal layer of the retina to the photoreceptors to be encoded. Photoreceptor cell bodies inhabit the ONL, and can be divided into the classes of rods and cones, which contain different types of photopigments. Rods are sensitive to low levels of light (termed scotopic conditions) and cones are sensitive to higher levels of light (termed photopic conditions). Regardless of the kind of photopigment within a photoreceptor, transduction always occurs within the outer segment given that this portion of the cell houses the 11-cis retinal chromophore, which is bound to the photoreceptor's opsin. When a photoreceptor absorbs a photon, the conformation of the chromophore changes from 11-cis retinal to all-trans retinal, which then separates from the opsin. Once separated, the opsin activates the protein transducin whose alpha subunit, which is bound to GTP, dissociates itself and then activates phosphodiesterase (PDE). At this point, PDE hydrolyzes cGMP, which leads to the

sodium channels closing. When these sodium channels close, the cell hyperpolarizes, which results in a decrease in the amount of glutamate it releases.

Following the ONL is the OPL, where the primary connections being formed are those between the photoreceptors and the bipolar cells (BCs), whose cell bodies are housed in the INL. There are numerous kinds of BCs in this layer, but they can be generally categorized into ON-center and OFF-center cells. In other words, BC receptive fields exhibit a center/surround architecture with the center being either ON or OFF, and the surround being the opposite. The functional distinction between these two groups is defined by the manner in which they respond to the aforementioned decrease in glutamate from the hyperpolarization of photoreceptors in response to photon capture. Sign-inverting ON BCs depolarize in response, while sign-conserving OFF BCs hyperpolarize instead. This signal is then transmitted to the amacrine and ganglion cells through the connections formed in the IPL.

Amacrine and ganglion cell activity is the first source of any spiking activity in the retina, as all cellular responses prior to this point in processing produce graded potentials. While amacrine cells help to mediate retinal ganglion cell (RGC) activity and do produce their own action potentials, the RGCs are responsible for the majority of the spiking activity at the retinal level, which is sent onward via the optic nerve for processing throughout different regions of the brain. Due to the nature of the BC signals that act as input, as well as the pattern of connections between BCs and RGCs that take place in the IPL, RGC receptive fields also typically exhibit a center/surround architecture. Therefore, ON-center RGCs exhibit a high spiking rate in response to an increase in light intensity, while OFF-center RGCs show a high spiking rate in response

to decrease in light intensity. Since both increments and decrements of light are encoded, the retina is therefore able to signal any point of intensity change throughout the visual scene, regardless of its polarity. These various signals from the RGCL are transferred via the optic nerve, where they exit the retina and proceed toward higher levels of processing in the brain.

Overview of the Electroretinogram (ERG)

The function of many of the aforementioned levels of retinal processing can be non-invasively measured through the use of the electroretinogram (ERG). Although it is recorded at the corneal level, the ERG reflects the gross potential of the retina in response to a light stimulus (see Figure 2). Traditionally the ERG stimulus consists of a full-field uniform flash of light, a stimulus that is now distinguished as the flash ERG. Varying the intensity, duration, and polarity of this flash alters the characteristics of the response. The standard light-adapted flash ERG (Marmor et al., 2009) uses brief square-wave flashes of white light, which are to be a maximum of 5 ms in duration and 3.0 $cd \cdot s \cdot m^{-2}$ in intensity and presented on a white 30 $cd \cdot m^{-2}$ background. This produces a small negative potential

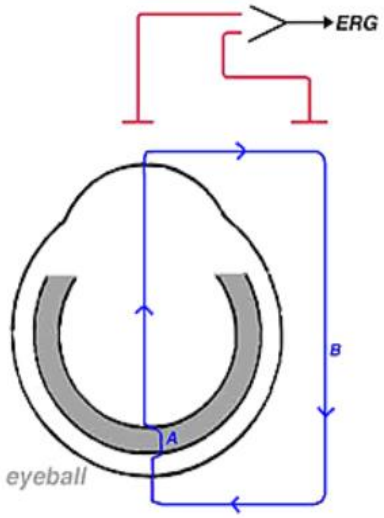

Figure 2. Schematic Representation of ERG Current. The current flow that measured in the ERG response is represented in blue. The (A) portion of that current is that which is generated in response to the transduction and encoding of light, and travels across the retina. Because other portions of the eye are conductive as well, the current also travels through the center of the eye, out to the cornea, and then back to the retina through the surrounding tissues (B). It is this portion of the current that we measure, as the ERG is recorded at the corneal level. From http://webvision.med.utah.edu.

known as the a-wave, followed by a larger positive potential known as the b-wave. After the b-wave comes a large negative potential known as the photopic negative response PhNR), but this waveform component is not recognized by the current standards for this paradigm. An example of the complete resulting waveform is shown in Figure 3A.

In addition to the standard flash paradigm, long-duration flash stimuli (Figure 3B) act as an alternative stimulus option that allows additional waveform components to be observed in the response (Pangeni, Lammer, Tornow, Horn, & Kremers, 2012; Vukmanic, Godwin, Shi, Hughes, & DeMarco, 2014). This alternative employs stimulus durations of approximately 150-250 ms (rather than 5 ms, as is used in the standard flash

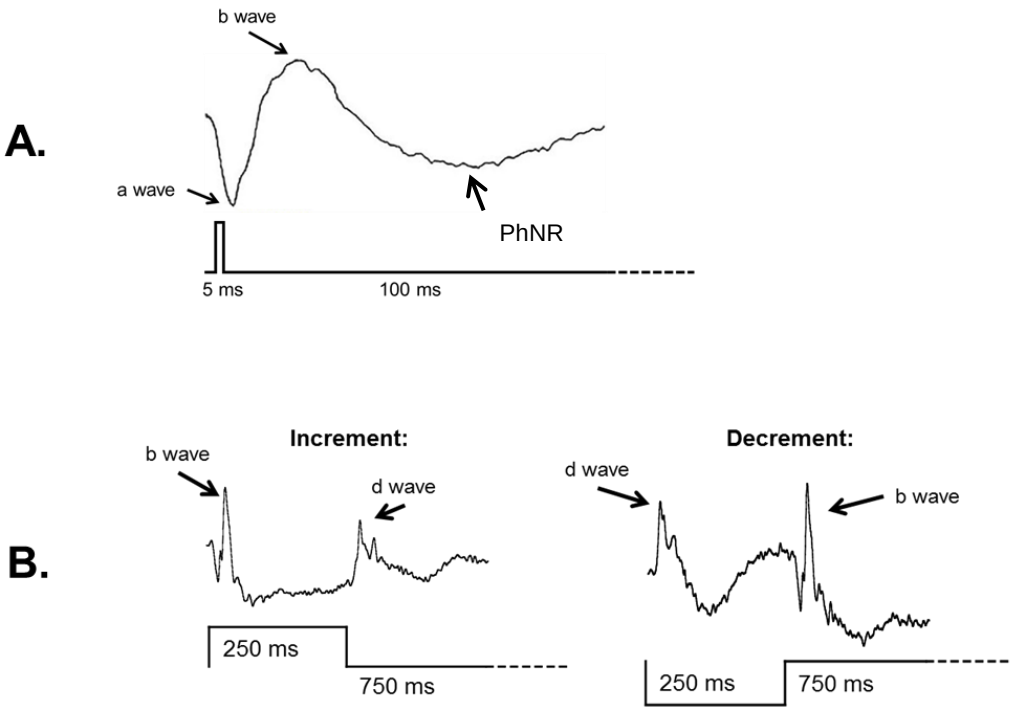

Figure 3. Flash ERG Stimulus Options. The standard brief flash stimulus (A) and long-duration flash stimulus (B) are compared, along with their respective responses. Note that the d-wave is only seen in response to long-duration decrements and cannot be seen in the response to a brief flash. Modified from Vukmanic et al., 2014.

paradigm), providing the retina with sufficient time to recover from its initial response over the course of the flash duration. Due to this recovery period, both b-waves and d-waves can be observed in response to a single flash's onset and offset, respectively. This is in contrast to the standard brief-duration flash response in which the b-wave and the d-wave are mixed due to lack of sufficient time for separation.

Origins of the a-wave

The first change in potential is the a-wave, which is a small negative potential whose leading edge reflects the hyperpolarization initiated by photoreceptors (Hood & Birch, 1995; Robson, Saszik, Ahmed, & Frishman, 2003). The latter portion of the a-wave appears to be largely driven by hyperpolarizing second-order neurons, which was most notably shown when cis-2,3-piperidine-dicarboxylic acid (PDA) was applied to the macaque retina (Bush & Sieving, 1994). Upon application of PDA, which blocks transmission from the photoreceptors to hyperpolarizing second-order neurons, the flash ERG response no longer showed an a-wave in response to a flash of any luminance within 1 log td above the photopic threshold. The effects of PDA continuously decreased (indicated by an increase in a-wave amplitude) until about 4 log td, at which point the effect was still present, but plateaued. Based on this trend, the authors presume the source of the a-wave at higher intensities (particularly those >4 log td) to be hyperpolarization of cones. Therefore, a combination of hyperpolarizing photoreceptors and second-order neurons is understood to be the source of this component, with the degree of contribution from each of the two cell classes varying with flash intensity.

Origins of the b-wave

The b-wave is the first positive potential seen in the flash ERG response, and is largely shaped by a combination of ON (depolarizing) and OFF (hyperpolarizing) bipolar cell responses. More specifically, depolarizing bipolar cells (DBCs) seem to provide the main source of the positive potential, and hyperpolarizing bipolar cells (HBCs) decrease the amplitude and duration of the b-wave, shaping the response. Evidence for this idea was first seen in the non-human primate retina when 2-amino-4-phosphonobutyric acid (APB), PDA, and kynurenic acid (KYN) were applied (Sieving, Murayama, & Naarendorp, 1994). The application of APB, which diminishes the response of DBCs but does not affect the response of HBCs, led to a severe decrease in b-wave amplitude, but an increase in a-wave and d-wave amplitude. However, when PDA and KYN were applied together to suppress responses from hyperpolarizing postreceptoral neurons (including both HBCs and horizontal cells), the resulting response showed a sustained positive plateau that lasted for the duration of the flash, making it difficult to identify

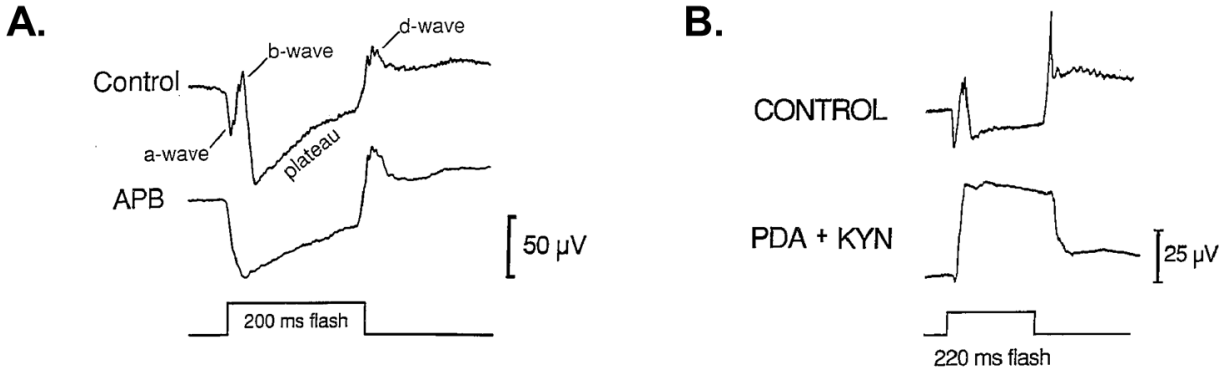

Figure 4. Effects of APB, PDA, and KYN on the b-wave. The b-wave seems to largely originate in DBCs, as applying APB severely diminishes or even extinguishes the response (A). However, the HBCs and horizontal cells must serve to shape and limit the response, as application of PDA + KYN yields a large positive potential that lasts for the entire duration of the flash (B). Modified from Sieving et al., 1994.

specific waveform components (see Figure 4). Based on these results, it can be surmised that the b-wave is largely driven by DBCs, but is shaped and limited in duration by HBCs and horizontal cells.

Origins of the d-wave

Upon applying APB and PDA to pharmacologically assess the origins of the d-wave in macaque retina (Ueno et al., 2006), it appears that both photoreceptors as well as HBCs combine to drive the positive component of this waveform. More specifically, the HBC component largely drives the first peak of the d-wave, and the photoreceptors drive the second peak of this waveform. As expected, the ON pathway hyperpolarizes in response to a decrement of light. Therefore, the ON pathway does not add to the positive potential seen in the d-wave, but rather serves to shape the response. See Figure 5 for the contributions from each of the aforementioned pathways.

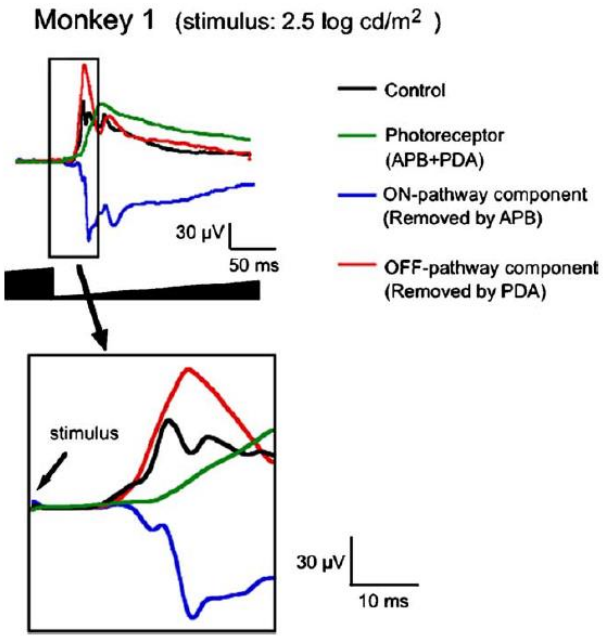

Figure 5. Effects of APB and PDA on the d-wave. The original d-wave (in black) is compared to the portion of the d-wave originating in photoreceptors (green), the ON pathway (blue), and the OFF pathway (red) in macaque. These results suggest that the OFF pathway provides the primary source of the initial portion of the response, with the photoreceptors providing the latter portion of the positive potential, and the ON pathway component serves to shape the response. From Ueno et al., 2006.

Origins of the Photopic Negative Response (PhNR)

Appearing as a negative potential after the b-wave (see Figure 3A), the PhNR is a component of the standard flash ERG that is known to reflect non-linear spiking activity of the retina, rather than linear activity like that which drives the a-, b-, and d-waves. As shown in macaque retina (Viswanathan, Frishman, Robson, Harweth, & Smith, 1999), the PhNR was severely reduced or eliminated in response to increment flashes when the retina was subject to tetrodotoxin (which blocks spiking activity) or experimental glaucoma (which lowers the functionality of the RGCL), though the a- and b-wave components remained unchanged. These authors therefore concluded that the RGCL likely drives this response, though its timing suggests that it may be mediated by glial cells. A reduction in the PhNR of human glaucoma patients provides further evidence that the RGCL is likely to be the source of this response (Preiser, Lagreze, Bach, & Poloschek, 2013), as glaucoma affects integrity of the optic nerve and, consequently, the RGCL.

Multifocal Electroretinogram (mfERG)

In contrast to the presentation of full-field flashes which yield one holistic response across the retina, the multifocal electroretinogram (mfERG) offers an alternative method of assessment that produces localized responses across the retina. To accomplish this, the mfERG stimulus consists of a 23° × 23° hexagonal array whose spatial and temporal properties seek to equalize the degree of cone stimulation as a function of eccentricity. Spatially, the hexagons are centered on the fovea and stretched by a factor that reflects the variations in cone receptive field density across the central retina, which seems to be optimized when the stretch factor is adjusted based on the specific recording

equipment and parameters being used for that session (Poloschek & Bach, 2009). Temporally, the flashes of the individual hexagons follow an m-sequence, a pseudorandom order of presentation that maximizes the signal-to-noise ratio for these localized responses while ensuring that they remain uncorrelated across various regions of the retina (Sutter & Tran, 1992). The localized responses from each hexagon exhibit highly similar response characteristics of those seen in a full-field flash ERG response, but seem to vary somewhat depending on whether ON responses, OFF responses, or an addition of the two is being assessed (Rodrigues, da Silva Filho, Silveira, & Kremers, 2010). Although the mfERG has been shown to be useful in a variety of contexts, all of the responses to be investigated in this work are ones which represent the holistic response of the retina; therefore, the mfERG will not be employed.

Overview of the Pattern Electroretinogram (PERG) Response

In addition to the early stages of retinal processing, the ERG is also capable of reflecting the later processes that take place primarily in the RGCL. Instead of a uniform flash of light, the PERG utilizes a spatial stimulus, typically a checkerboard or grating pattern, which reverses in contrast. Half of the stimulus displays an increment of light as the other half displays a decrement of light, yielding no change in net luminance as the polarities of each section reverse simultaneously. Since the responses to increment and decrement flashes of light are primarily reflective of large graded potentials, it is thought that these signals linearly cancel via simultaneous stimulation of early retinal ON- and OFF-retinal pathways. Due to this cancellation of larger linear potentials of opposite polarities, the smaller remaining response is understood to represent remaining non-linear spiking activity, which primarily originates in the RGCL.

Current source density (CSD) analysis has shown that even the precise sources and sinks of the retinal currents evoked differ based on whether the stimulus is a uniform flash of light or a contrast-reversing pattern, implying that the PERG generates a different bioelectric field. For instance, the predominant source-sink pair for the flash ERG seems to be in the distal half of the retina, whereas the predominant pair for the PERG appears to be in the more proximal half of the retina near the nerve fiber layer (Baker, Hess, Olsen, & Zrenner, 1988). Additionally, the differences between the fields imply that the PERG dipole is likely orthogonal to the eye axis, whereas the flash ERG dipole seems to be relatively coaxial (Chou & Porciatti, 2012), further distinguishing the responses to these two kinds of stimuli. These results from various CSD-based analyses are in alignment with the aforementioned understanding that the flash ERG response is largely representative of the earlier, linear retinal processes that generally originate in the photoreceptors and bipolar cells (Evers & Gouras, 1986; Stockton & Slaughter, 1989; Ueno, Kondo, Niwa, Terasaki, & Miyake, 2004), whereas the PERG represents the non-linear activity of the retina which primarily originates in retinal ganglion cells and amacrine cells. Further explanation and evidence of the PERG response origins are discussed in detail later in this dissertation.

Standards for Recording and Analyzing the PERG Response

Although there are numerous variations of the methods used to record the PERG response, the International Society for Clinical Electrophysiology of Vision (ISCEV) sets the standards for both clinical and research-based recordings. Since these standards are re-evaluated and updated every five years, the specifications from the most recent update (Bach et al., 2013) are referenced in this review.

Stimulus Presentation. The standard stimulus for the PERG is a black and white checkerboard that reverses in contrast, resulting in the simultaneous transition of black checks to white checks and white checks to black checks. Each check is 0.8° × 0.8° (±0.2° on each side), with the entire stimulus field being approximately 15° × 15° (±3° for each side). A high contrast level between the white and black checks is ideal, with the minimum acceptable level being 80%. Contrast is to be measured based on the difference between the luminance values of the light and dark checks, which is most appropriately determined by the formula for Michelson contrast due to the patterned nature of the stimulus.

Additionally, the PERG should be recorded under photopic conditions, with the white checks being no dimmer than 80 candelas per meter squared (cd/m^2). For transient recordings, where the entire response to a contrast reversal is completed before another contrast reversal occurs, the checks should reverse at a rate of 4.0 ± 0.8 reversals per second (rps). For steady-state recordings, the response to a contrast reversal has not fully completed before another reversal occurs. In these cases, ISCEV recommends using the higher reversal rate of 16 ± 3.2 rps. For all PERG recordings, regardless of reversal rate, it is imperative that eye movements are minimized, which is accomplished by the placement of a fixation point in the middle of the stimulus. It is also necessary for the subject to see the stimulus clearly. Therefore, ISCEV maintains that the eye should not be dilated, and any optical correction necessary to attain a clear image should be employed.

Key Components of the Waveform. The prominent waveform components in a PERG response vary based on whether it is a transient or a steady-state recording. In transient recordings, the waveform can be separated into individual components, whereas steady-state recordings only allow for holistic analysis. For this reason, only specific components of the transient waveform will be discussed here. The standard, transient PERG in human is composed of three main components (Figure 6). The first is a small negative wave that occurs around 35 ms after the beginning of the response, and is therefore termed N35. The next component is known as P50, as it is a larger, positive component that occurs approximately 50 ms after the onset of a pattern reversal. This portion of the response is the most commonly-assessed waveform component. After P50, a large negative component follows, occurring at approximately 95 ms into the response, and is therefore termed N95. Although N35 is sometimes used as a reference point, it is primarily P50 and N95 that have been of greatest interest to researchers and clinicians using the PERG, and are therefore much more frequently reported. It should be noted that the preferred name of each component tends to differ with species.

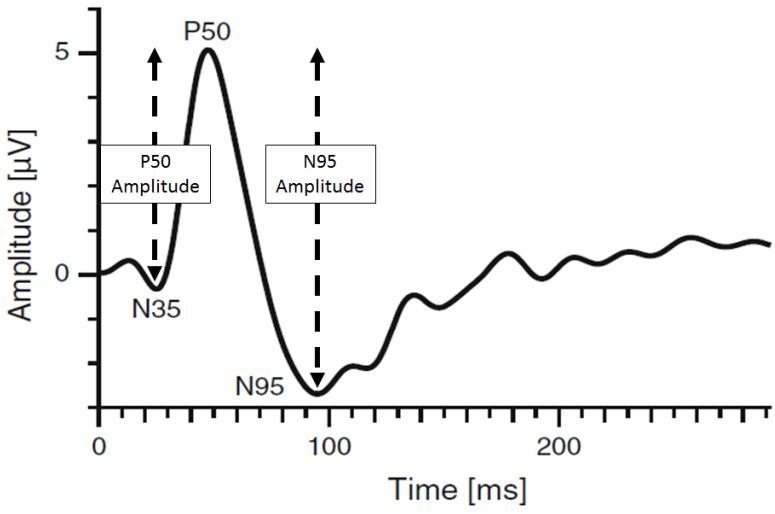

Figure 6. Transient PERG Waveform Components. The transient PERG waveform consists of 3 key components: N35 (a negative potential occurring at approximately 35 ms after stimulus onset), P50 (a positive potential occurring at approximately 50 ms after stimulus onset), and N95 (a negative potential occurring approximately 95 ms after stimulus onset). Modified from Bach et al., 2013.

Analyzing the PERG Response. For transient responses, both amplitude and time-to-peak (also known as implicit time) are to be reported for each waveform component of interest. N35 is not currently of clinical interest and there is no standard for assessing its amplitude. However, P50 amplitude is commonly measured, and extends from the trough of N35 to the peak of P50. (If N35 is not readily apparent, the measurement is simply made from the average baseline of the response to the peak of P50.) Similarly, N95 amplitude is to be measured from the peak of P50 to the trough of N95. (See Figure 6 for amplitude measurements.) For any waveform component, the implicit time can be measured in milliseconds from the onset of the response to the peak or trough of that component.

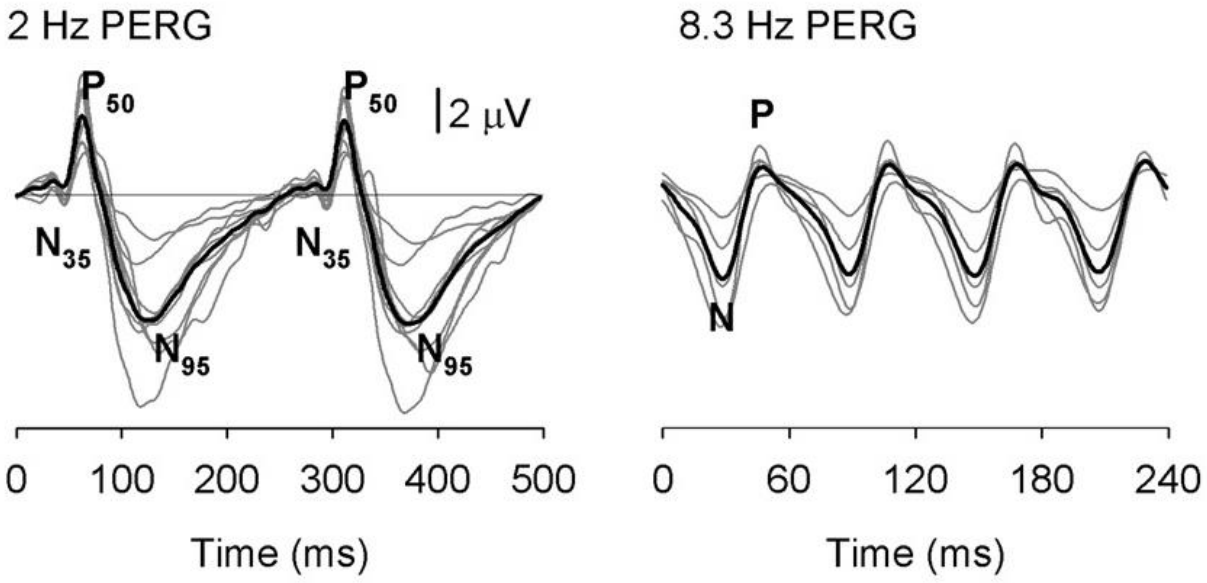

Figure 7. Comparison of Transient and Steady-State Responses. Transient responses are shown on the left, from a stimulus that was reversing at 2 Hz (4 rps). Steady-state responses are shown on the right, from a stimulus that was reversing at 8.3 Hz (16.6 rps). Note that P50 and N95 are distinguishable in the transient responses, but that only key positive (P) and negative (N) peaks can be identified in the steady-state responses due to the difference in morphology. These responses are recorded from non-human primates, but show the same morphological markers as those found in human. From Luo & Frishman, 2011.

For steady-state PERG responses, the phase shift of the response relative to the stimulus and the amplitude of this response should both be measured by assessing the second harmonic after the waveform has been subject to Fourier analysis. If phase shift is reported instead of implicit time, it should be specified as to whether the phase shift is increasing or decreasing with implicit time. Since the morphology of a waveform response to a steady-state stimulus is different from that of a transient waveform, attempts to identify individual components of steady-state responses are discouraged. (See Figure 7 for a comparison of transient and steady-state response morphology.)

Cellular Origins of the PERG Response

Contributions from Retinal Ganglion Cell Layer (RGCL)

As previously mentioned, the PERG is thought to be primarily driven by the RGCL. Much of the support for this theory comes from animal models and human case studies that compare PERGs in healthy subjects and those with damage to the RGCL. For example, PERG responses were measured in each eye of an adult man who had undergone a surgically-induced unilateral optic nerve section 30 months prior to recording (Harrison, O'Connor, Young, Kincaid, & Bentley, 1987). Because the optic nerve of one eye had been severed, retrograde degeneration resulted in RGC death in that eye by the time these recordings were made, but the eye was understood to be otherwise unaffected. This expectation was supported by the observation that there were no significant differences in flash ERG response between the two eyes. In contrast, the PERG was severely reduced in the eye that had experienced the optic nerve section relative to the eye that was still fully healthy, indicating that a significant portion of the response must rely on the functional integrity of the RGCL (Harrison et al., 1987).

Similarly, the PERG has also been assessed in various animal models of optic nerve sections. In cats, optic nerve sections tend to result in a PERG response that gradually decreases when recorded over a period of months after the surgery (reflecting the RGC degeneration) until it plateaus at a very low-amplitude response once RGCs are no longer functional (Tobimatsu, Celesia, Cone, & Gujrati, 1989; Vaegan, Anderton, & Millar, 2000). Other work in cat has found that the PERG is extinguished entirely only 4 months after optic nerve section, when most (but not all) of RGC functionality is thought to be lost (Maffei & Fiorentini, 1981). Each of these three studies has also shown that the flash ERG responses were unaffected by the section of the optic nerve, which indicates that earlier retinal layers are minimally affected (if at all) and corroborates the aforementioned case study in human. Despite the discrepancy in the exact degree of PERG amplitude reduction between studies, it still seems to be clear that the functionality of the RGCL plays a vital role in driving the PERG response in cat.

Although cats have been some of the most commonly-studied animals for observing the effects of optic nerve section as they pertain to the PERG response, these effects have been investigated in other animal models as well. Rats, for example, also showed a greatly diminished PERG response four months after optic nerve section, suggesting that they too are highly (but not fully) dependent on the integrity of the RGCL (Berardi, Domenici, Gravina, & Maffei, 1990). In pigeon, however, the PERG amplitude decreased immediately following the section, but then gradually returned to normal amplitude within 24 weeks. Therefore, the PERG response in pigeon must not be generated from the RGCL, indicating that the pigeon may not act as a proper model of the PERG response in human (Blondeau, Lafond, & Brunette, 1987).

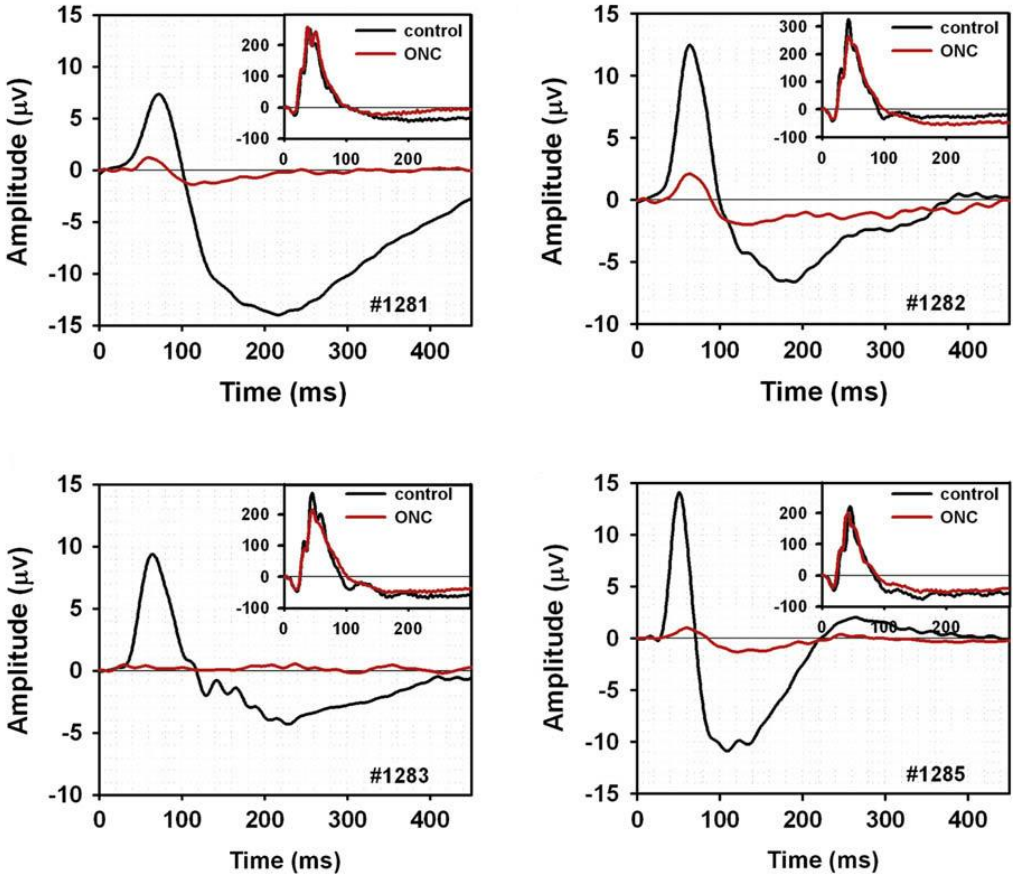

Figure 8. Reduction of the PERG Response after Optic Nerve Crush. Individual PERG responses from 4 mice both before an optic nerve crush (black lines), as well as 39-42 days after an optic nerve crush when RGC degeneration had taken place (red lines). Although the PERG responses were severely reduced after RGC degeneration from the optic nerve crush, the flash ERG responses remain unchanged (insets in upper right corner of each graph). This acts as further confirmation of an RGC origin for the PERG response since those were the only cells affected from the crush, and only the PERG was reduced while the flash ERG (which reflects earlier retinal processes) was unaffected. From Miura et al., 2009.

Similar to the uses of optic nerve section reported above, optic nerve crush has been used in mice for the same purpose of examining the dependence of PERG responses on the RGCL. Instead of severing the optic nerve as in the case of a section, an optic nerve crush involves literally a crushing pressure on the exposed optic nerve, typically with a blunt instrument. Like the optic nerve section, this procedure results in the atrophy of the RGCs, but leaves all other retinal functioning intact. When PERG responses are

recorded from mice who have experienced optic nerve crush, the result is generally a severe and irreversible reduction in PERG amplitude, though some mice have shown that the response is eliminated entirely (Chou, Park, Luo, & Porciatti, 2013; Miura, Wang, Ivers, & Frishman, 2009). Post-crush PERG responses and flash ERG responses are compared in Figure 8, which shows the expected finding of a reduction in PERG amplitude and an unaltered flash ERG response. In summary, these studies across various species show that an intact and functional RGCL is required to produce the PERG response.

Contributions from the ON and OFF Pathways

Two of the most fundamental visual pathways are the ON and OFF pathways, each of which begins at the bipolar cell layer of the retina and continues on through the cortex. As previously described, the ON pathway is excited by increments of light, while the OFF pathway is excited by decrements of light. Because these differential excitatory responses can be seen in the RGCL of the retina, it is important to understand the weightings of each of their contributions to the PERG response since there are equal degrees of local luminance onsets and offsets at any given time in viewing the PERG stimulus. This question has been addressed most directly through the use of animal models in which the ON and OFF pathways can be assessed separately via pharmacological manipulation.

As shown in Figure 9, mice were injected with APB to block the synapses between ON-bipolar cells and photoreceptors (blocking the ON pathway for all stages of processing), and PDA to block signal transmission to OFF-pathway bipolar cells and all RGCs (blocking the OFF pathway for all of the following levels of processing). When

APB was applied, the mouse PERG response no longer exhibited a P1 component (equivalent to the P50 component in human), indicating that the ON pathway is a key source of the P1 component in mouse. An application of tetrodotoxin (TTX), which blocks all spiking activity, followed the APB application, which led to the abolition of the N2 component (equivalent to the human N95) that had previously been isolated from APB. When PDA was applied alone in a different group of mice, both the P1 and N2 components were severely reduced. Taken together, these results suggest that the ON

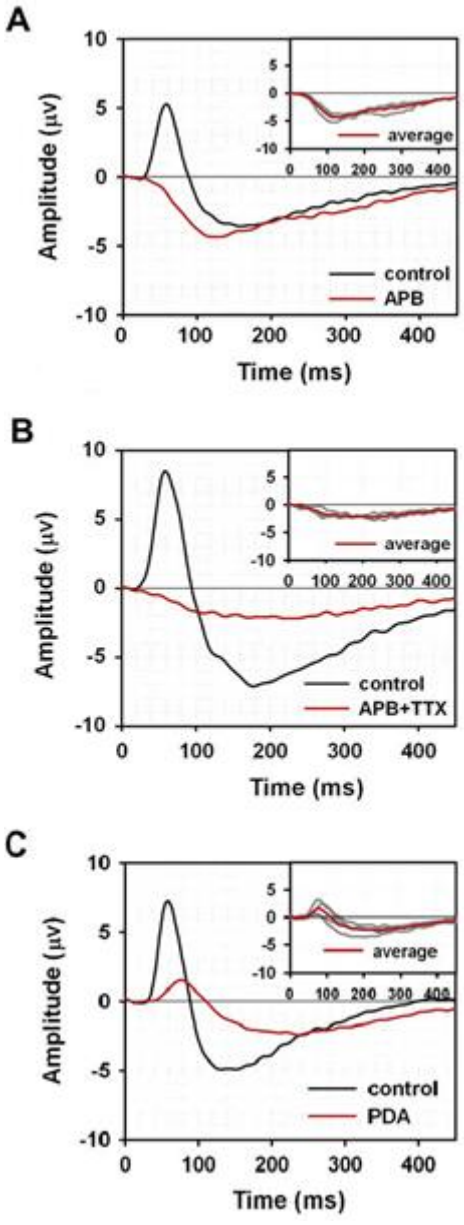

Figure 9. Effects of APB, APB+TTX, and PDA on PERG Recordings in Mouse. Averaged PERG recordings from four mice are shown both before (black lines) and after (red lines) various injected treatments. (Individual traces are shown in the inset graphs in the top right of each main graph). An injection of APB, which blocks the ON pathway, eliminated P1 (A), and the addition of TTX (which blocks spiking activity) after APB resulted in the elimination of both P1 and N2 (B). Injection of PDA, which blocks OFF pathway activity, reduced both P1 and N2 amplitude. Modified from Miura et al., 2009.

pathway acts as the primary origin of the P1 response, whereas the OFF pathway seems to contribute to both the P1 and N2 response in mouse (Miura et al., 2009).

Some differences were found when these drugs were applied in macaque (Luo & Frishman, 2011). When APB was applied alone, both the P50 and N95 components were reduced to half of their original amplitudes, indicating that the ON pathway must extensively contribute to the overall response. Upon the application of PDA alone, N95 was eliminated, but P50 amplitude was increased, suggesting that the OFF pathway drives the N95 response and limits the P50 response in this model. Spiking activity was also shown to play a key role in generating the transient PERG response, as TTX eliminated the reduced, but present P50 seen in those monkeys who served as models for experimental glaucoma. Given these findings, the authors conclude that while the ON and OFF pathways must contribute to the transient PERG response components somewhat differently, they seem to be of approximately equal weighting in regards to each of their levels of contribution to the holistic response amplitude in non-human primate.

In steady-state PERG responses recorded in this same study, application of APB severely reduced response amplitude to the point of nearly extinguishing it. Applying PDA to healthy animals seemed to generally increase the amplitude of the steady-state PERG, though these results were somewhat inconclusive given that it actually decreased response amplitude for one of the macaques tested. While TTX did not fully eliminate the steady-state PERG response, it drastically decreased it in each of the animals tested. When these three resulting responses from different pharmacological manipulations are considered together, they imply that steady-state PERG responses in non-human primate are largely driven by the ON pathway with relatively little contribution from the OFF

pathway. Further, retinal spiking activity seems to be a significant component of the steady-state PERG response, just as it did in the transient PERG response (as detailed in the previous paragraph).

Stimulus Factors that Affect the PERG

Pattern Type

Although the standard for PERG recordings is a square-wave reversing checkerboard (Bach et al., 2013), any patterned stimulus that reverses in contrast and maintains a constant net luminance with light and dark portions equally distributed throughout the stimulus is satisfactory to record a PERG response. Therefore, the effect of varying pattern type has been explored by multiple studies. One way in which this has been investigated was through the comparison of checkerboard and grating stimuli, though this has yielded conflicting results. In one of the key early studies to make this comparison, PERG responses elicited from square-wave checks and square-wave stripes of the same spatial frequency were found to be equal in amplitude, implying there was no effect of changing the pattern type (Armington, Corwin, & Marsetta, 1971). However, when a later study compared square-wave checks to both sine- and square-wave gratings, the checks consistently elicited a larger response in both human and pigeon subjects (Vaegan & Arden, 1987). These two examples represent a general debate of the effects of pattern type that still continues in the literature today.

Temporal Frequency

Another element of the PERG stimulus that can affect its respective response is the rate at which the contrast reverses, known as the temporal frequency (TF). One way in which the response is affected is through the frequently-demonstrated trend of

response amplitude changing as a function of TF. Although there is clearly an effect of TF on PERG response amplitude, reports vary as to exactly how the response changes with reversal rate. One of the major disputes in the literature is the number of peaks seen in the curve derived from amplitude plotted as a function of TF. Some reports give evidence for one peak at a somewhat lower TF (Berardi et al., 1990; Berninger & Schuurmans, 1985; Brannan, Bodis-Wollner, & Storch, 1992; Heine & Meigen, 2004; Siegel, Marx, Bodis-Wollner, & Podos, 1986), whereas others have found two different peaks, with one being a lower TF and the other being a higher TF, with a dip in amplitude occurring between the two peaks (Falsini & Porciatti, 1996; Hess & Baker, 1984; Odom, Maida, & Dawson, 1982; Porciatti & Sartucci, 1996).

Within those reports that have provided evidence for only one peak TF, the exact TF of that peak varies somewhat. Animal models have also been included in these reports, but their use as models seem valid as their peaks fall in the same TF range as those reported from human subjects. In rat, the peak seems to be between 8 and 12 rps (Berardi et al., 1990), and in macaque, it is reported to be 12 rps (Siegel et al., 1986). In humans, there is slightly higher variability, as reported peaks have consisted of approximately 4.8 rps (Brannan et al., 1992) and 11.1 – 16.2 rps (Heine & Meigen, 2004), while another report indicates a peak of 10 rps that occurred for N95 only, with no peak shown in P50 (Berninger & Schuurmans, 1985). As previously mentioned, transient responses are known to be elicited from stimuli that reverse at lower TF rates, while steady-state responses result from higher TF rates (Sokol, Jones, & Nadler, 1983). Since these peaks fall within a range that includes both higher TFs of the transient range and

lower TFs of the steady-state range, they do not provide a reliable consensus as to whether transient or steady-state stimuli might elicit larger responses.

Similarly, the results that indicate two peaks in human responses show some variability, as well. Some reports indicate a first peak of very low TF, up to 4 rps, and a second peak of slightly higher TF, being in the range of 8-16 rps (Hess & Baker, 1984; Odom et al., 1982). Others, however, indicate that both peaks occur at higher TFs, with the first peak being in the range of 12 – 24 rps and the second peak in the range of 32-40 rps, and an absolute cutoff between 50 and 60 rps (Falsini & Porciatti, 1996; Porciatti & Sartucci, 1996). It is possible that this variability (both regarding the number of peaks reported as well as the discrepancies as to what those peaks may be) might be related to the fact that these studies used very different ranges of spatial frequencies in their stimuli, as there is a growing body of evidence that suggests the presence of an interaction between TF and spatial frequency (Berninger & Schuurmans, 1985; Heine & Meigen, 2004; Hess & Baker, 1984; Siegel et al., 1986).

Spatial Frequency

Although the effect of spatial frequency on the PERG has been investigated in a large number of studies, there is a high degree of variability across the many results. While most investigations have yielded some degree of spatial tuning (defined as amplitude change as a function of spatial frequency), some failed to find any effect of spatial frequency whatsoever. This complete lack of spatial tuning was found both in human, at a reversal rate of 3 rps (Kirkham & Coupland, 1983), and in pig, at a reversal rate of 8 rps (Janknecht, Wesendahl, Feltgen, Otto, & Bach, 2001). However, Janknecht and colleagues noted that their results in pig may not have been indicative of a true lack

of spatial tuning, as the data showed a high degree of variability and generally low amplitudes under most conditions. Since this only leaves one known study to date that has failed to find spatial tuning, it is highly possible that the spatial frequency of a stimulus does have at least a minimal effect on the PERG response.

Other studies have found a minor effect of spatial tuning, albeit only under certain conditions for some. For instance, Armington and Brigell (1981) found that lower to middle spatial frequencies showed no difference in amplitude, but that increasing the spatial frequency (up to a maximum of 5.46 cycles per degree [cpd] for this study) did result in a slight reduction in amplitude. Similarly, a later study (Bach & Holder, 1996) found that amplitude decreased monotonically with increasing spatial frequency past approximately 2 cpd, which was true for both the standard 15°×15° stimulus field as well as the larger 30°×30° stimulus field. Both of these studies evaluated the effects of spatial frequency at transient TFs. However, when spatial tuning was investigated across three different TFs, it was only found to be present at the higher two reversal rates (7.5 and 15 rps), but not at the lowest rate tested (1.88 rps) (Sokol et al., 1983). Therefore, the specific TF chosen may play a pivotal role in determining the degree of spatial tuning seen in the response.

Despite those accounts documenting little to no spatial tuning being present in the PERG response, many others have found spatial tuning consistently across a range of different conditions. Some of these results indicate similar findings to those from Sokol and colleagues (1983) in that amplitude is shown to monotonically decrease as spatial frequency increases (Armington et al., 1971; Korth, 1983). Similarly, a low-pass function has also been found in rat (Berardi et al., 1990). Perhaps the most common finding has

been that the human spatial tuning curve is actually bandpass (Arden & Vaegan, 1983; Porciatti et al., 1989; Thompson & Drasdo, 1989), though these reports do not show a widespread agreement as to where the peak of this function occurs. Despite this variability of peak spatial frequency, when a bandpass nature of the PERG's spatial tuning is seen, it appears to be independent of contrast, luminance, or temporal frequency (Hess & Baker, 1984). In addition to the claims of the function being potentially low-pass or bandpass, there is also some evidence to suggest that the PERG response amplitude increases with spatial frequency (Leguire & Rogers, 1985), though most findings would disagree with this report.

In addition to the variability regarding the degree of spatial tuning present, there is also some variability regarding the potential interaction between transient waveform components (P50 or N95) and spatial tuning. When the trends between the two waveform components differ, it seems that P50 shows limited spatial selectivity that is only present under low-contrast conditions (Korth & Rix, 1985), or no spatial tuning at all (Berninger & Schuurmans, 1985; Wu, Armington, & Reeves, 1992). However, N95 appears to be consistently spatially tuned when evaluated independently (Berninger & Schuurmans, 1985; Korth & Rix, 1985; Wu et al., 1992). A wide-scale review of this literature echoed this trend, and suggested that steady-state recordings would also be more likely to show spatial tuning than would transient responses. Therefore, while there is some discrepancy as to the exact shape of the spatial tuning curve, it does appear that any spatial tuning present is likely to vary with the precise stimulus parameters used.

Contrast

Contrast level between the dark and light checks in the PERG stimulus has been varied extensively to evaluate its effect on the PERG response, yielding a widespread consensus that PERG amplitude increases monotonically with contrast (Arden & Vaegan, 1983; Korth, 1983; Leguire & Rogers, 1985; Thompson & Drasdo, 1989). However, it appears that this increase does not begin until contrast exceeds 1 – 20% (Hess & Baker, 1984). This effect of contrast does not seem to hold when hemifield stimuli are compared, regardless of whether they are nasal/temporal or superior/inferior (Katsumi, Tetsuka, Mehta, Tetsuka, & Hirose, 1993), though further investigation will be necessary to confirm this. Since the relationship between the standard PERG and contrast is so robust, it is imperative to maximize stimulus contrast so that the already-small response amplitude can be maximized, as well. It should also be noted that bright ambient lighting can lead to a decrease in contrast at the level of the screen itself, indicating that the PERG should be recorded under lower photopic conditions to obtain the strongest and most reliable responses (Bach & Schumacher, 2002).

The effect of adapting to the PERG stimulus has also been assessed at various contrast levels in an effort to understand how it may potentially affect PERG amplitude, though the literature does not seem to show a strong consensus on this issue. Upon watching a steady-state PERG stimulus at 99% contrast, it was found that the amplitude continuously decreased over time, an effect which was not found when the contrast was lowered to 25% (Porciatti, Sorokac, & Buchser, 2005). In opposition to this finding, the presentation of the PERG with swept contrast changes (where the contrast is either continuously increasing or decreasing within a single presentation) had no effect on the

PERG contrast threshold, regardless of the direction of the sweep (Brigell, Peachey, & Seiple, 1987). Although these results would imply that adaptation was not taking place, it may be the case that adaptation to the PERG is possible, but only over a prolonged viewing period.

An interaction between contrast and spatial tuning has also been suggested by some investigations. Generally, spatial selectivity seems to be more prevalent when stimuli are of higher contrast levels, with lower contrast levels showing little to no spatial selectivity (Korth & Rix, 1984; Sokol et al., 1983; Tetsuka, Katsumi, Mehta, Tetsuka, & Hirose, 1992), though some evidence points to this only being the case for P50, with N95 showing spatial selectivity at all contrast levels (Korth & Rix, 1985). Contrast sensitivity functions (CSFs) have also been evaluated in the PERG, and have been compared to those determined psychophysically. When plotted as a function of spatial frequency, the PERG CSF peaked at a lower spatial frequency relative to the traditional psychophysical CSF (Peachey & Seiple, 1987). Using the PERG to determine one's CSF has therefore been shown to be a valuable tool to evaluate one's retinal contrast sensitivity rather than one's cortical contrast sensitivity, which is likely to be reflected in the psychophysical CSF.

In addition to interacting with spatial frequency, the effects of contrast also seem to have an interaction with temporal frequency. The first demonstration that the contrast transfer function (CTF), which plots amplitude as a function of contrast, changes in shape when temporal frequency is altered was shown by Zapf and Bach (1999). Their data indicated that below approximately 7 rps, the CTF increases linearly with contrast. However, as temporal frequency increases, their data indicate that the CTF becomes

increasingly exponential. To further investigate this trend, another study evaluated the CTF with an even larger range of stimulus parameters that also added the use of a linearity index (Ben-Shlomo, Bach, & Orfi, 2007). Upon doing so, it was found that the linearity index value (where 1 = completely linear and 0 = a step function) generally decreased as temporal frequency increased. Additionally, these authors demonstrated that the stimulus could be reversed at rates of up to 10 rps before the CTF began decreasing in linearity. Together, these studies indicate the importance of acknowledging temporal frequency when comparing results from stimuli that differ in contrast.

Luminance versus Contrast Origins of the Response

Much of the reason that the PERG response is thought to be primarily contrast-based is due to the lack of net change in luminance across the stimulus. Because increments in luminance are consistently occurring to the same degree and at the same rate as decrements in luminance, the expectation is that the linear ON activity will average with the linear, and opposite, OFF activity to yield a null result for these earlier levels of processing, leaving only contrast-based activity to be recorded. One can test this hypothesis by modeling the PERG response using increment and decrement flashes.

Modeling the PERG response from flash ERG responses was first tested by Arden & Vaegan (Arden & Vaegan, 1982), who summed increment and decrement responses and compared the result to the standard PERG response in humans. The summed response was consistently larger than the PERG response across an extensive range of local background luminance. Later, this same principle was applied to the macaque retina, both in healthy animals and in those which had been established as models of experimental glaucoma (Viswanathan, Frishman, & Robson, 2000). Increment and

decrement responses were halved and then summed to create PERG simulations in this study, so as to account for the fact that only half of the stimulus field is displaying an increment or decrement in the actual PERG stimulus at any given time. These results indicated that for both healthy and glaucomatous animals, the simulated PERG seemed to accurately represent the implicit times of both P50 and N95 of actual PERG responses from stimuli recorded at the lowest spatial frequency of 0.1 cpd, but then showed increasing delay with increasing spatial frequency (other tested spatial frequencies included 1.5 and 3 cpd). For all spatial frequencies, however, the amplitude of the simulation exceeded that of the actual PERG response.

More recently, PERG simulations have been carried out with human data using this same model of halving and then summing increment and decrement responses (Simpson & Viswanathan, 2007). In human, it was shown that the model was able to accurately reflect the waveform of the actual PERG response, and with no more variability than that which was found in those actual PERG responses. However, the PERG responses that were modeled only accounted for a very limited set of possible parameters, namely a 42°×32° grating (which is much larger than the standard 15°×15° checkerboard) and a spatial frequency of either 0.04 or 1 cpd, reversing in contrast at a rate of 2 times per second. Since this work, this same model has been expanded for use across four different temporal frequencies (2, 4, 6.2, and 16.6 rps) in macaque so as to test the accuracy of both transient and steady-state simulations (Luo & Frishman, 2011).

Results of this further testing indicated that in non-human primate, both the implicit time and the amplitude of the P50 component of the simulation were significantly different from the implicit time and amplitude of the P50 component from

the PERG response, whereas there were no differences in either of these measures between the simulation and PERG response for the N95 component (Luo & Frishman, 2011). Therefore, it may be the case that changes in temporal frequency affect the accuracy of the model differently for these two waveform components, though this has not yet been confirmed in humans.

Conversely, previous evidence in cats has shown that spatial frequency, which is a measure of the size of the elements in the stimulus, may determine whether the response is more luminance- or contrast-driven, as finer patterns yielded a contrast-based response while coarser patterns yielded a luminance-based response (Tobimatsu et al., 1989). Regardless of the exact degree to which luminance and contrast each drive the PERG response, though, it is clear that the resulting waveform from a patterned stimulus is much smaller and somewhat different in morphology relative to the resulting waveform from a uniform flash of light. Therefore, the PERG must reflect characteristically different activity than that of a flash ERG, even if the exact relationship between the two responses and their respective origins is still unknown.

Application of the PERG in Disease States

Since the PERG is useful in clinical contexts, it is necessary to understand how each of the various diseases that have been documented specifically affects the PERG response in order to increase the response's diagnostic value, as well as the accuracy with which one may use the PERG to monitor disease progression. Despite the clear benefits of examining PERG responses from clinical populations, it can be difficult to study an isolated disease in human patients since there are often comorbidities present. Additionally, the same disease can show a high degree of variability in its effects across a single patient

base, making it difficult to compare results across subjects, and particularly across studies. Because of these constraints, animal models of diseases affecting the PERG can also be extremely valuable when assessing the ways in which this response is affected within a specific clinical context. Therefore, several of the more common disease states that can employ PERG for diagnostic and/or monitoring purposes have been investigated in both human and animal models, which are both discussed in more detail below.

Ocular Hypertension

Ocular hypertension (OHT), a condition in which the eye experiences unusually high intraocular pressure but does not immediately cause damage to the optic nerve, is a major marker in identifying glaucoma suspects. Because of this, OHT is carefully monitored by ophthalmologists, which may include the use of PERG recordings since it typically affects the integrity of the RGCL. When OHT was induced unilaterally via laser in a rat model, the PERG amplitude (measured from the peak of P1 to the trough of N2, parallel to the human N95 amplitude) was reduced by approximately 45%, which was correlated with the degree of loss of RGCs (Ben-Shlomo et al., 2005). These data mimic the changes seen in the human PERG response recorded from OHT patients, as PERG amplitudes in OHT patients have been shown to be consistently lower than those of healthy controls in response to steady-state patterns (Falsini et al., 2008; Ventura, Golubev, Feuer, & Porciatti, 2010).

Transient PERG responses have also been informative in human OHT patients, as they have allowed for the evaluation of specific waveform components independently. For instance, one investigation found no change in N95 amplitude, but did find a negative correlation between intraocular pressure and P50 amplitude. Since retinal nerve fiber layer

(RNFL) thickness (which decreases with RGC death) was not correlated with P50 amplitude, however, these data suggest that the changes seen in the PERG may represent a lowered functionality of the RGCs due to higher intraocular pressure rather than actual RGC death (Uva et al., 2013). These conclusions are further strengthened by the observation that transient changes in intraocular pressure can lead to temporary, reversible decreases in PERG amplitude as measured in responses to steady-state patterns (Giuffre, Falsini, Gari, & Balestrazzi, 2013).

Often, OHT patients are only evaluated using steady-state stimuli since that is the most sensitive (and therefore the most common) stimulus type used to diagnose and monitor glaucoma, generally making it more advantageous than transient PERG recordings. For example, when compared with optical coherence tomography (OCT) and frequency-doubling technology (FDT) perimetry (two other methods of assessing OHT), the transient PERG was the least sensitive measure of the three options tested (Cellini, Toschi, Strobbe, Balducci, & Campos, 2012). Because the transient PERG is not often used in clinical evaluation of OHT due to its relative lack of sensitivity, further investigation using transient stimuli for research purposes is needed to definitively show how and to what extent individual waveform components are affected in the PERG responses of OHT patients.

Glaucoma

Glaucoma is a disease in which damage to the optic nerve is experienced, with visual field defects resulting from this damage. Usually, the optic neuropathy seen in glaucoma is a product of elevated intraocular pressure due to a buildup of aqueous humor (Foster, Buhrmann, Quigley, & Johnson, 2002). Unfortunately, this disease is highly

prevalent, as it currently affects about 60 million people worldwide, and has led to blindness in about 8.4 million of these individuals (Cook & Foster, 2012). Further, glaucoma is projected to affect approximately 79.6 million by 2020, with an estimated 11.2 million of those patients becoming blind because of the disease (Quigley & Broman, 2006). Because the PERG response originates in the RGCL, the PERG has been one tool of use in predicting, diagnosing, and monitoring glaucoma, as explained in more detail below.

Predicting Glaucoma. One way in which clinicians may use the PERG in the context of populations at risk for glaucoma is in predicting which glaucoma suspects are most likely to later develop the disease. Although there is some debate as to whether or not the PERG is a useful measure of glaucoma prediction, a review of the literature pertaining to the PERG as a predictive tool found that it was generally useful in detecting damage from RGC loss (often indicating early glaucoma) before any deficits were noticeable in one's visual field (Bach & Hoffman, 2008). One way in which this investigation has been furthered since the time of the aforementioned review is through the comparison of the PERG against three different forms of perimetry that are also known to be used to diagnose and monitor glaucoma. All tools yielded a similar level of accuracy of glaucoma diagnosis with the exception of FDT perimetry, which yielded a slightly higher diagnostic accuracy. Despite this difference, the authors explicitly note that the PERG is not to be discounted since it is a more objective measure of RGC functionality given that it does not rely on behavioral responses (Tafreshi et al., 2010).

Following this study, the PERG was assessed longitudinally for its ability to predict which patients with OHT would progress to a diagnosis of glaucoma within four years. More specifically, the clinical utility of evaluating the PERG response from a single visit

was compared to that gained from multiple visits over time. While the PERG was indeed found to successfully predict which patients would develop glaucoma, trends acquired from multiple visits did not lead to significantly more predictive power than did the data from a single visit (Bode, Jehle, & Bach, 2011), which suggests that one recording session yields a sufficient amount of data to predict the development of glaucoma.

In addition to knowing how much data is needed to predict this disease, it is also pertinent to recognize characteristic differences between those who may develop glaucoma and those who are already in its early stages. To establish what differences should be expected, PERG responses from glaucoma suspects were compared to those from patients with early primary open angle glaucoma. Both groups showed an increase in N95 implicit time, but only early glaucoma patients showed a decrease in N95 amplitude, indicating that changes in implicit time may be characteristic of RGC dysfunction while changes in amplitude may be characteristic of cell death (Jafarzadehpour, Radinmehr, Pakravan, Mirzajani, & Yazdani, 2013). Although these data all exemplify the PERG's ability to predict which glaucoma suspects will experience progression to the disease itself, it is still unclear if the PERG is equally able to predict the progression of severity past disease onset (Ventura, Golubev, Feuer, & Porciatti, 2013).

Simulated and Experimental Glaucoma. Efforts to isolate the origins of the PERG response in glaucoma have often led to simulated and experimental models of the disease, since these allow for more highly- and uniformly-controlled conditions. In human, healthy control populations can be used to produce results that simulate those of glaucomatous patients by altering the stimulus to mimic what a patient would see. Upon reducing the contrast, luminance, clarity and area of the stimulus to simulate conditions

experienced in glaucoma, Porciatti and Ventura (2009) reported that the amplitude and implicit time of the PERG were independently affected in their data. Therefore, these two measures most likely represented two different aspects of RGC activity. The previously-discussed results of Jafarzadehpour and colleagues (2013) seem to provide further support for this idea within an actual clinical population, indicating both that the simulation was probably an accurate representation of the PERG response in glaucoma, and that amplitude and implicit time may well reflect independent processes.

Animal models can also be useful ways to explore the effects of glaucoma on the PERG, with one of the most useful models being the macaque. Two macaque studies implemented unilateral experimental glaucoma by elevating the intraocular pressure via laser, and then allowing the resulting OHT to progress into glaucoma. In one of these studies, the resulting PERG response showed a severely reduced N95 and a moderately reduced P50 relative to the healthy eye (Viswanathan et al., 2000). The other study, however, showed that experimental glaucoma completely eliminated both P50 and N95 (Luo & Frishman, 2011). Despite the minor discrepancy regarding the degree of amplitude reduction, it is clear that the PERG response from the macaque model is consistently reduced in amplitude when experimental glaucoma is induced in otherwise-healthy animals. A similar result has been found in a mouse model of glaucoma, which was monitored over time with disease progression. As expected, the amplitude of the PERG in mice with experimental glaucoma declined with age until the PERG response was completely eliminated, showing that the mouse is also a reliable model in which to measure functional inner retinal degradation (Porciatti, Saleh, & Nagaraju, 2007).

PERG Amplitude Decrease in Humans. Across many of the earlier reports of PERG measurements in glaucomatous eyes, PERG response amplitude was reduced or even eliminated while the flash ERG showed no significant changes (Rimmer & Katz, 1989). More recent investigations have shown this reduction in both components of the transient PERG, as well as the general amplitude measurement of the steady-state PERG (Bach & Hoffman, 2008), as seen in Figure 10. Unfortunately, many of the investigations conducted in both transient and steady-state conditions have led to a somewhat high degree of variability, both within and between studies. Since finding this pattern, the PERG ratio was developed in hopes of reducing such variability. To calculate this ratio, the PERG amplitude from the upper hemifield of the stimulus is divided by the PERG amplitude from the lower hemifield of the stimulus so as to account for the known trend of RGC loss occurring predominantly in only one hemifield for most glaucoma patients. Although the PERG ratio has been shown to reduce the higher levels of variability often found across PERG recordings in glaucoma patients, it does maintain the risk of missing

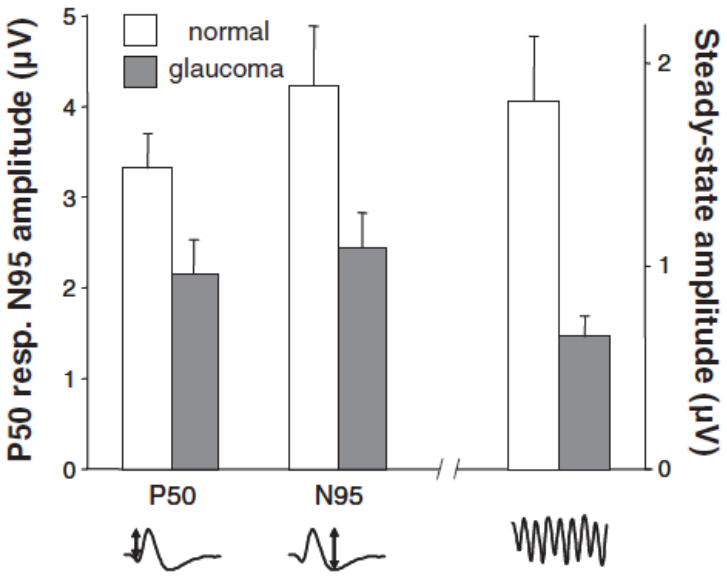

Figure 10. Amplitude Reduction in Transient and Steady-State PERG Recordings in Healthy and Glaucomatous Eyes. As is exemplified here, individuals with glaucoma (grey bars) exemplify lower PERG amplitudes relative to those with healthy eyes (white bars). This is true for both P50 and N95 in the transient PERG, as well as the sole amplitude measurement taken made in the steady-state PERG. From Bach & Hoffman, 2008.

peripheral and symmetrical RGC loss and is therefore only applicable for limited purposes (Graham, Wong, Drance, & Mikelberg, 1994).

More recent studies have investigated the precise changes in PERG responses from glaucoma populations in more detail. For example, reductions in RNFL thickness have been shown to correlate with the decrease in PERG amplitude for those with early glaucoma, but not for those with OHT. Therefore, it has been suggested that the changes in the PERG from OHT are generally from damage to the optic nerve head and retinal function, whereas the changes seen in the PERG of those with early glaucoma likely reflect both functional losses as well as loss in RNFL thickness (Falsini et al., 2008). Within glaucoma patients specifically, the degree and nature of adaptation to steady-state PERG stimuli were assessed as a function of severity, and compared to a group of healthy controls. Adaptive changes associated with the phase of the PERG response were significantly correlated with disease severity, despite the fact that adaptive changes associated with the amplitude of the PERG response were not. Therefore, when assessing the PERG within glaucoma patients to determine differences in severity, response phase may actually act as a more reliable and accurate marker than amplitude (Porciatti et al., 2013).

Other Diseases Affecting the PERG

Although OHN and glaucoma populations are the most frequent clinical applications of the PERG, other maladies have also been reported as causing changes in PERG activity. For instance, reduced to absent PERG responses have been found across patients that represent a range of varying ocular diseases affecting the optic nerve after development (Fiorentini, Maffei, Pirchio, Spinelli, & Porciatti, 1981; Guy et al., 2014;

Rodriguez-Mena et al., 2013; Talla et al., 2013), as well as cases in which the optic nerve is unsuccessful in fully developing to begin with (McCulloch, Garcia-Filion, Fink, Chaplin, & Borchert, 2010; McCulloch, Garcia-Filion, van Boemel, & Borchert, 2007). However, the disease or visual impairment of interest does not have to primarily or even directly affect the optic nerve to alter the PERG; scotomas (Junghardt, Wildberger, Robert, & Torok, 1993), amblyopia (Rimmer & Katz, 1989), diabetes without the presence of retinopathy (Ventura et al., 2010), Parkinson's disease (Armstrong, 2011; Garcia-Martin et al., 2014), and even depression (Bubl, Kern, Ebert, Bach, & Tebartz van Elst, 2010) have all been linked to reductions in PERG amplitude. Based on the varied assortment of diseases and dysfunctions in which the PERG may be affected, all comorbidities should be noted when interpreting PERG results in a clinical setting.

CHAPTER II

GENERAL METHODS AND ANALYSES

Although the PERG response has been well-established over the course of several decades, some assumptions regarding the dogma of this response have yet to be verified. One such assumption is that the local increment and decrement responses elicited by the PERG stimulus linearly cancel, leaving only the non-linear retinal activity to be seen in the response. Another underlying idea is that any spatial tuning seen in the PERG response to varying the check size of the PERG stimulus is reflective of the spatial tuning that has previously been seen in responses from individual RGCs. The present work sought to investigate the validity of these two assumptions. Experiment 1 aimed to model the PERG response from flash stimuli, and Experiment 2 evaluated the degree of spatial tuning seen in response to PERG stimuli whose elements had been scaled by a scaling factor that mimicked the approximate rate of change of RGCf size. After successfully modeling the PERG response in Experiment 1, Experiment 3 sought to verify this response in a population of glaucoma patients and determine its translational value in this patient population. Although some methods varied by experiment, others were common to all three investigations. Such general methods and analyses are described below.

General Methods

Participants

Individuals were recruited through the University of Louisville's online subject pool (via Sona Systems, Ltd. recruitment software), as well as through flyers placed around campus. Upon assessing intrasubject variability from pilot data ($\sigma^2 = 1.24$), an effect size of $f = 0.64$ was found for our recordings for $\alpha = 0.05$ and $\beta = 0.95$. Based on this effect size, a minimum of 12 participants were needed for each temporal frequency in each of the three experiments, since data from each temporal frequency were considered separately. All participants for Experiments 1 and 2 were adults with normal or corrected-to-normal vision, between the ages of 18 and 55 years.

Apparatus and Stimuli

Monocular ERG responses were recorded using DTL electrodes (Dawson, Trick, & Litzkow, 1979) from healthy human subjects. Silver cup electrodes were used for both the ground and the reference. The ground electrode was centered on the forehead and the reference electrode was placed on the ipsilateral temple. The ERG signal was amplified 10,000x, analog filtered from 0.1 – 100 Hz, and digitized at a rate of 1000 samples per second with online artifact rejection (±100 μV). Although ISCEV recommends against the use of a notch filter (Bach et al., 2013), pilot data showed no difference in waveform amplitude or morphology when used in the conditions that characterize the work described here, so it was implemented to reduce 60 Hz noise and therefore increase the signal-to-noise ratio. To further reduce the artifact of noise on waveform measurements, all recordings were subjected to a zero-phase first-order low-pass Butterworth filter with a cutoff of 30 Hz. As seen in Figure 11, this filter did not alter the morphology of the

response. Impedance was measured prior to recording, and had to be less than 5 kΩ for the subject to be able to participate in any part of this study.

Stimuli were generated using a graphics-generating software package (Vision Research Graphics, Durham, NH) run on a standard PC, and were displayed on a Hitachi SuperScan Pro 21" CRT monitor that was positioned 36 in from the subject. The height and width of each stimulus was 14.3° ×14.3°. All stimuli were square-wave flashes (in the case of PERG simulations using the flash ERG) or counterphase reversals (in the case of PERG recordings) and were presented on a uniform gray background (52.35 cd/m^2) background (52.35 cd/m^2) that was approximately equal to the average luminance value between the light (104.50 cd/m^2) and dark (0.20 cd/m^2) sections of the PERG stimulus. All stimuli were presented both at transient (4 rps) and steady-state (15 rps) temporal frequencies.

General Analyses

Each ERG waveform assessed as part of the comparative data analysis represented the average of a minimum of 100 responses, though typically 120 – 180 were recorded. Before assessing any of these averaged waveforms, each was normalized to a baseline of 0 μV. For responses to transient stimuli, amplitudes of P50 waveform components were measured from the trough of N35 to the peak of P50, while N95 amplitudes were measured from the peak of P50 to the trough of N95. Implicit time was also measured for both P50 and N95, and was defined for each as the number of milliseconds from the onset of the flash or contrast reversal to the point at which the peak or trough occurred for that waveform component. For responses to steady-state stimuli, Fourier analysis was used to determine the amplitude and phase shift via assessment of

the second harmonic (which represents the reversal rate). Since transient and steady-state waveforms are known to characteristically differ, no comparisons were made between the two types of stimulation.

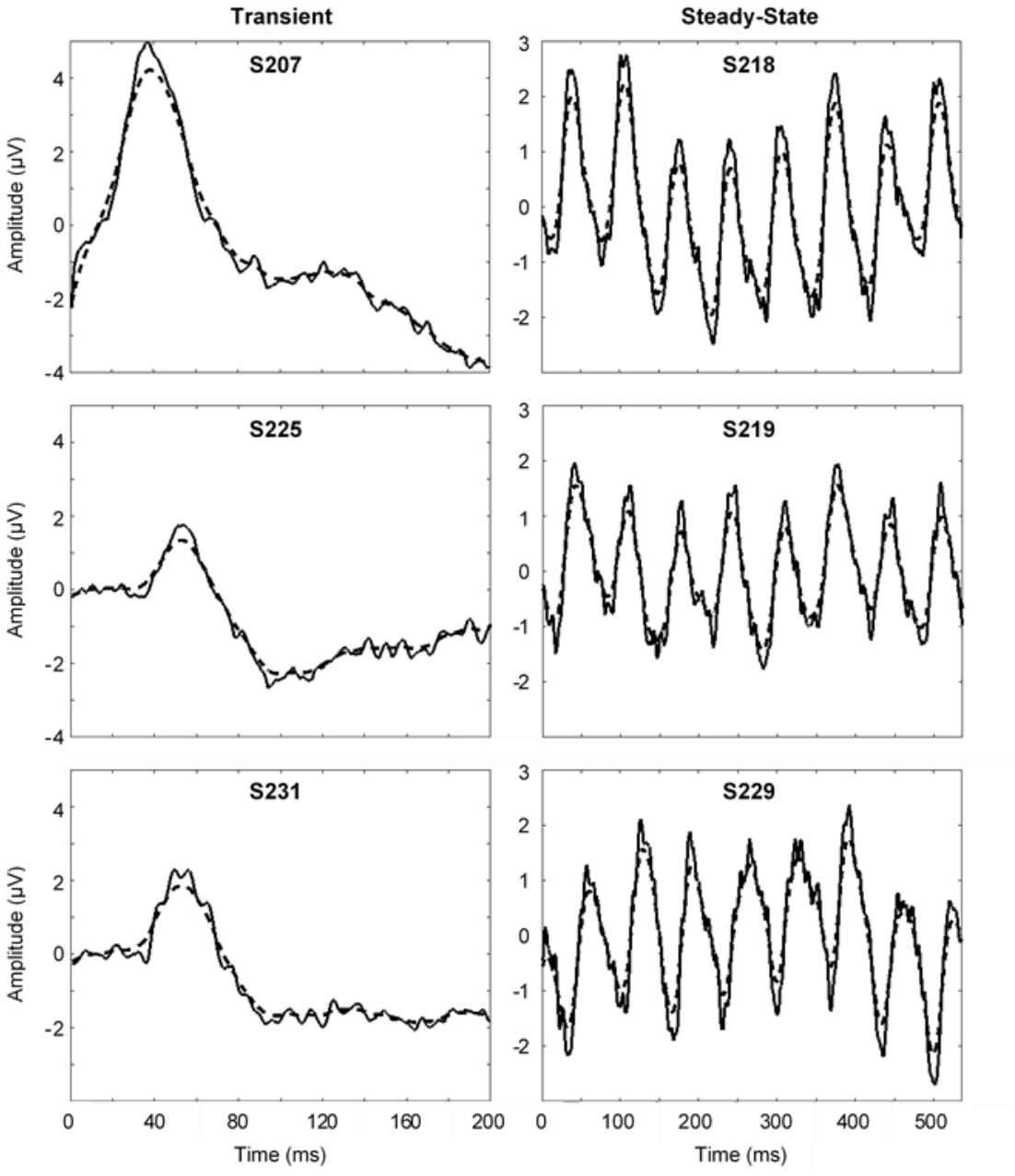

Figure 11. Effect of Low-Pass Filtering. A zero-phase, first-order, low-pass Butterworth filter with a 30 Hz cutoff was applied to each recording before analysis to remove excess noise. As seen in the subset of PERG responses shown above, the filtered waveforms (dashed lines) reflected the true morphology of the original signals (solid lines).

CHAPTER III

EXPERIMENT 1: MODELING THE PATTERN ELECTRORETINOGRAM IN HEALTHY ADULTS

Experiment 1: Modeling the Contributions of Luminance and Local Spatial Contrast on PERG Response

Hypothesis: The PERG response is the result of linear cancellation of simultaneous increment and decrement retinal responses, and can therefore be modeled by a summation of ERG responses elicited by increment and decrement flashes.

Aim: Create a model of the PERG that incorporates amplitude scaling, temporal timing, and retinal area stimulated by increment and decrement retinal responses.

Rationale: As reviewed in Chapter I, previous attempts to model the PERG from flash ERG responses have relied on the assumption that responses from the retinal ON- and OFF-pathways, as reflected in the b-wave and d-wave responses, are opposite-polarity graded potentials which sum to leave only the non-linear, RGC-driven activity.

There are two implicit assumptions underlying this standard model. The first assumption is that the b-wave and d-wave responses can be added together without further consideration of retinal processing that may take place subsequent to the generation of the b- and d-wave responses, for example, in the inner-plexiform layer. Further retinal processing may scale increment and decrement responses separately, or

alter the phase relationship of the responses, ultimately affecting the morphology of the resulting PERG response.

The second assumption is that the spatial content of the PERG stimulus and the associated processing of local contrast edges by the retinal circuits can be ignored when modeling the PERG response using flash ERG responses. Implicit in this assumption is that the retinal area stimulated by the light and dark checks is half that of a uniform flash stimulus of the same stimulus field size. As previously discussed, prior models of the PERG response have simply averaged together the b-wave and d-wave responses generated from long-duration flash stimuli to create a simulated PERG waveform. While the PERG response may result from the cancellation of simultaneous retinal responses to light increments and decrements, this cancellation process may involve retinal circuits that respond differently to a pattern stimulus versus a flash stimulus. Therefore, simply summing the b-wave and d-wave responses from a uniform field may not take into account amplitude scaling or timing factors that result from the retinal response to a patterned stimulus.

One would also expect these factors to be altered by the temporal frequency of the stimulus pattern (i.e. transient versus steady-state PERG paradigms). This is of particular concern given the findings that the transient PERG has approximately equal contributions from the ON and OFF pathways, whereas the steady-state PERG seems to originate largely within the ON pathway (Luo & Frishman, 2011). Based on mixed results from previous experiments that have attempted to simulate the PERG (Arden & Vaegan, 1983; Luo & Frishman, 2011; Simpson & Viswanathan, 2007; Viswanathan et al., 2000), I propose that these assumptions may not be valid and should to be tested further.

Procedure. Pupils were dilated and visual accommodation was relaxed with 2.5% phenylephrine hydrochloride and 1% tropicamide. In the absence of accommodation, and to maintain acuity, subjects viewed all PERG stimuli through corrective lenses. Responses were recorded from both PERG stimuli and flash stimuli in an effort to simulate the PERG response using flash ERG protocol. PERG recordings followed the ISCEV standards (Bach et al., 2013), using the recommended checkerboard with 0.8° checks and a mean luminance of 52.35 cd/m^2 (black checks = 0.20 cd/m^2, white checks = 104.50 cd/m^2), with a maximized contrast of 99.62% between black checks and white checks. Two different categories of flash stimuli were used to create the PERG

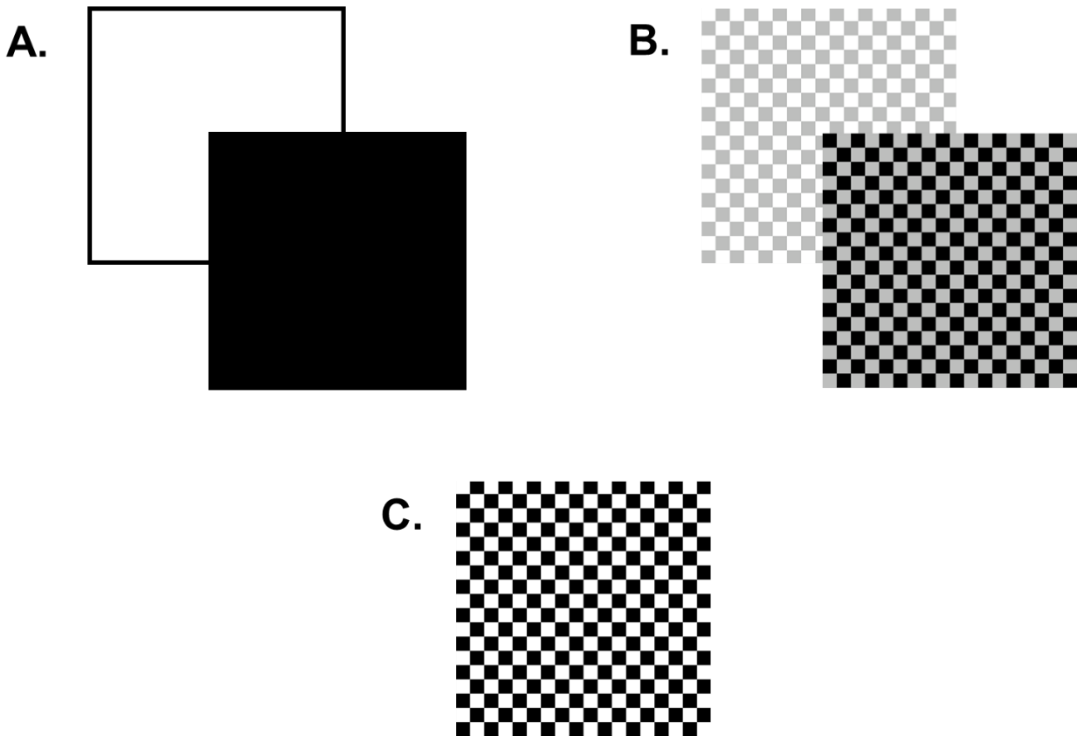

Figure 12. Stimuli Used in Experiment 1. Experiment 1 seeks to model the standard PERG response by summing increment and decrement responses from flash stimuli. To accomplish this, simulations were created from both uniform flash stimuli (A) as well as checked flash stimuli (B) to model the response seen from a standard PERG stimulus (C).

simulations (see Figure 12). One category (Figure 12A) consisted of uniform light that alternated between black (decrements) and white (increments), while the other category (Figure 12B) alternated between checkerboards of gray and white checks (increments) and gray and black checks (decrements).

The gray used in the checked flash stimuli was the same luminance as that of the local background (52.35 cd/m^2), which represented an average between the luminance values of the increments and decrements. All flash stimuli used the same reversal rates as those of the PERG stimuli (4 and 15 rps), and also used the same luminance values of the increment and decrement portions of the PERG stimulus. Because increment and decrement stimuli were presented separately in the flash stimuli conditions, the contrast within a checkerboard PERG stimulus was higher than that of each individual flash stimulus (i.e. an increment or decrement flash against a local gray background of 52.35 cd/m^2), but matched the modulation depth between increment and decrement stimuli.

Analyses. For both transient and steady-state responses, PERG recordings from standard checkerboards were compared to simulations created from summed increment (ON) and decrement (OFF) responses to either uniform flashes of light or checked flashes of light. Since the flash ERG responses used for PERG simulations were recorded in one waveform, each was split into its ON and OFF components so that they could each be normalized to a baseline of 0 μV and then summed to produce that participant's simulation. Once simulations from both uniform flashes and checked flashes were created, error was calculated between each simulation and the PERG response waveform, with a lower degree of error indicating a better fit.

Because each of the two uniform flash stimuli was as large as the PERG stimulus, the simulation from combined flash responses represents twice as much retinal stimulation as that of the PERG response. This study, however, also used checked flash stimuli, which provided the same degree of actual stimulation as the increments and decrements seen within the PERG stimulus. To determine if this difference in degree of retinal stimulation affected the simulation, two paired-samples *t*-tests compared the error of the uniform-flash simulation to that of the checked flash simulation for transient and steady-state conditions, respectively. Since past authors (Luo & Frishman, 2011; Simpson & Viswanathan, 2007; Viswanathan et al., 2000) have tried to account for this luminance discrepancy by averaging the b- and d-wave amplitudes, two paired-samples *t*-tests were used to compare the goodness of fit from the averaged uniform-flash b- and d-waves to that of the summed checked flashes. One of these *t*-tests made this comparison for transient responses, with the other being for those which were steady-state.

In designing this experiment, however, it was recognized that even separate flashes in the appropriate spatial layout with the same amount of luminance as that found in the PERG stimulus would not necessarily create the best-fitting simulation since these flashes were not being processed simultaneously. To account for this possibility, algebraic manipulations of the simulations created from uniform flash stimuli were also compared to the original PERG response. The first of these manipulations consisted of scaling the amplitude of the increment and decrement responses before summing to create the simulation. Pilot data had consistently shown that the simulation from uniform flashes was larger in amplitude than the actual PERG waveform (see Figure 13 for a sample of these pilot data), which may be due to a difference in the gain mechanism(s)

between uniform flashes and checked flashes, as previously mentioned. Therefore, the amplitudes of both increment and decrement responses were scaled in increments of 5% down to a waveform that was 25% of the original response. Each possible combination of scaled increment and decrement responses was evaluated.

The second of these manipulations aimed to account for known differences in response kinetics between the ON and OFF pathways (Chichilinsky & Kalmar, 2002) by shifting the b-wave along the x-axis before summing it with the d-wave. Specifically, it was shifted both forward (occurring after the start of the d-wave) and backward (occurring before the start of the d-wave) in 2 ms intervals, up to a total of 10 ms in each direction. Since it is currently unclear exactly how response kinetics are characterized in the context of the increment and decrement combinations within the PERG stimulus, this wide range of timing possibilities helped to account for the potential for either pathway to respond to its respective stimulus components more quickly. Finally, permutations of each degree of scaling and phase shifting were also assessed to account for possible interactions between these two sets of processes.

Each participant's simulation was compared to his or her original PERG response of the appropriate temporal frequency via an error metric calculated by totaling the sum of squared differences between the PERG waveform and the simulation of interest. In other words, the difference between the PERG response and its respective simulation was calculated for each point in time, and then squared. After a squared value of this nature had been attained for each millisecond in time (200 ms for transient responses, 536 ms for steady-state responses), they were summed to account for the total area of difference between the two waveforms, which acted as the participant's error for that comparison.

For each participant, error was normalized to a peak value of 1 by dividing all error values by the maximum error value obtained across all simulations within that temporal frequency. The simulation with the lowest degree of error was labeled as the best fit for each subject. Since these algebraic manipulations produced many different simulations, there was some variability in the specific scaling and time-shifting parameters that represented the model of best fit for each individual. For this reason, the average of individual best-fit parameters was calculated to create an averaged model of best-fit for each temporal frequency. Upon calculating this average, these parameters were rounded to their closest integer value of the interval appropriate for that measure (i.e. 2 ms for time-shifting, 5% for amplitude-scaling).

After individual and averaged best-fit parameters were established for both transient and steady-state conditions, a paired-samples *t*-test compared the degree of error from the simulation using the averaged best-fit parameters to the simulation using each individual's best-fit parameters. One such *t*-test was conducted for best-fit parameters found under transient conditions, and another was conducted for best-fit parameters found under steady-state conditions. Further, an additional set of paired-samples *t*-tests compared the individual best fits to the checked flash simulation to see which produced the lowest error. In each set of comparisons, Holm's procedure was used to maintain a family-wise error rate of 0.05.

All of the comparisons that have been discussed thus far have focused on the holistic degree of error between a simulation and the original PERG waveform. However, comparisons of transient waveforms also allow for the possibility of evaluating this degree of error as it pertains to the specific waveform components of P50 and N95. As

detailed in Chapter I, these two response components have been shown to differ somewhat in origin (Luo & Frishman, 2011; Miura et al., 2009), and therefore may differ somewhat in the degree to which they can each be successfully modeled in the context of the present PERG simulations. For this reason, the same comparisons that were made to assess the fits of holistic waveform simulations were used to assess the fits of the portions of the waveform that represent P50 (35 to 65 ms) and N95 (85 to 115 ms). The ranges for each of these components were selected based on where these components were found in pilot data.

Results. As previously described, each categorical comparison yielded two paired-samples *t*-tests: one which compared results within transient stimuli, and one which compared results within steady-state stimuli. For all comparisons, each value assessed represented the degree of error between that simulation and the actual PERG response. All statistics (both descriptive and inferential) were performed on the degree of normalized error present in each simulation, as described in more detail in the above Analyses section. Because of this, all values reported are representative of such error, but it should be noted that the present results are discussed in regards to goodness of fit. Since degree of error and goodness of fit are inversely related, the inference used to describe these results is that lower error indicates a better fit.

Averaged differences between amplitudes and implicit time/phase measurements of the simulations and the actual PERG response are reported in Table 1. For each set of *t*-tests, Holm's procedure is employed to maintain a family-wise error rate of 0.05. For this reason, adjusted α-values are reported alongside all *t*-values, degrees of freedom, and *p*-values in Table 2 for holistic waveforms (transient and steady-state), and in Table 3 for

transient waveform components (P50 and N95). It should be noted that while 37 participants took part in this experiment, only 24 of them participated in the checked-flash stimuli conditions. Therefore, any comparisons made to the checked-flash simulation were only using the data from those 24 participants so as to keep all comparisons within-subject.

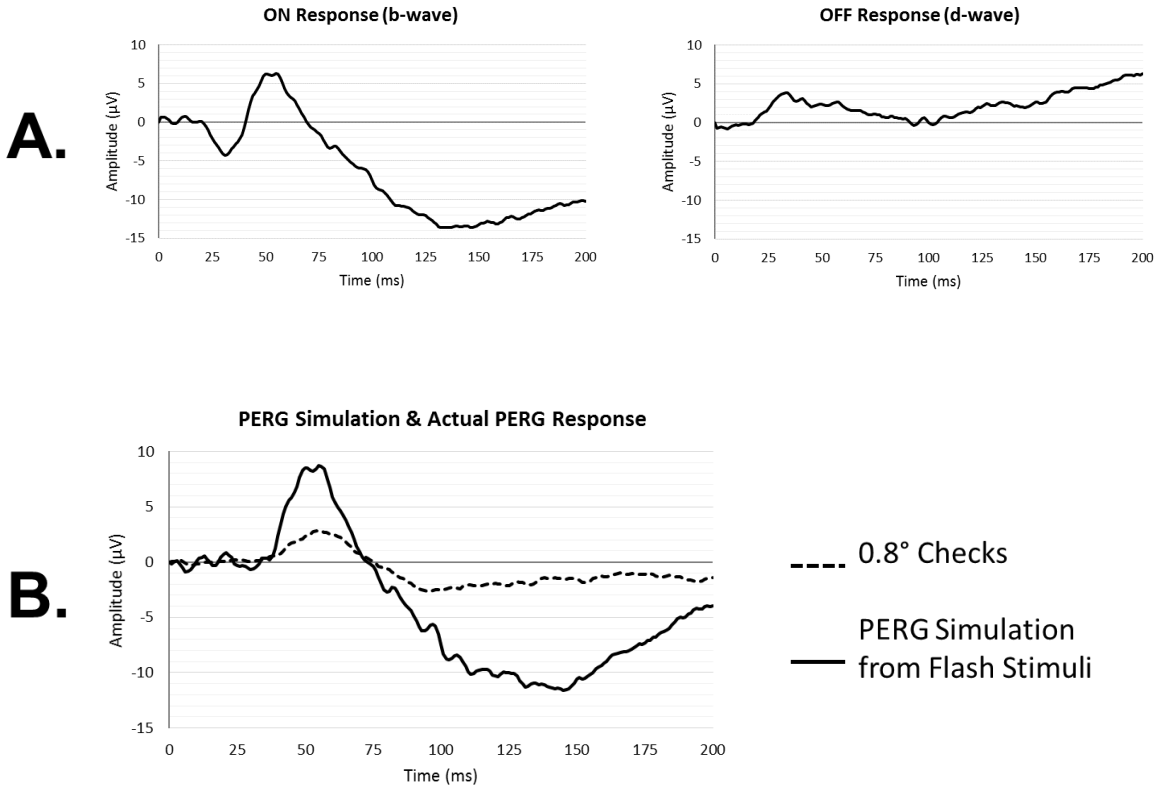

Figure 13. Experiment 1 Pilot Data. For each subject, both ON/b-wave responses and OFF/d-wave responses were recorded in response to uniform flash stimuli (A). These responses were then summed and normalized to create a simulation of the PERG (B, solid line). As is seen here, the PERG simulation is of greater amplitude than the PERG response to the standard checkerboard for both waveform components (B, dashed line). Additionally, N2 displays a greater implicit time than does N95. Since this model shows much of the same morphology, but some amplitude and timing differences, further manipulations such as flashing checked stimuli and algebraic alterations will be employed in an effort to improve the accuracy of the model. Data displayed are from subject 229.

To better understand the effect that each variable had on the resulting degree of error, see Figures 14 and 15 for the effects of scaling and time-shifting, respectively. As seen in Figure 14, the goodness of fit was more drastically impacted by the degree to which the b-wave was scaled relative to the degree by which the d-wave was scaled for both transient and steady-state simulations. Additionally, the range of fit success was highly similar for transient simulations and steady-state simulations when comparing these effects of scaling. However, when the effect of time-shifting the b-wave was assessed, the pattern of results differed between transient and steady-state simulations.

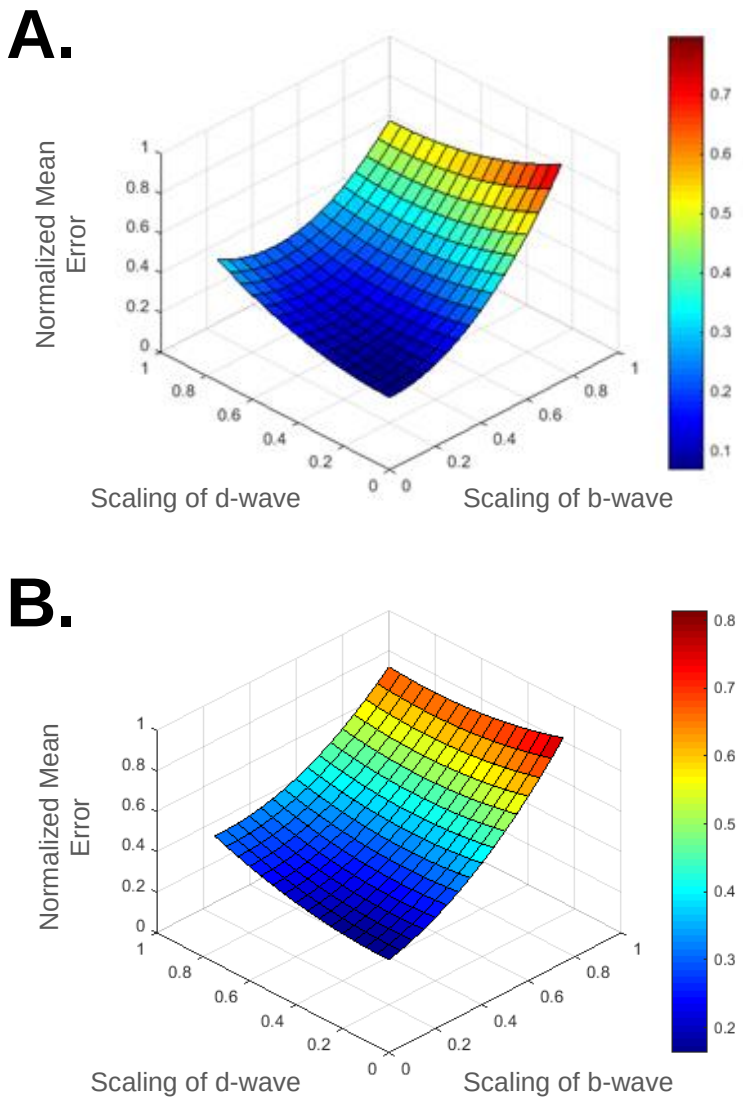

Figure 14. Averaged Degree of Error as a Function of Scaling. The averaged degree of error between the PERG response and simulations, excluding time-shifting, is plotted as a function of scaling factor for the b-wave and d-wave. Despite some minor differences, the pattern of these effects are highly similar for both transient **(A)** and steady-state **(B)** simulations. In both cases, the degree to which the b-wave is scaled has a much more drastic effect on the goodness of fit than does the degree to which the d-wave is scaled.

For transient simulations, goodness of fit increased with the delay of the b-wave, with the most optimal fit resulting from shifting the b-wave to start 10 ms after the d-wave. In the case of steady-state simulations, goodness of fit decreased with the delay of the b-wave, with the most optimal fit resulting from shifting the b-wave to start 10 ms before the d-wave. Overall, time-shifting alone resulted in more successful fits for transient simulations than it did for steady-state simulations (as seen in Figure 15).

For both transient and steady-state conditions, the uniform-flash simulations (raw sums of b-waves and d-waves) were far greater in amplitude than the actual PERG responses. This was expected given that the flash stimuli used to create the b-waves and d-waves that contributed to the uniform-flash simulation each comprised the same stimulus field size as that of the PERG. Because of this, the uniform-flash simulation is representative of twice the amount of stimulation as that of the PERG response, and is therefore expected to produce a larger-amplitude response relative to the PERG. In the case of the individual best-fit simulations, however, both the amplitude and timing tend to align well with those respective measures of the actual PERG response. To see examples of individual simulations and actual PERG responses, see Figure 16. Averaged PERG responses and simulations can be found in Figure 17.

To eliminate this confound of differences in retinal stimulation, the present study also employed checked-flash stimuli, which represented both the correct degree of luminance and accurate spatial layout of the increment and decrement flashes within the PERG stimulus. To evaluate the efficacy of these checked-flashes relative to the uniform flashes, goodness of fit was compared between the simulations created from each of these two stimulus types using two paired-samples *t*-tests (one for transient conditions and one

for steady-state conditions). For transient stimuli, the simulation created from uniform flashes ($M = 0.600$, $SD = 0.256$) yielded a worse fit than that which was created from checked flashes ($M = 0.343$, $SD = 0.219$; $t(23) = 3.976$, $p = 0.001$). The same result was found when the steady-state uniform-flash simulation ($M = 0.722$, $SD = 0.160$) was compared to the steady-state checked-flash simulation ($M = 0.268$, $SD = 0.192$; $t(23) = 9.026$, $p < 0.001$), indicating that the degree of retinal stimulation has a significant impact on how well these simulations are able to fit the true PERG response.

Since transient responses are often evaluated in regards to their individual components, this same comparison was made for both P50 and N95 with two additional *t*-tests. The goodness of fit for the P50 component was found to be greater for the uniform-flash simulation ($M = 0.580$, $SD = 0.243$) relative to the checked-flash simulation ($M = 0.175$, $SD = 0.237$; $t(23) = 4.786$, $p < 0.001$), mimicking the pattern found for the holistic responses to both transient and steady-state stimuli. However, when the goodness of fit for N95 was compared between the uniform-flash simulation ($M = 0.478$, $SD = 0.275$) and the checked-flash simulation ($M = 0.430$, $SD = 0.325$), no difference was found ($t(23) = 0.543$, $p = 0.593$). This may be due to the findings of Luo and Frishman (2011) that showed contributions of luminance-based responses to both the steady-state PERG and P50 component of the transient PERG, but not to the N95 component.

Previous work (reviewed in Chapter I) has also found this confound of differing degrees of retinal stimulation between that which is seen in from the PERG stimulus versus separate uniform-flash stimuli. To account for this, most authors have created their simulations by halving the amplitudes of the b-wave and d-wave and then adding these

two waveforms together (Luo & Frishman, 2011; Simpson & Viswanathan, 2007; Viswanathan et al., 2000). This is mathematically equivalent to averaging the original b-wave and d-wave. While averaging may control for the difference in luminance, it does not account for the flashes being presented in a different spatial arrangement, which may also contribute to the PERG response. To determine if there was an effect of presenting the flashes within a spatial context, two paired-samples *t*-tests compared the goodness of fit from the simulation created by averaging the b- and d-waves with that from the checked-flash simulation. One *t*-test was used for each temporal frequency, and two additional *t*-tests were used to assess the P50 and N95 components of transient responses.

When the transient uniform flash simulation was scaled to 50% of its original amplitude (the equivalent of averaging the b- and d-waves), the fit from this scaled simulation ($M = 0.134$, $SD = 0.073$) was better than that of the transient checked flash simulation ($M = 0.175$, $SD = 0.237$; $t(23) = -4.619$, $p < 0.001$). When comparing just the P50 component of the 50% uniform-flash simulation ($M = 0.084$, $SD = 0.059$) to the P50 component of the checked-flash simulation ($M = 0.175$, $SD = 0.237$), however, no difference was found ($t(23) = -1.701$, $p = 0.102$). In contrast, the N95 component of the 50% uniform-flash simulation ($M = 0.095$, $SD = 0.058$) was a better fit than the checked-flash simulation ($M = 0.430$, $SD = 0.325$; $t(23) = -4.989$, $p < 0.001$). For steady-state responses, no difference in goodness of fit was found between the 50% uniform-flash simulation ($M = 0.277$, $SD = 0.082$) and the checked-flash simulation ($t(23) = 0.264$, $p = 0.794$). These results further support the idea of luminance-based contributions to the responses to the transient P50 component and the steady-state PERG response, but not to the N95 component of the transient response (Luo & Frishman, 2011).

Individual best-fit parameters were averaged across participants to determine a more general model that may be applied to all participants without having to customize individual parameters. The present data yielded transient averaged best-fit parameters that shifted the b-wave to begin 0.126±0.871 ms before the d-wave, scaled the b-wave down to 33.694±1.885% of its original amplitude, and scaled the d-wave down to 45.315±3.452% of its original amplitude. Steady-state best fits were produced by shifting the b-wave to begin 9.258±0.312 ms before the d-wave, scaling the b-wave down to

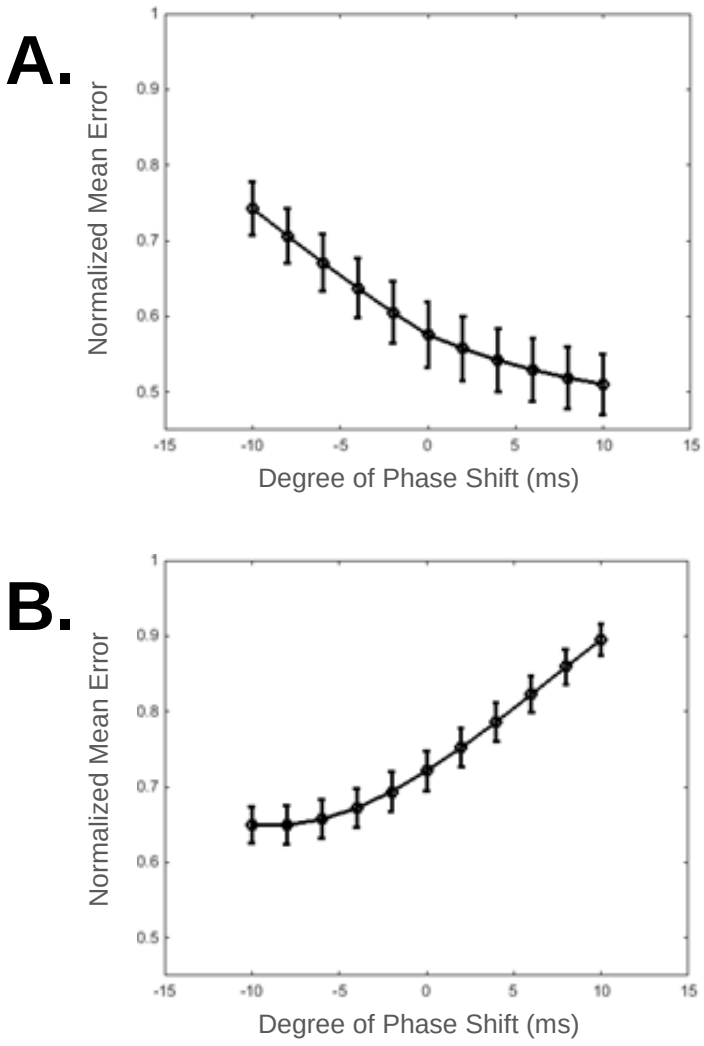

Figure 15. Averaged Degree of Error as a Function of Time-Shifting. The averaged degree of error between the PERG response and simulations that were not scaled is plotted as a function of b-wave time shift along the x axis. For transient simulations **(A)**, the optimal fit appears to result from the b-wave starting 10 ms after the d-wave before summing, whereas for the steady-state simulations **(B)**, the best fit is found when the b-wave starts 10 ms before the d-wave prior to summing. Note that time-shifting alone produces better fits in transient stimuli relative to steady-state, as is indicated by the lower range of error.

25.161±0.147% of its original amplitude, and scaling the d-wave down to 30.564±1.161% of its original amplitude. For both of these conditions, each of these values were rounded to the nearest integer value that represented a multiple of the time-shifting or scaling integers being used in the model. This yielded a transient best-fit This yielded a transient best-fit that involved no time-shifting, a 35% scaled b-wave, and a 45% scaled d-wave. The steady-state best fit was rounded to a time shift of -10 ms, a 25% b-wave, and a 30% d-wave.

To determine if the simulation produced from a set of averaged best-fit parameters yielded as good of a fit as that from the individual's best fit parameters, the goodness of fit from these two simulations were compared with additional paired-samples *t*-tests. In the case of transient stimuli, the simulation from an average of best-fit parameters ($M = 0.081$, $SD = 0.063$) was not as good of a fit as the simulation from individual best-fit parameters ($M = 0.032$, $SD = 0.035$; $t(36) = 7.612$, $p < 0.001$). This same result was found when averaged best-fit simulations were assessed in steady-state conditions ($M = 0.228$, $SD = 0.106$) and then compared to steady-state individual best-fits ($M = 0.127$, $SD = 0.057$; $t(36) = 8.750$, $p < 0.001$).

When the individual components of the transient simulations were assessed, however, P50 showed no difference in fit between averaged best-fit simulations ($M = 0.059$, $SD = 0.069$) and individual best-fit simulations ($M = 0.078$, $SD = 0.122$; $t(36) = -1.162$, $p = 0.253$). In the case of the N95 component, the simulations produced from averaged best-fit parameters ($M = 0.085$, $SD = 0.106$) did not fit the N95 of the PERG as well as those produced from individual best-fit parameters ($M = 0.035$, $SD = 0.043$, $t(36) = 3.541$, $p = 0.001$). Therefore, the P50 component of the transient simulation was the

only component measured that would not require an individualized set of parameters to achieve the best possible fit.

Although these individualized best-fit parameters seemed to yield the best fit, it was unclear if these parameters were merely compensating for the luminance difference and the lack of spatial layout in the stimulus field, or if they were accounting for additional variations in the response caused by simultaneous presentation of the flashes. To assess this, goodness of fit was compared between individual best-fit simulations and checked-flash simulations for all conditions. Neither transient checked-flash simulations ($M = 0.343$, $SD = 0.219$) nor steady-state checked-flash simulations ($M = 0.268$, $SD = 0.192$) were able to produce as good of a fit as their respective individual best-fit simulations (transient: $M = 0.033$, $SD = 0.037$, $t(23) = -6.770$, $p < 0.001$; steady-state: $M = 0.128$, $SD = 0.062$, $t(23) = 4.391$, $p < 0.001$).

For the P50 component of the transient response, individual best-fits ($M = 0.093$, $SD = 0.148$) were no different from checked-flash simulations ($t(23) = 1.829$, $p = 0.080$). In contrast, N95 showed the same pattern as each of the comparisons of holistic simulations in that the checked-flash simulations ($M = 0.430$, $SD = 0.325$) did not yield as good of a fit as the individual best-fit simulations ($M = 0.037$, $SD = 0.037$; $t(23) = 6.018$, $p < 0.001$). Therefore, with the potential exception of P50, it appears that there is some sort of difference in retinal processing of the PERG that must be accounted for when its increment and decrement portions are viewed simultaneously rather than separately.

Finally, due to some participants' reports of afterimages following the stimuli, the potential of adaptation during stimulus viewing was assessed. Since this possibility had

not been considered in the original design of the experiment, the precise amount of viewing time was not controlled for from subject to subject because of artifact rejection. Due to this limitation, adaptation effects were assessed by comparing the amplitude of from an average of the first 25 trials to that of the last 25 trials from the same stimulus. These 25-trial blocks were each subsets of the total number of trials averaged together to represent a single measurement for that individual. It is also possible that adaptation may have occurred more quickly within just a few trials. As is common with ERG recordings, however, the variability of single-trial measurements was far too great to determine if this was the case.

Three paired-samples *t*-tests were performed to assess the degree of adaptation in P50, N95, and steady-state amplitudes from checkerboard PERG stimuli. There was one participant for whom the file with recordings of individual trials had become corrupted, and was therefore excluded from this analysis. Each test compared the average amplitude of the first 25 responses to that of the last 25 responses for the same stimulus in an attempt to evaluate if this amplitude had decreased over the length of recording for that stimulus. For P50, the amplitude from the first 25 responses ($M = 2.309$, $SD = 1.154$) was not found to differ from the amplitude of the last 25-responses ($M = 2.349$, $SD = 1.124$; $t(35) = -0.248$, $p = 0.805$). Similarly, no difference was found between the amplitude of the first 25 responses ($M = 4.661$, $SD = 1.783$) and the last 25 responses ($M = 4.032$, $SD = 2.145$) for N95 responses ($t(35) = 1.542$, $p = 0.132$). However, in the case of steady-state responses, the amplitude from the first 25 responses ($M = 1.016$, $SD = 0.334$) was greater than the amplitude from the last 25 responses ($M = 0.871$, $SD = 0.298$; $t(35) = 4.543$, $p < 0.001$).

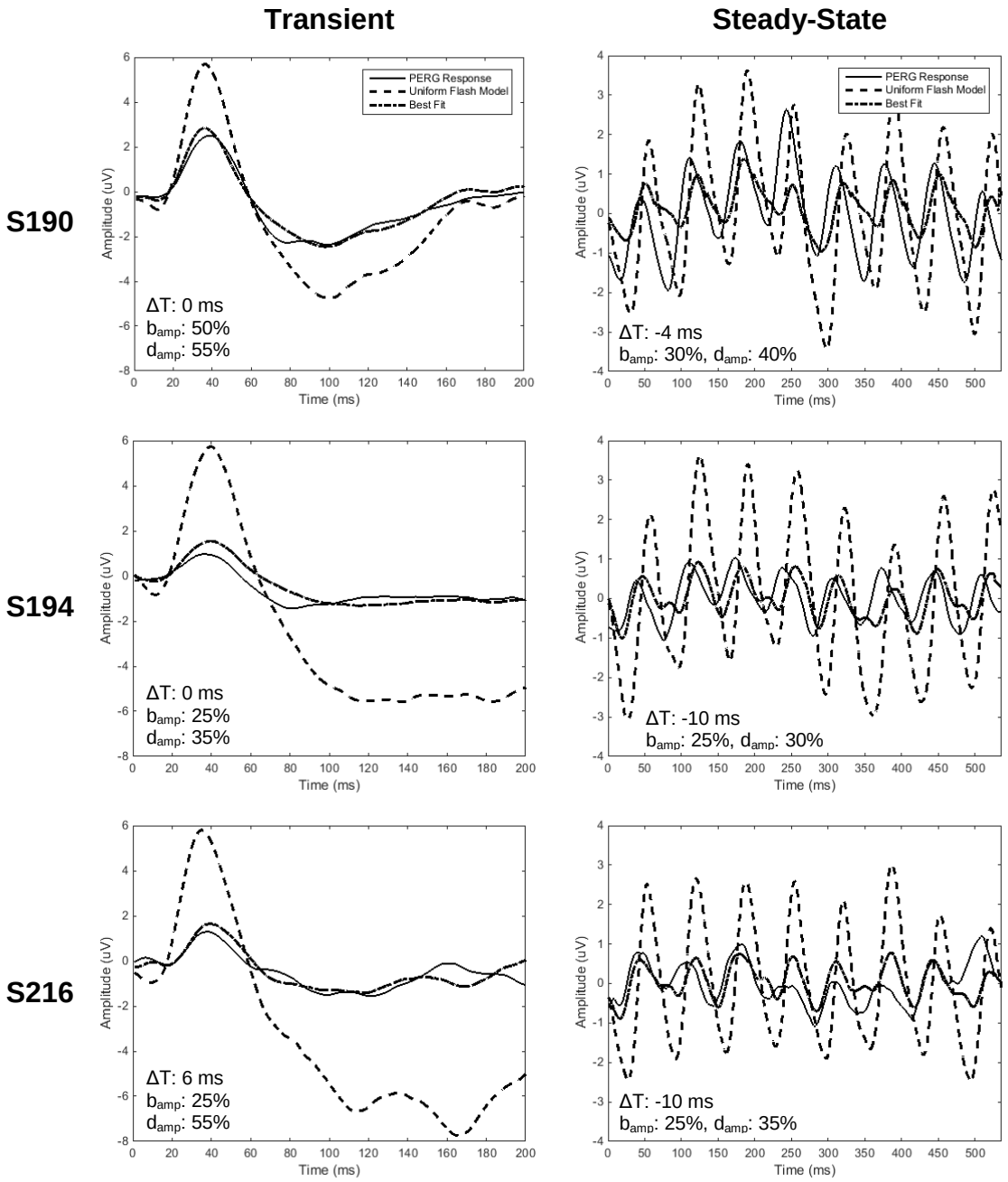

Figure 16. Comparisons of Experiment 1 PERG Responses and Simulations. Samples of individual data are shown from three representative subjects (S190, S194, and S216) in response to both transient stimuli (left) and steady-state stimuli (right). For each plot, the PERG response (solid lines) is compared with the simulation created from simply summing the b- and d-waves from uniform flash stimuli (dashed lines), as well as with the simulation that yielded the lowest degree of error and therefore represented the best fit for that subject (dot-dashed lines). The amount of time shift (ΔT), b-wave scaling (b_{amp}), and d-wave scaling (d_{amp}) that was employed to create the best fit for each subject is shown in the bottom left of each graph. Negative ΔT values represent the b-wave beginning before the start of the d-wave, and positive values represent the b-wave starting after the beginning of the d-wave.

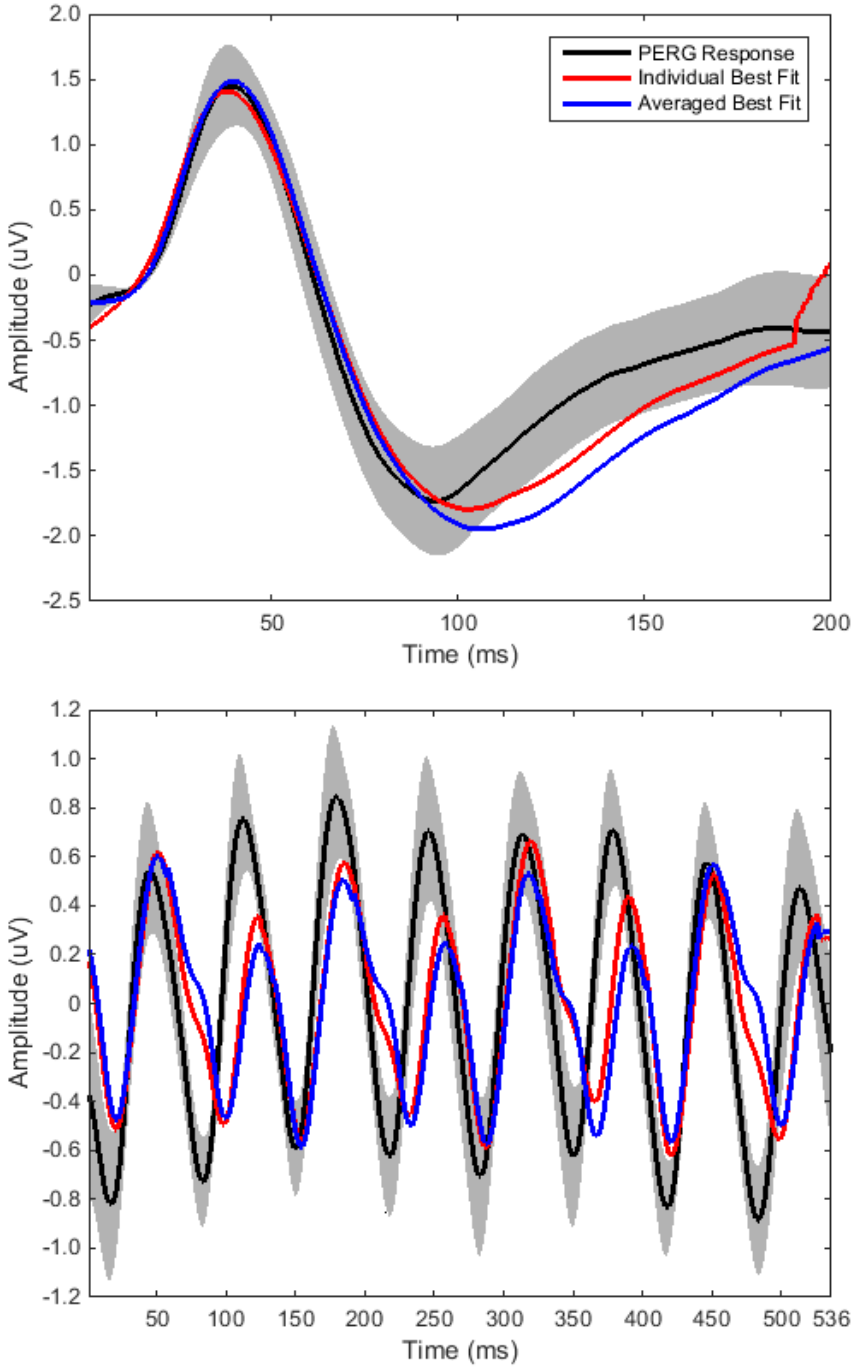

Figure 17. Averaged Experiment 1 PERG Responses and Simulations. For both transient (top) and steady-state (bottom) conditions, three waveforms are shown which represent the average of all participants' PERG responses (solid black line), individual best-fit simulations (solid red line), and averaged best-fit simulations (dashed red line), respectively. Each of these waveforms are shown on top of the 95% confidence interval for the PERG response (gray fill) to see how the averaged simulations compare to the variability of the PERG response.

	100% Uniform Flash	50% Uniform Flash	Checked Flash	Averaged Best Fit	Individual Best Fit
Differences in Amplitude (μV)					
Transient					
P50 Average	3.458	0.965	0.629	0.626	0.610
P50 Standard Error	0.198	0.087	0.067	0.082	0.077
N95 Average	7.269	1.925	3.206	1.145	0.615
N95 Standard Error	0.444	0.229	0.313	0.131	0.099
Steady-State					
Average	1.343	0.215	0.366	0.387	0.329
Standard Error	0.073	0.019	0.051	0.043	0.039
Differences in IT (ms)/PS (deg)					
Transient					
P50 Average	1.820	1.820	2.875	1.829	2.441
P50 Standard Error	0.190	0.190	0.425	0.197	0.397
N95 Average	14.351	14.351	15.014	12.685	11.261
N95 Standard Error	1.348	1.348	1.237	1.357	1.299
Steady-State					
Average	98.614	63.966	88.032	75.512	65.095
Standard Error	8.851	16.660	12.318	11.452	10.219

Table 1. Amplitude and Implicit Time/Phase Differences. Average differences and their respective standard errors are listed for the amplitude and implicit time ("IT," transient) or phase shift ("PS," steady-state) of each simulation relative to the actual PERG waveform, with transient simulations listing P50 and N95 waveform components separately.

Stimulus Comparison	***t***	df	***p***	Adjusted α
Transient				
100% Uniform Flash and Checked Flash	3.976	23	0.001*	0.050
50% Uniform Flash and Checked Flash	-4.619	23	<0.001*	0.025
Averaged Best Fits and Individual Best Fits	7.612	36	<0.001*	0.013
Checked Flash and Individual Best Fits	6.770	23	<0.001*	0.017
Steady-State				
100% Uniform Flash and Checked Flash	9.026	23	<0.001*	0.013
50% Uniform Flash and Checked Flash	0.264	23	0.794	0.050
Averaged Best Fits and Individual Best Fits	8.750	36	<0.001*	0.017
Checked Flash and Individual Best Fits	4.391	23	<0.001*	0.025

Table 2. Error Comparisons among PERG Simulations. Comparisons (listed in far left column) are listed with their respective *t*-values, degrees of freedom, *p*-values, and adjusted α values based on Holm's procedure. Note that two sets of planned comparisons are being made (one for each temporal frequency), yielding two different sets of adjusted α values. Comparisons that are significantly different are denoted by an asterisk (*) next to their respective *p*-values. Means and standard deviations are reported in the text.

	t	df	*p*	Adjusted α
P50				
100% Uniform Flash and Checked Flash	4.786	23	<0.001*	0.013
50% Uniform Flash and Checked Flash	-1.701	23	0.102	0.025
Averaged Best Fits and Individual Best Fits	-1.162	36	0.253	0.050
Individual Best Fits and Checked Flash	1.829	23	0.080	0.017
N95				
100% Uniform Flash and Checked Flash	0.543	23	0.593	0.050
50% Uniform Flash and Checked Flash	-4.989	23	<0.001*	0.017
Averaged Best Fits and Individual Best Fits	3.541	36	0.001*	0.025
Individual Best Fits and Checked Flash	6.018	23	<0.001*	.013

Table 3. Error Comparisons among Waveform Components of Transient PERG Simulations. Comparisons (listed in far left column) are listed with their respective *t*-values, degrees of freedom, *p*-values, and adjusted α values based on Holm's procedure. Note that two sets of planned comparisons are being made (one for each temporal frequency), yielding two different sets of adjusted α values. Comparisons that are significantly different are denoted by an asterisk (*) next to their respective *p*-values.

Summary. This experiment evaluated the accuracy and usefulness of simulating the PERG response with only flash ERG stimuli. Based on the results reported here, it appears that a single model that simply averages the b- and d-wave responses does not adequately describe any one subject's PERG response. Customized best-fit parameters for both transient and steady-state waveforms provide better fits to individual data, implying that a singular model will not always provide satisfactory fits to an individual's PERG response. For transient responses, it may also be the case that the spatial component of the PERG stimulus has a large impact on the transient PERG response, as the checked-flash simulation yielded a lower error relative to the uniform-flash simulation that had been scaled to 50% of its original amplitude (which should account for the luminance difference).

This spatial component may not play as large of a role in steady-state responses, however, as there was no difference in error found between the 50% scaled uniform-flash simulation and the checked-flash simulation when the temporal frequency was changed to 15 rps. For both transient and steady-state simulations, it may be the case that there is still some difference in gain mechanisms when flashes are shown separately versus simultaneously given that individuals' best-fit parameters yielded lower degrees of error relative to the checked-flash simulations. Due to all of these limitations, it may be the case that the transient PERG response cannot be reliably simulated from separate presentations of flash stimuli.

Just as the success of the PERG simulation was shown to vary somewhat with temporal frequency, so too was it shown to vary between the two waveform components of transient simulations. P50 seems to be more reliably replicated, as the only comparison

that yielded a significant difference in error was that of the 100% uniform-flash simulation to the checked-flash simulation. This difference is expected based on the luminance discrepancy alone, and shows that P50 does change in size when more stimulation is present. However, the comparison between the 50% uniform-flash simulation and the checked-flash simulation yielded no difference in the degree of error for the P50 component, implying that the spatial context of the stimulus is not imperative for its use in simulating the PERG response. Further, the P50 fit did not improve when the parameters were customized to the individual, regardless of whether that individual fit was compared to averaged best-fit parameters or checked-flash simulations. This wide range of equally-useful options suggests that P50 may be reliably simulated in most individuals.

In contrast, the N95 component appears to be much less generalizable. When the 100% uniform-flash simulation was compared with that of the checked-flash simulation, no difference in N95 error was found, indicating that luminance is not likely to be a key variable in simulating this component. However, when the 50% uniform-flash simulation was compared to the checked flash simulation, N95 error differed between the two waveforms. Given that the scaling of the uniform-flash simulation should control for the luminance difference between the two, this finding suggests that the spatial context of the stimulus has the capacity to substantially alter the fit of a PERG simulation within the N95 range.

A difference in N95 error was also found between simulations from averaged best-fit parameters relative to those from individual best-fit parameters. Similarly, N95 error also differed between checked-flash simulations and those from individual best-fit

parameters. Since no one simulation was found to be equally as successful as those simulations using individuals' best-fit parameters, it may be the case that N95 cannot be reliably simulated using a single model with standardized parameters. Due to this stark difference between the success of simulating N95 versus P50, it may also be the case that the N95 component was what led to the low reliability of replicating the holistic transient response. See Chapter VI for further possible implications from this experiment.

Based on the results of analyzing potential adaptation over the course of the recording session for PERG stimuli, it appears that no significant adaptation is taking place for transient stimuli since both the P50 and N95 amplitudes do not differ between the first 25 trials and the last 25 trials. However, there was some evidence for adaptation during steady state recording, which could be lowering the resulting amplitude for each stimulus. Since the precise amount of time spent viewing each stimulus was not standardized across participants, there is no way to precisely define the degree to which the responses would have been affected by adaptation. Given that all analyses were within-subject comparisons, however, it may be inferred that this possibility would not drastically affect the results. It may, however, suggest that future studies should regulate the amount of time each participant spends viewing each stimulus, as this finding should extend to all PERG and ERG recordings.

CHAPTER IV

EXPERIMENT 2: OPTIMIZING THE PERG STIMULUS BASED ON A MODEL OF RETINAL GANGLION CELL RECEPTIVE FIELD SIZE

Experiment 2: Optimizing the PERG Stimulus Based on a Model of Retinal Ganglion Cell Receptive Field Size

Hypothesis: The PERG will reflect the spatial response properties of the retinal ganglion cells, and the response will be optimal when the spatial properties of the stimulus reflect the spatial scaling of RGC receptive field size across the retinal area stimulated.

Aim: Determine the degree of tuning of the PERG response to spatially scaled stimuli based on a model of retinal ganglion cell receptive field size as a function of eccentricity.

Rationale: As reviewed in Chapter I, numerous studies point to the source of the PERG as originating from the RGCs. Further, the amplitude of the PERG response is often found to be sensitive to the spatial characteristics of the stimulus presented. Considering both of these findings, it is likely that this spatial tuning of the PERG response reflects the well-established spatial tuning seen in the RGCs (Enroth-Cugell & Robson, 1966). Because RGC bodies (Curcio & Allen, 1990) and their respective receptive fields (RGCf) change in size with eccentricity, I predict that scaling a PERG

stimulus to account for such changes in RGCf across eccentricity will optimally stimulate the RGCs involved in the PERG response.

To test this idea, I generated a custom stimulus in which the spatial frequency changes continuously based on a model of the human retina (Watson, 2014) which predicts RGCf size changes as a function of eccentricity. Using a combination of the known RGC counts from Curcio and Allen (1990) and the degree of displacement estimated by Drasdo and colleagues (Drasdo, Millican, Katholi, & Curcio, 2007), Watson (2014) was able to model the predicted RGCf density across central and peripheral regions of the human retina. Since this model is currently the most thorough prediction of RGCf in across the retina, it was used to design the scaled stimuli for this experiment.

The precise degree to which stimulus spatial frequency impacts the size of the PERG response remains an empirical question due to mixed results from various studies. Based on the idea that spatial tuning does indeed have a strong effect on response amplitude, I propose that a PERG stimulus that is spatially scaled to mimic the continuous change in RGCf size will provide optimal stimulation to the RGCs involved in the PERG response. This stimulus should yield a response of a higher amplitude relative to the response from a standard PERG stimulus of uniform spatial frequency. A larger-amplitude PERG response would provide a better signal-to-noise ratio and allow for more reliable measurements, potentially leading to earlier detection of disease onset and more accurate monitoring of disease progression. To control for the general effect of spatial scaling, I assessed the degree of spatial tuning of PERG responses to uniform

checkerboard stimuli that vary in check size. Two temporal frequencies (one transient, one steady-state), 8 variations of scaled spatial frequency, and 5 check sizes for checkerboards of uniform spatial frequency were tested.

Procedure. The PERG was recorded using a set of custom-made stimuli that controlled for the proportional changes in retinal ganglion cell receptive field size within the stimulated portion of the retina, based on the model of RGCf density proposed by Watson (2014). More specifically, this scaling aimed to create a stimulus in which the RGCf density under one cycle of the grating was equal to that which falls under any other cycle, regardless of any potential difference in eccentricity between these two cycles. Since RGCf density decreases as eccentricity increases, it follows that the spatial frequency needed to maintain the same RGCf density within each cycle need to be highest in the center of the grating and lowest at the grating's outer edges. It would be impractical for the parameters of the stimuli to mimic actual RGCf size since the stimuli would be too small to elicit a PERG response; instead, the variation in spatial frequency as a function of eccentricity followed the rate of change as modeled by Watson.

Each pattern was presented as a square stimulus in which the spatial frequency is highest in the center and continuously decreasing in each direction toward the periphery (see Figure 17A). Although Watson's formula includes a different set of parameters for each meridian, PERG stimuli must be symmetrical so as to provide the same net luminance in each direction. Therefore, the same formula was used for each meridian so that the changes in spatial frequency would be consistent in each direction, ensuring that there would be no difference in the size of the bars (spatial frequency) based on meridian and therefore no net change in luminance when the contrast reverses. To accommodate

this need, all of the values that were specific to each meridian were averaged to model the average change in RGCf as a function of eccentricity. With these parameters averaged across meridian, RCGf density is defined as

$$d_{gf}(r) = \ 33162.3 \ * \left[0.9869\left(1 \ + \frac{r}{1.043}\right)^{-2} + 0.0131 \exp\left(\frac{-r}{14.5633}\right)\right] \quad (1)$$

where d_{gf} is RGCf density and r is eccentricity in degrees visual angle.

However, to use RGCf density as a means of determining the necessary spatial frequency at a given eccentricity, it must be compared to the RGCf density within the region of a single cycle of spatial frequency at the centermost point of the stimulus. This latter RGCf density measurement can be calculated by

$$spatial\ frequency = \ 33162.3\ /x \quad (2)$$

where x represents the centermost spatial frequency, and 33162.3 is the estimated RGCf density at an eccentricity of 0°. This density found within a single cycle of the centermost spatial frequency must next be compared to the density at eccentricity r that is calculated in Equation 1. This comparison then determines the necessary spatial frequency at eccentricity r as

$$spatial\ frequency\ = \frac{\left\{33162.3 * \left[0.9869\left(1+\frac{r}{1.043}\right)^{-2}+0.0131\exp\left(\frac{-r}{14.5633}\right)\right]\right\}}{\left(\frac{33162.3}{x}\right)} \quad (3)$$

where *x* is the centermost spatial frequency at which the scaling begins. Since this was a novel PERG stimulus that had not previously been tested, the optimal center spatial frequency for this stimulus was unknown. Because of this, I tested a total of eight scaled stimuli, each with the same scaling factor but differing in center spatial frequency (0.394, 0.625, 0.991, 1.57, 2.49, 3.94, 6.25, and 9.91 cpd). These center spatial frequencies were

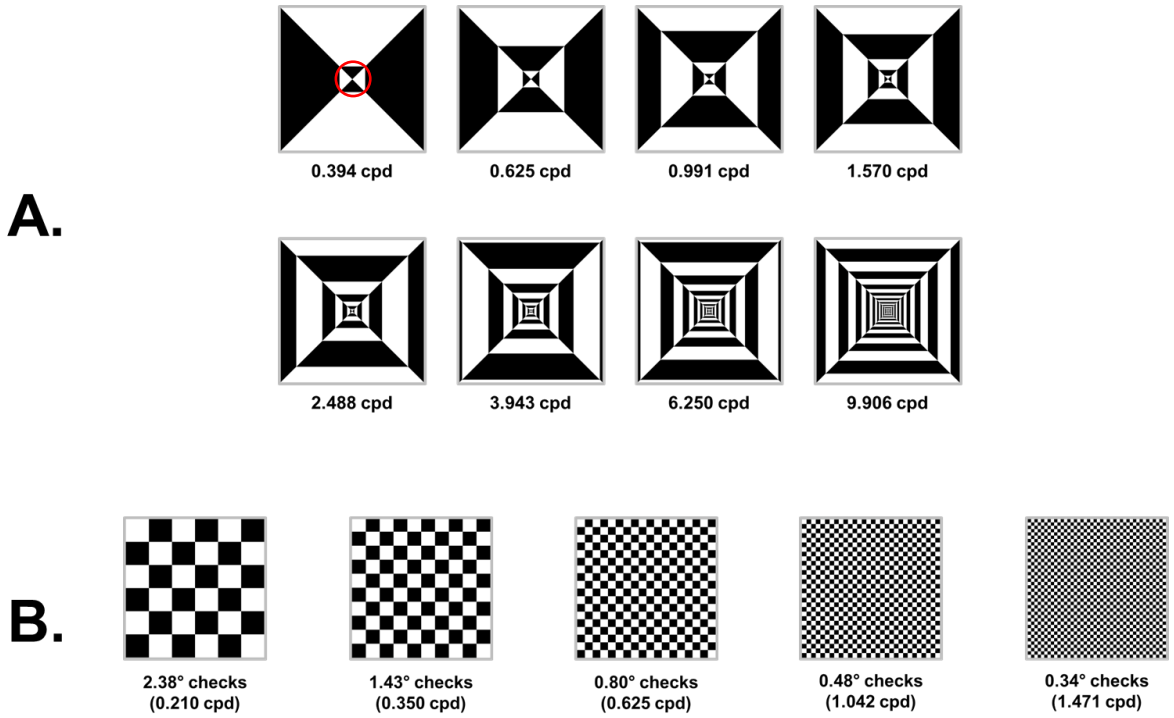

Figure 18. Experiment 2 Stimuli. Responses from PERG stimuli that have been scaled to approximate the proportional changes in RGCf size across the central 14.3° of the retina that is being stimulated (A) will be compared to those from checkerboard stimuli with uniform check sizes of 0.34°, 0.48°, 0.80°, 1.43°, and 2.38° (B). All scaled stimuli use the same scaling factor for the rate of change of spatial frequency, but 8 different center spatial frequencies are compared. (This portion is circled in red for the stimulus that begins at 0.394 cpd.)

determined by moving in increments of 0.2 log steps above and below the standard PERG spatial frequency of 0.625 cpd. (See Figure 18 for all stimuli tested.)

As a control for the efficacy of the spatially scaled stimulus, spatial tuning was also assessed across a series of checkerboards, each of which had a uniform spatial frequency across the stimulus. For the most closely-matched comparison to scaled gratings, responses to five different uniform check sizes of a similar spatial frequency range were compared (0.34°, 0.48°, 0.80°, 1.43°, and 2.38°checks; see Figure 17B for corresponding spatial frequencies), which included the standard PERG checkerboard (0.80° checks). The degree and nature of the spatial tuning curves from both the scaled gratings as well as the checkerboards were compared to assess the effectiveness of scaling the spatial frequency within the stimulus rather than simply changing the uniform spatial frequency across stimuli. Since the scaled stimulus was a hybrid between a grating and a checkerboard pattern, responses from a grating of uniform 0.625 cpd bars (which are spatially equivalent to a 0.8° check size) were also recorded for comparison.

Analyses. Amplitude and implicit time were measured for each response using the same methods as those described in Experiment 1. Also as in Experiment 1, comparisons were only made within each temporal frequency. Implicit time/phase shift was not evaluated inferentially since it was not the measure of interest, but it is reported descriptively for each stimulus used. First, a pair of repeated-measures ANOVAs were used to separately compare response amplitude for checkerboard stimuli and scaled gratings, with each pair consisting of one ANOVA to assess amplitudes of transient responses, and one to assess amplitudes of steady-state responses. Two-way ANOVAs were performed on transient responses to include waveform component (P50 and N95) as

a factor. One-way ANOVAs were performed on steady-state responses since only one amplitude measure was necessary for each waveform. All following pairwise comparisons were made using Holm's procedure to maintain a family-wise error rate of 0.05.

For each of three amplitude measurements (P50, N95, and steady-state), two *t*-tests were conducted. The first of these were used to compare the amplitude between the 0.625 cpd grating and the standard checkerboard to ensure that there was no difference in response amplitude. Based on their interchangeable nature throughout PERG literature, these two stimuli were expected to yield the same amplitude under both transient and steady-state conditions. The second *t*-test therefore compared the highest amplitude found in each of the two stimulus categories (scaled gratings and uniform checkerboards) to determine if one type of stimulus could produce a larger-amplitude response than the other. As employed in Experiment 1 and in the pairwise comparisons of this experiment, Holm's procedure was used to maintain a family-wise error rate of 0.05.

Results. Amplitudes are reported for all Experiment 2 responses in Table 4, and implicit times/phase shifts are reported in Table 5. Upon assessing the P50 and N95 amplitudes from responses to transient checkerboard stimuli through a 2x5 factorial ANOVA, it was found that there was a sphericity violation for the variable of check size, as indicated by Mauchly's Test of Sphericity ($\chi^2(9) = 47.406$, $p < 0.001$). Therefore, degrees of freedom were adjusted to reflect the Greenhouse-Geisser sphericity estimates for this factor ($\varepsilon = 0.511$). There was no main effect of check size ($F(2.045, 40.897) = 2.677$, $p = 0.080$), but as expected, there was a main effect of waveform component ($F(1, 20) = 153.175$, $p < 0.001$).

There was also an interaction between check size and waveform component ($F(4, 80) = 6.412$, $p < 0.001$). Due to the presence of this interaction, simple effects of P50 and N95 were also evaluated via two one-way ANOVAs. Sphericity violations were found for amplitudes as a function of check size both P50 ($\chi^2(9) = 18.831$, $p = 0.027$) and N95 ($\chi^2(9) = 33.379$, $p < 0.001$), so degrees of freedom were corrected to the Greenhouse-Geisser sphericity estimates in both cases (P50 $\varepsilon = 0.700$; N95 $\varepsilon = 0.543$). A simple effect was found in the case of P50 ($F(2.800, 56.000) = 6.395$, $p = 0.001$), but not in the case of N95 ($F(2.174, 43.474) = 2.315$, $p = 0.107$).

For response amplitudes to steady-state checkerboards, a one-way ANOVA was conducted. Similar to the case of the transient 2x5 ANOVA, there was a sphericity violation for check size ($\chi^2(9) = 21.831$, $p = 0.010$) so degrees of freedom were corrected with Greenhouse-Geisser sphericity estimates ($\varepsilon = 0.653$). Unlike the case of transient checkerboard amplitudes, however, there was a main effect of check size for amplitudes of responses to steady-state checkerboards ($F(2.611, 52.218) = 3.148$, $p = 0.039$). After adjusting p-values of pairwise comparisons via Holm's procedure, one such comparison of 0.80 and 2.38 deg check sizes did reach significance ($p = 0.005$, adjusted $\alpha = 0.005$).

Next, separate ANOVAs were conducted to evaluate the effect of spatial tuning in the novel scaled grating stimuli. For transient responses, a 2x8 factorial ANOVA was performed. This yielded no main effect of center spatial frequency ($F(7, 140) = 1.505$, $p = 0.170$), but did yield a main effect of waveform component ($F(1,20) = 56.924$, $p < 0.001$). There was no interaction between these two factors ($F(7, 140) = 1.737$, $p = 0.105$). When this variable of center spatial frequency was assessed in steady-state amplitudes, a sphericity violation was found ($\chi^2(27) = 56.214$, $p = 0.001$) and degrees of

freedom were corrected with Greenhouse-Geisser sphericity estimates (ε = 0.521). This ANOVA showed a main effect of center spatial frequency ($F(3.648, 72.956) = 4.895$, $p = 0.002$), and a difference in amplitude between the center spatial frequencies of 0.394 and 3.943 cpd ($p = 0.001$, adjusted $\alpha = 0.002$). All of the spatial tuning results discussed here are depicted graphically in Figure 19.

To determine if there was a potential difference in the maximum possible amplitude from scaled gratings relative to checkerboards, 3 paired-samples *t*-tests were performed, each of which compared the scaled grating of maximum amplitude for that group to the checkerboard of maximum amplitude. In the case of the transient P50 component, amplitudes from 3.943 cpd scaled gratings ($M = 3.943$, $SD = 0.529$) were compared to those from 0.80 deg checkerboards ($M = 2.512$, $SD = 1.088$), but no difference in amplitude was found ($t(20) = -1.135$, $p = 0.270$). Similarly, when N95 amplitudes were compared between 2.488 cpd scaled gratings ($M = 3.527$, $SD = 0.971$) with those from 0.80 deg checkerboards ($M = 3.895$, $SD = 1.395$), there was no difference found for this component, either ($t(20) = -1.066$, $p = 0.299$). However, when amplitudes from steady-state responses were compared between 6.250 cpd scaled gratings ($M = 0.890$, $SD = 0.271$) and 0.80 deg checkerboards ($M = 1.020$, $SD = 0.220$), the checkerboards were found to yield a larger amplitude ($t(20) = -2.452$, $p = 0.024$). See Figure 18 for spatial tuning curves from both stimulus types for each of the two temporal frequencies.

Since the scaled gratings possess some elements of gratings and some elements of checkerboards, paired-samples *t*-tests were conducted to evaluate the null hypothesis of that there is no amplitude difference between uniform 0.625 cpd gratings and

checkerboards with 0.80 deg check sizes, which are equivalent in spatial frequency. For transient stimuli, P50 amplitudes for the 0.625 cpd gratings (M = 2.389, SD = 0.821) and checkerboards with 0.80 deg checks (M = 2.512, SD = 1.088) were found to be equivalent ($t(20) = -0.653$, $p = 0.521$), as expected. This same result was found when N95 amplitudes from 0.625 cpd gratings (M = 3.432, SD = 0.960) and 0.80 deg checkerboards (M = 3.895, SD = 1.395) were compared ($t(20) = -1.844$, $p = 0.080$). Similarly, no difference in amplitude was found between the steady-state 0.625 cpd grating (M = 1.110, SD = 0.348) and 0.8 deg checkerboard (M = 1.020, SD = 0.220; $t(20) = 1.306$, $p < 0.206$). These results ensure that none of the aforementioned effects were due to the stimulus being more or less similar to one of these two kinds of traditional PERG stimulus designs.

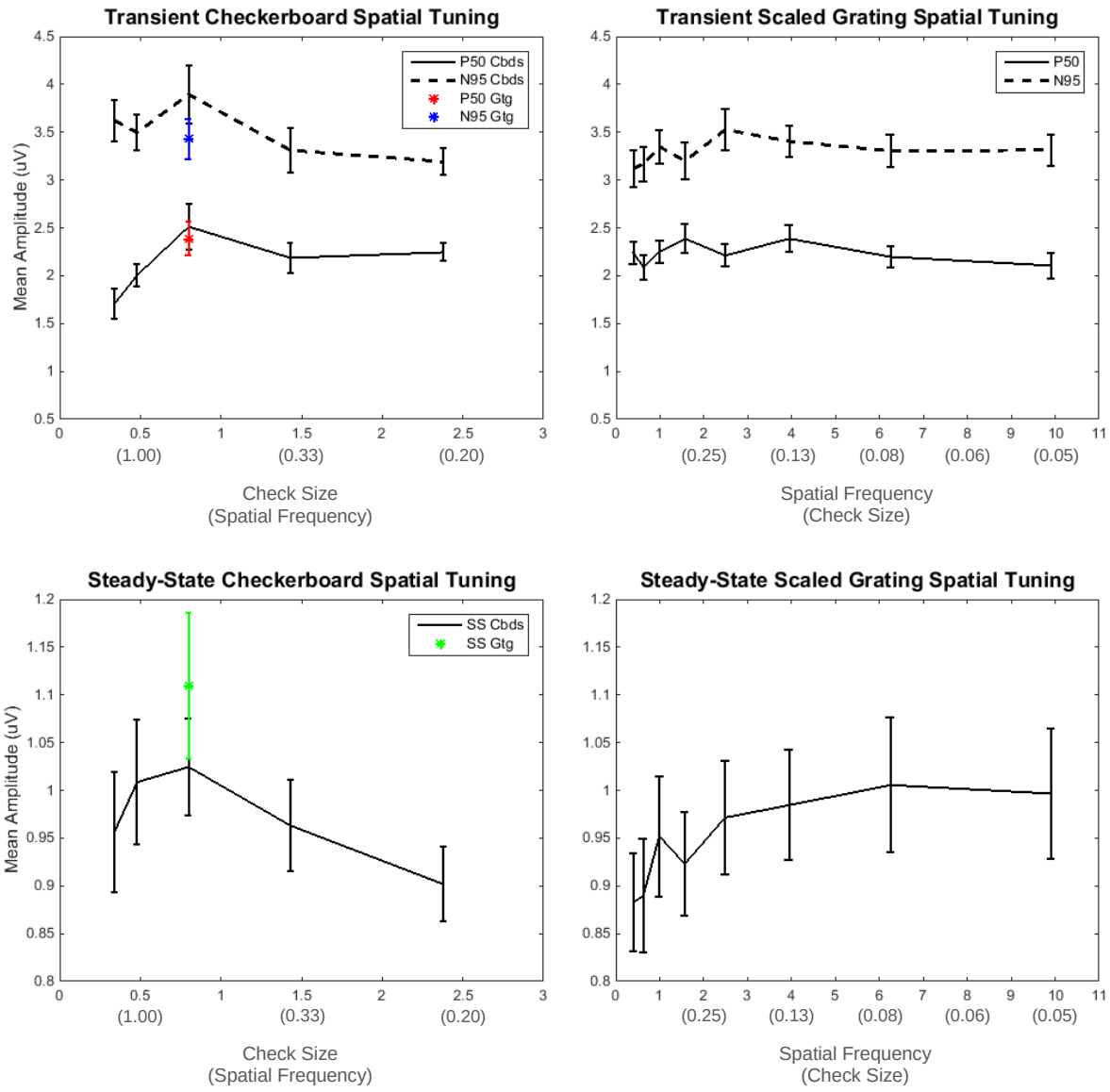

Figure 19. Spatial Tuning Curves for Checkerboard and Scaled Grating Stimuli. Amplitudes for transient (top row) and steady-state (bottom row) responses are plotted as a function of both check size and spatial frequency for uniform checkerboards (left column) and scaled gratings (right column). Also, amplitudes from uniform 0.625 cpd gratings are plotted on the checkerboard spatial tuning curves as a comparison to the 0.80 deg check size. The measure most appropriate for that stimulus type is listed as the top line of the x-axis, and the measure more appropriate for the other stimulus type is listed in parentheses below. Vertical bars represent standard error for that point.

Stimulus Type	SS Amp	P50 Amp	N95 Amp
Uniform Checkerboards			
0.340 deg	0.957±0.063	1.708±0.159	3.621±0.214
0.480 deg	1.009±0.066	2.004±0.116	3.496±0.183
0.800 deg	1.020±0.048	2.512±0.237	3.894±0.304
1.430 deg	0.963±0.048	2.186±0.162	3.310±0.235
2.380 deg	0.902±0.039	2.244±0.093	3.191±0.141
Uniform Grating			
0.625 cpd	1.110±0.076	2.389±0.179	3.432±0.210
Scaled Gratings			
0.394 cpd	0.883±0.051	2.241±0.115	3.120±0.191
0.625 cpd	0.890±0.059	2.085±0.128	3.169±0.180
0.991 cpd	0.952±0.063	2.252±0.116	3.347±0.178
1.57 cpd	0.923±0.054	2.386±0.151	3.198±0.189
2.488 cpd	0.972±0.060	2.211±0.114	3.527±0.212
3.943 cpd	0.984±0.058	2.387±0.138	3.404±0.166
6.250 cpd	1.006±0.070	2.197±0.113	3.303±0.166
9.906 cpd	0.997±0.068	2.105±0.137	3.314±0.162

Table 4. Average Amplitudes for Experiment 2 Stimuli. The average amplitude and standard error (in μV) are reported above for each stimulus tested in Experiment 2. Note that for transient responses, P50 and N95 amplitudes are reported separately. (See Chapter II for details on how amplitude was measured for each temporal frequency category.)

Stimulus Type	SS PS	P50 IT	N95 IT
Uniform Checkerboards			
0.340 deg	29.798±5.063	49.810±2.048	99.190±2.413
0.480 deg	15.826±9.888	49.762±2.065	98.333±2.212
0.800 deg	32.325±10.542	49.143±1.925	96.667±2.218
1.430 deg	27.876±9.886	48.476±2.121	95.429±2.373
2.380 deg	39.493±9.646	46.952±1.884	95.571±2.319
Uniform Grating			
0.625 cpd	85.791±14.899	48.714±1.780	97.857±2.267
Scaled Gratings			
0.394 cpd	114.291±11.193	46.381±1.839	96.619±2.227
0.625 cpd	104.141±14.462	46.000±1.807	95.476±1.891
0.991 cpd	99.815±14.989	46.619±1.907	96.810±2.001
1.57 cpd	95.757±15.769	46.905±1.907	97.714±2.337
2.488 cpd	97.315±13.679	46.095±1.806	96.762±2.003
3.943 cpd	90.720±16.418	47.190±1.768	96.619±1.724
6.250 cpd	99.769±11.173	47.905±1.995	96.952±2.305
9.906 cpd	75.763±17.585	48.286±1.886	94.476±1.908

Table 5. Average Implicit Times and Phase Shifts for Experiment 2 Stimuli. The average implicit times ("IT," in ms) and phase shifts ("PS," in deg) are reported above with their respective standard errors for each stimulus tested in Experiment 2. (See Chapter II for details on how implicit time and phase shift were calculated.)

Summary. Similar to the result from previous literature (as discussed in the beginning of this chapter), varying check size across uniform checkerboards produced mixed results in regards to altering amplitude. For transient responses, only P50 amplitude varied with check size, but N95 was not significantly affected. Like P50 amplitudes, steady-state amplitudes were also influenced by check size. This may suggest that the origins of the P50 component and the steady-state response are more similar to each other than are the origins of the N95 component and the steady-state response. When scaled gratings were used instead of uniform checkerboards, transient responses showed no difference in amplitude as a function of center spatial frequency. Steady-state response amplitude did vary with center spatial frequency, but the small range of amplitudes from the scaled gratings (0.883 to 1.006 μV) makes it unlikely that such scaling is of much practical benefit to employ.

It should be noted that while scaled gratings' center spatial frequencies (and therefore the ranges of spatial frequencies within the stimuli) were varied, the scaling factor remained the same for each of these stimuli so as to reflect the approximate change of RGCf size. Therefore, it is possible that some other scaling factor may optimize the response amplitudes to a greater degree than what was seen here. It is also possible that the windowing effects, produced by the limitations of the stimulus field size, altered the efficacy of the scaling by altering the spatial frequency that fell within the outermost range of the stimulus and comprised its edges. Finally, the continuous changes in spatial frequency across the scaled grating stimuli may be producing fewer effects on amplitude due to the presence of numerous spatial frequencies being presented to each region of the

retina. If this is the case, future investigations may consider definitive regions of differing spatial frequency rather than a continuous change as a function of eccentricity.

Neither transient nor steady-state response amplitudes differed between the 0.80 deg checkerboard and its 0.625 cpd uniform grating counterpart, indicating that the scaled grating amplitudes are not likely to be more heavily influenced by the degree to which these stimuli resemble checkerboards or uniform gratings. Upon comparing the maximum amplitude of the checkerboard responses to that of the scaled grating responses, there was no difference found for P50 or N95, indicating that there is no advantage to using scaled gratings over the traditional checkerboards with respect to amplitude. When this same comparison was made within steady-state responses, the maximum amplitude of the uniform checkerboards exceeded that of the scaled gratings, yielding further evidence that the use of these scaled gratings do not optimize the response. Given these results, it does not appear that scaling stimulus elements for the rate of change of RGCf size has a substantial effect on the response amplitude, at least for the pattern and scaling factors used here. It may also be the case that RGC contributions present in the PERG response are more representative of a single pooled response rather than the summation of individual RGC responses. For further discussion of the possible implications and limitations mentioned in this summary, see Chapter VI.

CHAPTER V

EXPERIMENT 3: MODELING THE PATTERN ELECTRORETINOGRAM IN ADULTS WITH GLAUCOMA

Experiment 3: Testing the Validity of Modeling the PERG in a Patient Population

Hypothesis: In glaucoma patients, simulations of PERG responses from sums of flash increments and decrements will show amplitude decreases proportional to those seen in actual PERG responses from the same patients.

Aim: Using the same modeling techniques as those from Experiment 1, validate the PERG simulation in a glaucoma patient population.

Rationale: As has been previously shown, PERG response amplitude is typically lower in the glaucoma population relative to healthy subjects due to the decrease in RGC functionality (Bach & Hoffman, 2008; Rimmer & Katz, 1989). Since the simulated PERG detailed in Experiment 1 was designed to mimic the same retinal processes that create the PERG response, it was expected that the amplitude of the PERG simulation would be decreased in glaucoma patients by the same proportion as that of an actual PERG response relative to those responses from these patients' healthy age-similar counterparts. The aim to test this hypothesis was therefore to record responses to PERG stimuli as well as flash increments and decrements in both glaucoma population and healthy controls so that PERG responses and simulations can be compared across these two groups. More specifically, the decrease in PERG response amplitude from glaucoma

patients (relative to healthy controls) was compared to the decrease seen between PERG simulations from the two groups.

Procedure. A subset of the procedures from Experiment 1 were replicated in a population of glaucoma patients at the University of Louisville Department of Ophthalmology and Visual Sciences. Criteria for patient selection included those with a diagnosis of primary open angle glaucoma or those who had been identified as glaucoma suspects. Participation was limited to those who did not exhibit any other conditions that had the potential to alter retinal thickness or quality of the image. Additionally, patients were required to have a history of reliable results from visual field testing (specifically, using the Humphrey Visual Field Analysis [HVA] 10-2, 24-2, OR 30-2) as well as an acuity of 20/40 or better in the eye from which the recordings were taken.

All experimental procedures were the same as those described in Chapter II, with the exception of recording responses from checked flash stimuli. These procedures were also employed in a sample of healthy age-similar controls to account for any effects of advanced age that may be seen in this patient sample. These controls were recruited from the population of healthy patients who are visiting the ophthalmology clinic for other concerns or for routine eye exams. Like the glaucoma sample, patients who constituted this control group were required to have an acuity of 20/40 or better in the eye being tested and could not exhibit any other conditions that had the potential to alter retinal thickness or quality of the image. Further, control group participants could not have ocular hypertension or a family history of glaucoma.

Patients recruited to participate in this study as those representative of the glaucomatous population were each categorized into one of four categories based on most

recent diagnosis: glaucoma suspect (GS), mild/early glaucoma, moderate glaucoma, or severe/advanced glaucoma. The resulting data consisted of that from 46 total participants, including 3 glaucoma suspects, 9 mild glaucoma patients, 10 moderate glaucoma patients, 15 severe glaucoma patients, and 9 control patients. Due to such a small number of glaucoma suspects participating, these individuals' data had to be combined with that of another group for inferential analyses. Upon comparing amplitudes and implicit times/phase shifts of PERG and flash data from these patients, it was determined that their data more closely resembled that of the control group relative to that of the mild glaucoma group. By definition, these suspects had experienced no glaucomatous changes at the time of recording, so it seemed that it would still be appropriate to combine their data with that of the 9 control patients, yielding a collapsed control/GS group of 12 individuals. These two collapsed categories will simply be referred to as the control group from this point forward.

In total, there were 34 glaucoma patients (mild, moderate, and severe) who participated, with a mean age of 69.09±1.61 (range, 50-88) years. In regards to racial demographics, this sample consisted of 17 African-American participants, 15 Caucasian participants, 1 Arabic participant, and 1 American Indian participant. The 12 control patients yielded a mean age of 61.00±3.52 (range, 38-81) years, and consisted of 4 African-American observers, 7 Caucasian observers, and 1 Asian-American observer. One eye was assessed for each patient, regardless of diagnostic category.

Analyses. Response amplitudes from PERG stimuli were compared between each category of glaucoma patients (mild, moderate, severe) and the control group for both transient and steady-state conditions via independent *t*-tests, so as to determine which

categories (if any) showed the expected decrease in response amplitude. Further, the same comparisons were also made for amplitudes of averaged best-fit simulations to determine if these simulations yielded the same pattern of results as did the PERG. (Averaged best-fit parameters were based on the group of interest; see Chapter III for methods of calculating these parameters.) Further, the amplitudes of both transient and steady-state b- and d-waves were also compared between the control group and each severity level of the glaucomatous group to determine if these amplitudes were the same between the two groups (as expected), or if they differed.

Since this particular experiment was largely focused on translational value of the PERG simulation, the only simulation of use would be an averaged set of parameters (which created in the averaged best-fit waveforms). Any trends seen in the averaged best-fit amplitudes would be likely to appear in the individual best-fit amplitudes as well, due to the averaged best-fit parameters consisting of the means of individual best-fit parameters. Along the same lines, the averaged best-fit simulations were expected to yield approximately the same amplitudes as the individual best-fit simulations. However, if this was not the case, it could be possible to find different trends in the amplitudes of the individual best-fit simulations, which may change the conclusions made by the results of the model. Therefore, to determine if there was any difference in amplitude between the simulations from averaged best-fit parameters versus those from individual best-fit parameters, a paired-samples *t*-test was conducted for each measure of amplitude (i.e. P50, N95, and/or steady-state) that showed a difference between the control group and any group of glaucoma patients.

To more precisely determine the effect of disease severity on amplitudes of PERG responses and PERG simulations, amplitudes were correlated with the HVA 10-2, 24-2, or 30-2 mean deviation (MD) value for each patient. This value acted as a quantifiable measure of total visual field loss, and therefore could be used as a continuous measure of disease severity. To assess the relationship between disease progression and response amplitude, two sets of correlations were performed for each measure of amplitude that yielded a difference between controls and at least one category of glaucoma patients (as described in the previous paragraph). The first set of these correlations evaluated the relationship between the MD values and the PERG response amplitudes, while the second compared the MD values to the response amplitudes from the averaged best-fit simulations of the PERG. Evaluating these relationships in the case of both the actual PERG response and the PERG response from averaged best-fit parameters led to a clearer understanding of whether the results from the PERG mimicked those from previous literature, and whether the averaged best-fit simulation followed the same trends.

Finally, the potential effect of age was assessed by comparing P50, N95, and steady-state PERG amplitudes that were recorded in young adults from Experiment 1, and older adults in the control group of Experiment 3. Previous literature has suggested that PERG amplitude decreases with age (Porciatti et al., 1989), so it was expected that the young adults who participated in Experiment 1 yielded higher-amplitude PERG responses than the older adults who comprised the control group in the present experiment. To assess this, three paired-sample *t*-tests were conducted to compare P50, N95, and steady-state amplitudes, respectively, between these two groups of participants.

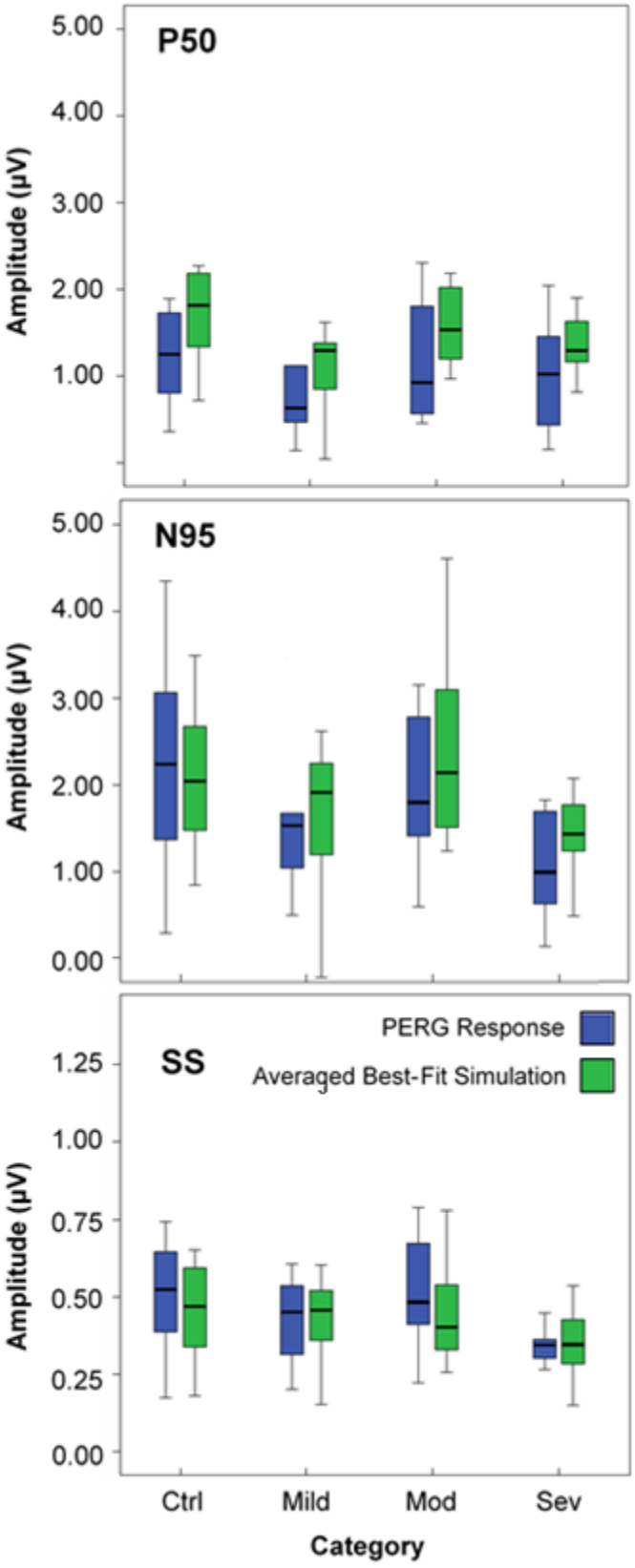

Figure 20. PERG and Best-Fit Amplitudes by Category. P50, N95, and steady-state amplitudes (in microvolts) are shown here for each category. While little difference was seen between patients and controls for the P50 component of transient waveforms, both the transient N95 amplitude and the steady-state amplitude tended to differ somewhat more between the controls and glaucoma patients. These patterns were highly similar between the amplitudes of the PERG and averaged best-fit simulations.

Results. Averaged amplitudes were recorded from all PERG responses, and can be found in the boxplots of Figure 20, with one boxplot per amplitude measurement (P50, N95, SS). As seen in these plots, the averaged PERG amplitude from controls was generally greater than that seen in glaucoma patients. Three *t*-tests assessed this relationship inferentially, with one test being used for each measure of amplitude (P50, N95, and SS). Holm's procedure was used to maintain a family-wise error rate of 0.05 for the three comparisons within each measure of amplitude. In the case of the P50, amplitudes from controls (M = 1.342, SD = 0.791) were the same as those from patients with mild glaucoma (M = 1.113, SD = 1.104; $t(19) = 0.556$, $p = 0.585$, adjusted $\alpha = 0.025$), moderate glaucoma (M = 1.414, SD = 1.287; $t(20) = -0.160$, $p = 0.874$, $\alpha = 0.05$), and severe glaucoma (M = 0.997, SD = 0.629; $t(25) = 1.266$, $p = 0.217$, adjusted $\alpha = 0.017$). In other words, for P50 there was no significant difference between the control group or any of the glaucoma groups.

Similarly, when N95 amplitudes were compared, the control population (M = 2.201, SD = 1.182) yielded no difference in amplitude relative to individuals with either mild (M = 1.719, SD = 1.081, $t(19) = 0.959$, $p = 0.350$, adjusted $\alpha = 0.025$), moderate glaucoma (M = 1.960, SD = 0.859, $t(20) = 0.536$, $p = 0.598$, $\alpha = 0.05$), or severe glaucoma (M = 1.198, SD = 0.887; $t(25) = 2.522$, $p = 0.018$, adjusted $\alpha = 0.017$). However, the boxplots show a trend for decreasing amplitude as a function of glaucoma severity, and if a single test had evaluated the difference in PERG amplitude between the control group and the group of patients with severe glaucoma, the amplitudes from the control group would have been seen as significantly larger due to the alpha value being 0.05 rather than 0.017. This was not the case due to correcting for multiple comparisons,

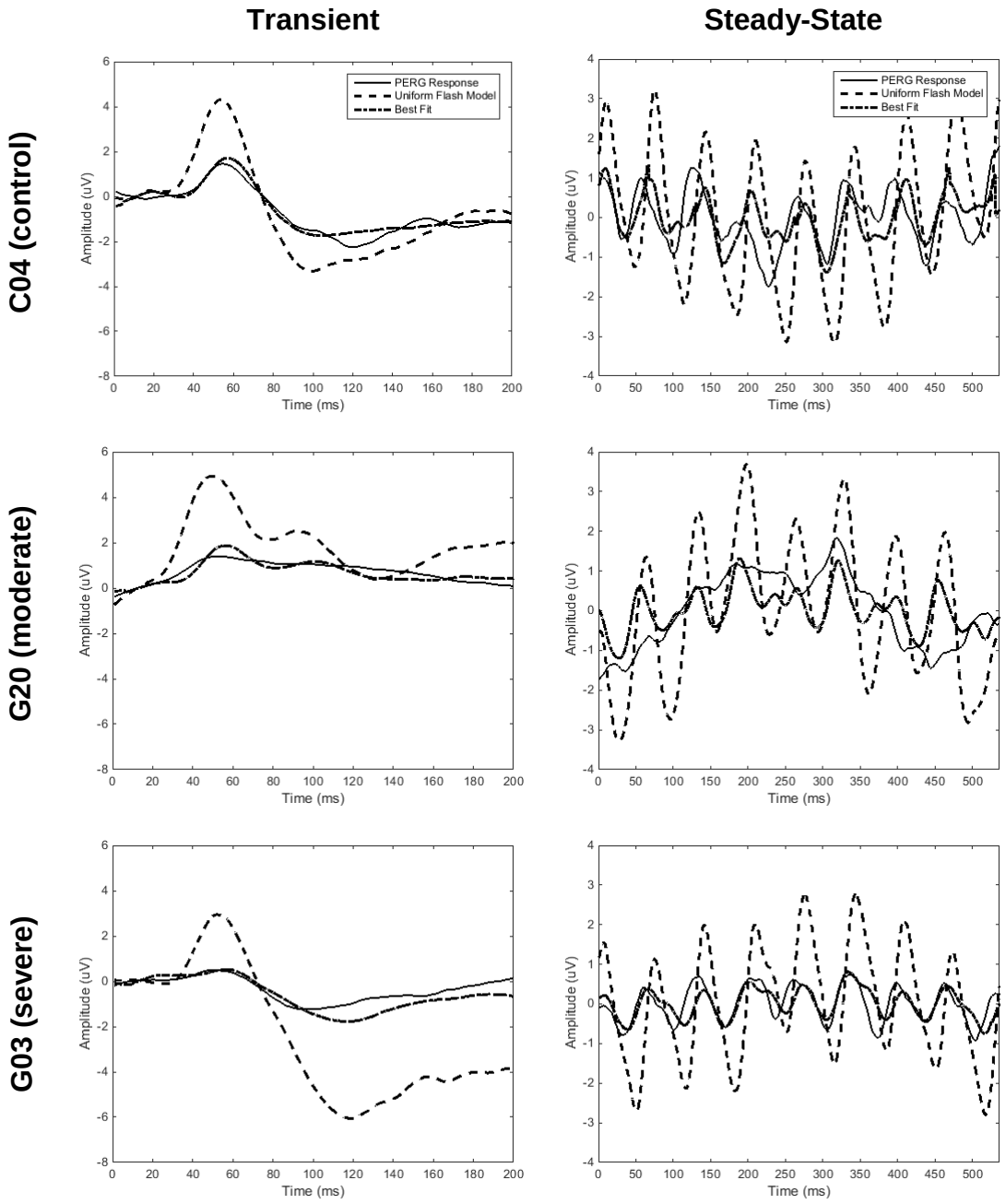

Figure 21. Comparisons of Experiment 3 PERG Responses and Simulations. Samples of individual data are shown from three representative subjects, in response to both transient stimuli (left) and steady-state stimuli (right). One subject was from the control group (C04), one was from the group with moderate glaucoma (G20), and another was from the group with severe glaucoma (G03). The amount of time shift (ΔT), b-wave scaling (b_{amp}), and d-wave scaling (d_{amp}) that was employed to create the best fit for each subject is shown in the bottom left of each graph. Negative ΔT values represent the b-wave beginning before the start of the d-wave, and positive values represent the b-wave starting after the beginning of the d-wave.

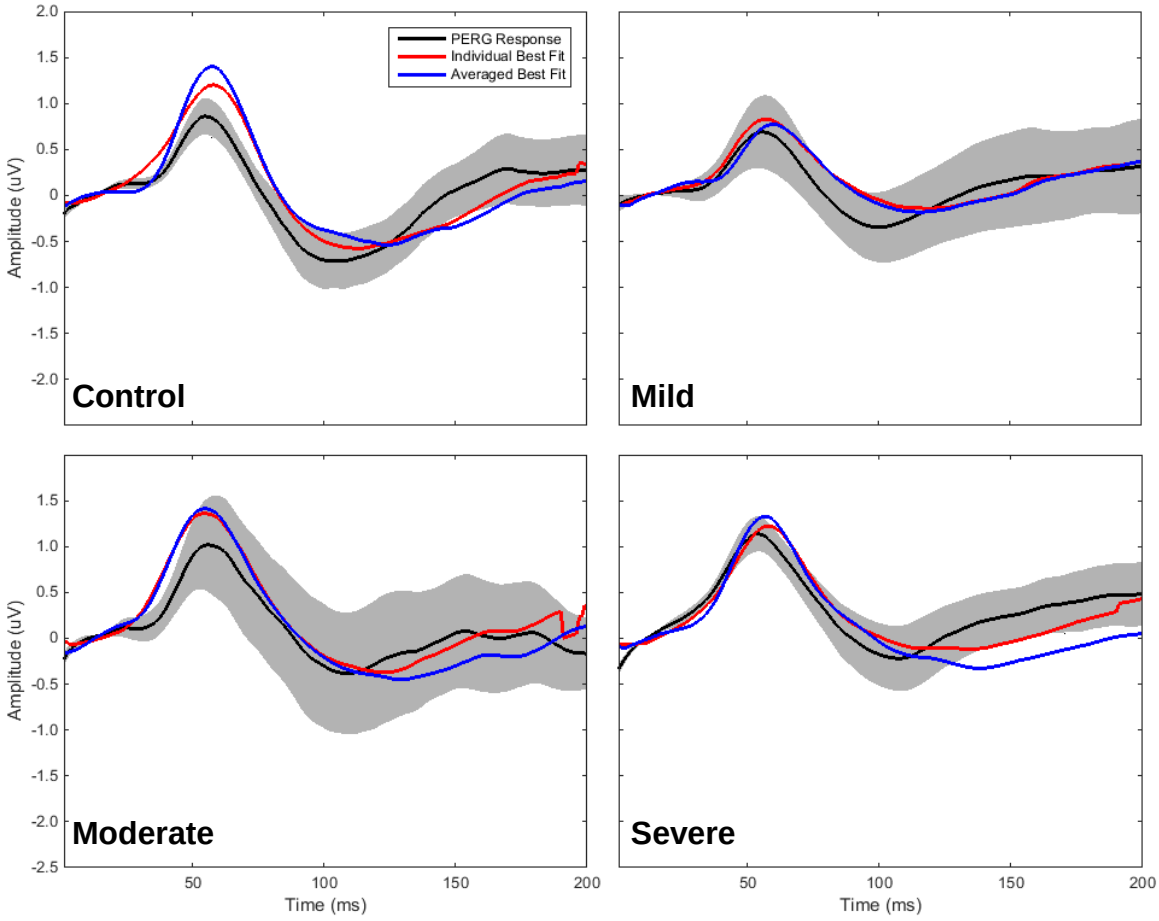

Figure 22. Comparisons of Experiment 3 Averaged Transient PERG Responses and Simulations. For each of the four participant groups of Experiment 3 (control, top left; mild, top right; moderate, bottom left; severe, bottom right), three waveforms are shown which represent the average of all of that group's participants' transient PERG responses (solid black line), individual best-fit simulations (solid red line), and averaged best-fit simulations (solid blue line). Each of these waveforms are shown on top of the 95% confidence interval for the PERG response (gray fill) to see how the averaged simulations compare to the variability of the PERG response. Note that the averages of the individual best fits (red) and the averaged best fits (blue) are often quite similar in each group, suggesting that it may be possible to find a set of common modeling parameters that successfully minimize the degree of error in the model across participants in each of the four categories shown here.

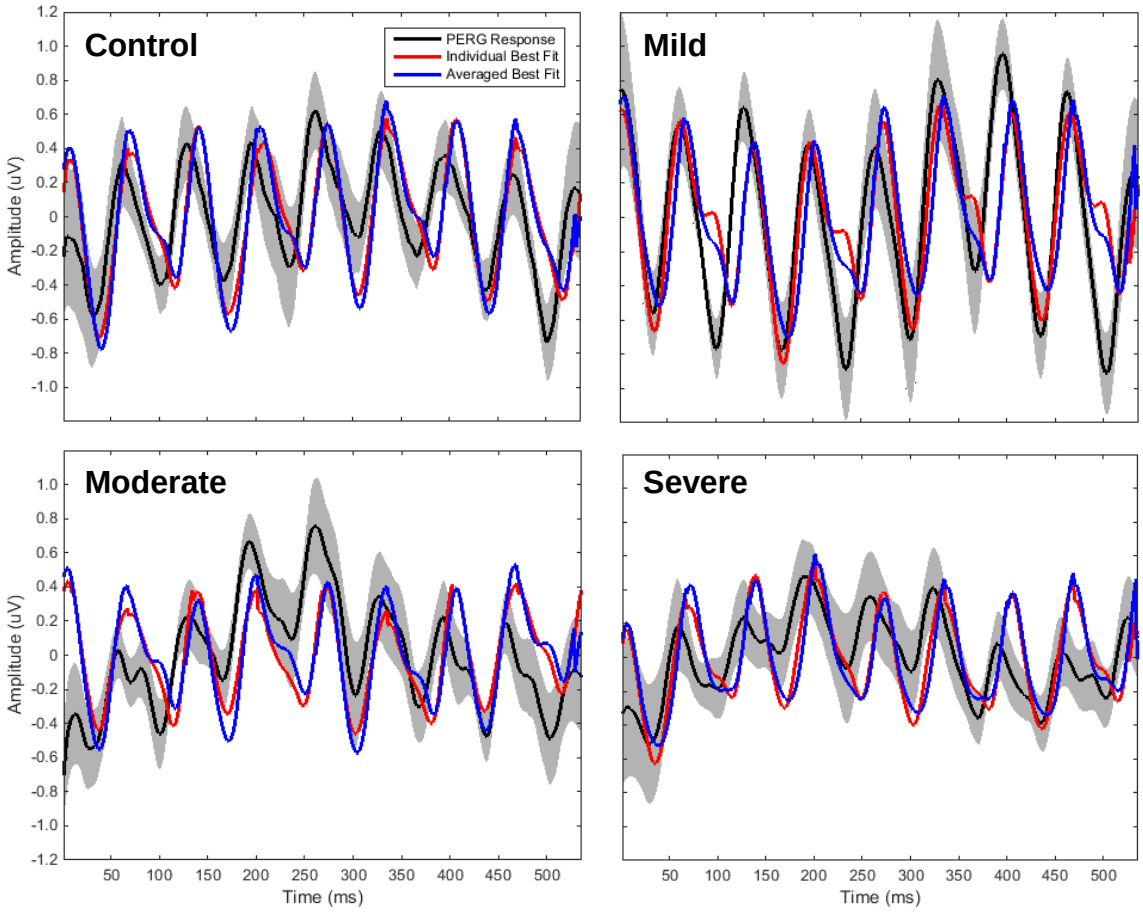

Figure 23. Comparisons of Experiment 3 Averaged Steady-State PERG Responses and Simulations. For each of the four participant groups of Experiment 3 (control, top left; mild, top right; moderate, bottom left; severe, bottom right), three waveforms are shown which represent the average of all of that group's participants' steady-state PERG responses (solid black line), individual best-fit simulations (solid red line), and averaged best-fit simulations (solid blue line). Each of these waveforms are shown on top of the 95% confidence interval for the PERG response (gray fill) to see how the averaged simulations compare to the variability of the PERG response. Note that like the averaged transient responses and simulations shown in Figure 22 the averages of the individual best fits (red) and the averaged best fits (blue) are often quite similar in each group, suggesting that it may be possible to find a set of common modeling parameters that successfully minimize the degree of error in the model across participants in each of the four categories shown here.

however. Upon assessing intrasubject variability from the N95 averaged best-fit amplitude data from control subjects ($\sigma_2 = 0.689$) and the patients with severe glaucoma ($\sigma_2 = 0.426$) shown here, an effect size of $f = 0.474$ resulted for $\alpha = 0.05$ and $\beta = 0.95$. Based on this effect size, a minimum of 94 total participants would be needed to show a significant difference between the N95 averaged best-fit amplitudes of these two groups. Therefore, although a large database may potentially show a significant difference between these two groups, it seems that the averaged best-fit simulation is not as sensitive of a measure as the PERG recording to detect N95 amplitude differences between these groups.

In evaluating steady-state PERG amplitudes, those from the control group (M = 0.573, SD = 0.305) were found to be no different relative to the group of mild (M = 0.411, SD = 0.154; $t(19) = 1.445$, $p = 0.165$, adjusted $\alpha = 0.025$) and moderate (M = 0.505, SD = 0.195; $t(20) = 0.600$, $p = 0.555$, $\alpha = 0.05$) glaucoma patients. However, when

	Transient			***Steady-State***		
Group	**TS**	**b %**	**d %**	**TS**	**b %**	**d %**
Control	2±1.67	30±2.82	35±4.06	-6±2.08	25±0.00	30±2.20
All Glaucoma	2±1.13	30±1.42	40±3.44	-4±1.19	25±0.49	30±1.32
Mild	6±1.82	25±0.00	45±8.01	-4±2.29	25±1.67	30±2.89
Moderate	0±2.11	30±3.88	45±8.23	-8±1.96	25±0.00	30±2.79
Severe	2±1.81	30±1.90	35±2.89	-2±1.91	25±0.53	30±1.84

Table 6. Averaged Best Fit Parameters by Category. Averaged time-shift ("TS", in milliseconds), b-wave weightings, and d-wave weightings are reported for each category of participants, along with their respective standard errors. Note that there is little variation between averaged best-fit parameters for patients in the control group versus those with glaucoma. Similarly, there was little variation across averaged best-fit parameters as a function of severity.

steady-state PERG amplitudes were compared between the control group and those with severe glaucoma ($M = 0.347$, $SD = 0.121$), the amplitudes from the control sample were found to be larger relative to these patients in the advanced stage of this disease ($t(25) = 2.621$, $p = 0.015$, adjusted $\alpha = 0.017$). Based on these results, it seems that the steady-state PERG was indeed found to be more sensitive to disease progression relative to the transient PERG.

To determine if the averaged best-fit simulations would follow these same trends, three additional sets of three *t*-tests compared the amplitudes of simulations from the control group to each category of glaucoma patients. (To see the averaged best-fit parameters for each group, see Table 6.) Similar to the results from PERG amplitude comparisons, P50 showed no difference in amplitude between the control group ($M = 1.715$, $SD = 0.509$) and those with mild ($M = 1.199$, $SD = 0.761$; $t(19) = 1.862$, $p = 0.078$, adjusted $\alpha = 0.025$) moderate ($M = 1.668$, $SD = 0.683$; $t(20) = 0.184$, $p = 0.856$, $\alpha = 0.05$), or severe glaucoma ($M = 1.362$, $SD = 0.337$; $t(18.297) = 2.067$, $p = 0.053$, adjusted $\alpha = 0.017$). The latter of these three tests showed that the assumption of homogeneity of variance between groups had been violated, as indicated by Levene's test ($F = 5.165$, $p = 0.032$), so degrees of freedom were adjusted accordingly.

In a similar manner, there were no differences in N95 amplitude found for these averaged best-fit simulations when the control group ($M = 2.134$, $SD = 0.830$) was compared to the group of patients with mild ($M = 1.533$, $SD = 0.979$; $t(19) = 1.520$, $p = 0.145$, adjusted $\alpha = 0.025$), moderate ($M = 2.352$, $SD = 1.043$; $t(20) = -0.547$, $p = 0.590$, $\alpha = 0.05$), or severe glaucoma ($M = 1.525$, $SD = 0.653$; $t(25) = 2.134$, $p = 0.043$, adjusted $\alpha = 0.017$). As in the case of the N95 PERG amplitudes, there would, in fact, be a

difference found between the control group and severe glaucoma patients if it were the only test evaluated, indicating that a similar trend may be taking place in these simulations. Upon assessing intrasubject variability from the N95 amplitude data from control subjects ($\sigma^2 = 1.397$) and the patients with severe glaucoma ($\sigma^2 = 0.787$) shown here, an effect size of $f = 0.747$ resulted for $\alpha = 0.05$ and $\beta = 0.95$. Based on this effect size, a minimum of 40 total participants would be needed to show a significant difference between the N95 amplitudes of these two groups.

The final set of three tests compared amplitudes from steady-state averaged best-fit simulations from the control group to each severity level of glaucoma. Similar to the results from PERG amplitude comparisons, the amplitudes from averaged best-fit simulations from the control group ($M = 0.455$, $SD = 0.158$) did not differ from those in

Waveform	Control	Mild	Moderate	Severe
Transient				
b-wave	3.40±0.52	2.70±0.71	2.85±0.40	2.83±0.22
d-wave	2.29±0.29	1.76±0.30	1.93±0.35	1.85±0.21
Steady-state				
b-wave	2.13±0.21	1.67±0.19	1.77±0.14	1.61±0.13
d-wave	1.06±0.16	1.02±0.12	0.98±0.14	1.03±0.11

Table 7. Flash Amplitudes of Controls and Glaucoma Patients. Amplitude comparisons were made between the control group and each category of the glaucoma patients in this study (mild, moderate, severe), with transient and steady-state b- and d-waves being assessed. Since Holm's procedure was used in each set of *t*-tests (each row of this table), each *p*-value denotes which alpha value was used for comparison via the superscripted daggers. As seen in previous literature, no amplitude differences were found for any of these comparisons.

the mild (M = 0.421, SD = 0.144; $t(19) = 0.506$, $p = 0.619$, adjusted $\alpha = 0.025$) or moderate (M = 0.438, SD = 0.151; $t(20) = 0.249$, $p = 0.806$, $\alpha = 0.05$) glaucoma categories. However, unlike the findings from PERG comparisons, there was no difference in amplitude found between the simulations from the control group and those with severe glaucoma (M = 0.346, SD = 0.110; $t(18.919) = 2.026$, $p = 0.057$, adjusted $\alpha = 0.017$). The degrees of freedom employed in this test were adjusted from 25 to 18.919 based on the results from Levene's test, which indicated that the assumption of homogeneity of variance had been violated ($F = 5.370$, $p = 0.029$). All of the amplitudes from averaged best-fits can also be seen in the boxplots of Figure 20.

Although previous literature has shown PERG amplitude differences between populations of control patients and glaucoma patients, it has generally shown that no significant differences in flash ERG amplitudes exist between these two groups (Bach & Hoffman, 2008). To determine if the current work reflected this idea, both b-wave and d-wave amplitudes were compared between controls and glaucoma patients, with Holm's procedure being employed within each temporal frequency. See Table 7 for a listing of these amplitudes by category (control, mild glaucoma, moderate glaucoma, and severe glaucoma) and their respective standard error values.

For transient stimuli, no difference in amplitude was found between the b-waves from the control group (M = 3.399, SD = 1.810) and those from patients with mild (M = 2.704, SD = 2.116; $t(19) = 0.810$, $p = 0.428$, adjusted $\alpha = 0.025$), moderate (M = 2.852, SD = 1.277; $t(20) = 0.801$, $p = 0.433$, $\alpha = 0.05$), or severe glaucoma (M = 2.834, SD = 0.844; $t(14.807) = 0.996$, $p = 0.335$, adjusted $\alpha = 0.017$). The latter of these three tests did not display homogeneity of variance according to the results of Levene's test ($F = 6.076$,

$p = 0.021$), and therefore required that its degrees of freedom be adjusted. Transient d-waves yielded the same pattern, with the control group ($M = 1.060$, $SD = 0.569$) yielding the same amplitude as that seen in mild ($M = 1.756$, $SD = 0.895$; $t(19) = 1.275$, $p = 0.218$, adjusted $\alpha = 0.017$), moderate ($M = 1.932$, $SD = 1.097$; $t(20) = 0.807$, $p = 0.429$, $\alpha = .05$), and severe glaucoma patients ($M = 1.852$, $SD = 0.825$; $t(25) = 1.259$, $p = 0.220$, adjusted $\alpha = 0.025$).

In the case of steady-state b-waves, amplitudes from control patients ($M = 2.134$, $SD = 0.738$) were also found to be the same as those from glaucoma patients with mild ($M = 1.672$, $SD = 0.568$; $t(19) = 1.561$, $p = 0.135$, adjusted $\alpha = 0.025$), moderate ($M = 1.774$, $SD = 0.441$; $t(20) = 1.354$, $p = 0.191$, $\alpha = 0.05$), and severe forms of the disease ($M = 1.615$, $SD = 0.496$; $t(25) = 2.183$, $p = 0.039$, adjusted $\alpha = 0.017$). Similarly, steady-state d-wave amplitudes did not differ between the control group ($M = 1.060$, $SD = 0.569$) and patients with mild ($M = 1.025$, $SD = 0.352$; $t(19) = 0.163$, $p = 0.873$, $\alpha = 0.05$), moderate ($M = 0.984$, $SD = 0.442$; $t(20) = 0.343$, $p = 0.735$, adjusted $\alpha = 0.017$), or severe glaucoma ($M = 1.028$, $SD = 0.437$; $t(25) = 0.168$, $p = 0.868$, adjusted $\alpha = 0.025$). These findings of no differences in flash ERG amplitude between the control group and glaucoma patients reinforces the idea purported in previous literature that flash ERG measurements are generally left unaffected in patients with glaucoma.

Given that the modeling parameters for the averaged best-fit simulations were created by calculating the means of the modeling parameters for individual best-fit simulations, it was expected that the simulations produced by these two sets of parameters should be highly similar. More specifically, it was expected that these two types of simulations would yield simulations of equal amplitude. This assumption was of

particular importance for the components of the PERG for which there was a difference in amplitude found between the control group and any category of glaucoma patients. Since both N95 and steady-state amplitudes were found to differ between the control group and glaucoma patients, each was assessed in its own paired-samples *t*-test to determine if that measure differed between the individual best-fit simulations and the averaged best-fit simulations across all participants.

When N95 amplitude was compared between the averaged best-fit simulations (M = 1.865, SD = 0.906) and the individual best-fit simulations (M = 1.805, SD = 0.929), no difference was found ($t(45) = 0.849$, $p = 0.400$). Similarly, no difference in steady-state amplitude was found between the averaged best-fit simulations (M = 0.409, SD = 0.142) and the individual best-fit simulations (M = 0.399, SD = 0.139; $t(45) = 1.043$, $p = 0.303$). These results confirm that the averaged set of modeling parameters are sufficient to achieve the same results as those seen from individualized parameters, and that individualized parameters are therefore unnecessary. Examples of individual data can be found in Figure 21, and examples of averaged waveforms can be found in Figures 22 and 23.

Since steady-state PERG amplitudes were found to differ between the control group and glaucoma patients, these amplitudes were correlated with MD values (as seen in Figure 24) to determine if there was a relationship between the amplitude in question and disease severity. Upon assessing this relationship between MD values (M = -7.386, SD = 8.020) and steady-state PERG amplitude (M = 0.411, SD = 0.164), amplitude was found to increase with MD values ($r(33) = 0.386$, $p = 0.024$), indicating that more severe cases of glaucoma yielded lower-amplitude responses. Since the transient N95

component also showed the potential for a difference in PERG amplitude between the control population and patients with glaucoma, MD values were also compared to N95 amplitudes ($M = 0.457$, $SD = 0.996$), revealing that the more severe cases of glaucoma yielded lower-amplitude PERG responses in this case, as well ($r(33) = 0.457$, $p = 0.007$). To determine whether or not the simulated PERG showed these same trends, MD values were also correlated with these amplitude measurements from the averaged best-fit simulations. In the case of these simulations, however, neither N95 ($M = 1.770$, $SD = 0.925$; $r(33) = 0.287$, $p = 0.100$) nor steady-state amplitudes ($M = 0.393$, $SD = 0.135$; $r(33) = 0.192$, $p = 0.276$) were correlated with MD values, indicating that this model is not likely to be useful to track disease progression.

In addition to assessing the effects of glaucoma, the effects of age were also evaluated by comparing PERG amplitudes from the young adults who participated in Experiment 1 to the older adults who participated as control subjects in the present experiment. Within transient PERG responses, young adults ($M = 2.828$, $SD = 0.986$) yielded larger-amplitude responses than the older adults in the control group of Experiment 3 ($M = 1.144$, $SD = 0.574$; $t(47) = 5.622$, $p < 0.001$, adjusted $\alpha = 0.025$). Similarly, the N95 component of transient PERG responses was also larger in the young adults ($M = 4.684$, $SD = 1.632$) relative to the older adults ($M = 1.972$, $SD = 1.191$; $t(47) = 5.298$, $p < 0.001$, $\alpha = 0.050$). The same was also true for steady-state amplitudes, with those from the younger adults ($M = 1.099$, $SD = 0.413$) being greater than those from the older adults ($M = 0.518$, $SD = 0.160$; $t(45.249) = 7.064$, $p < 0.001$). Note that the degrees of freedom in the steady-state comparison were adjusted to account for a lack of

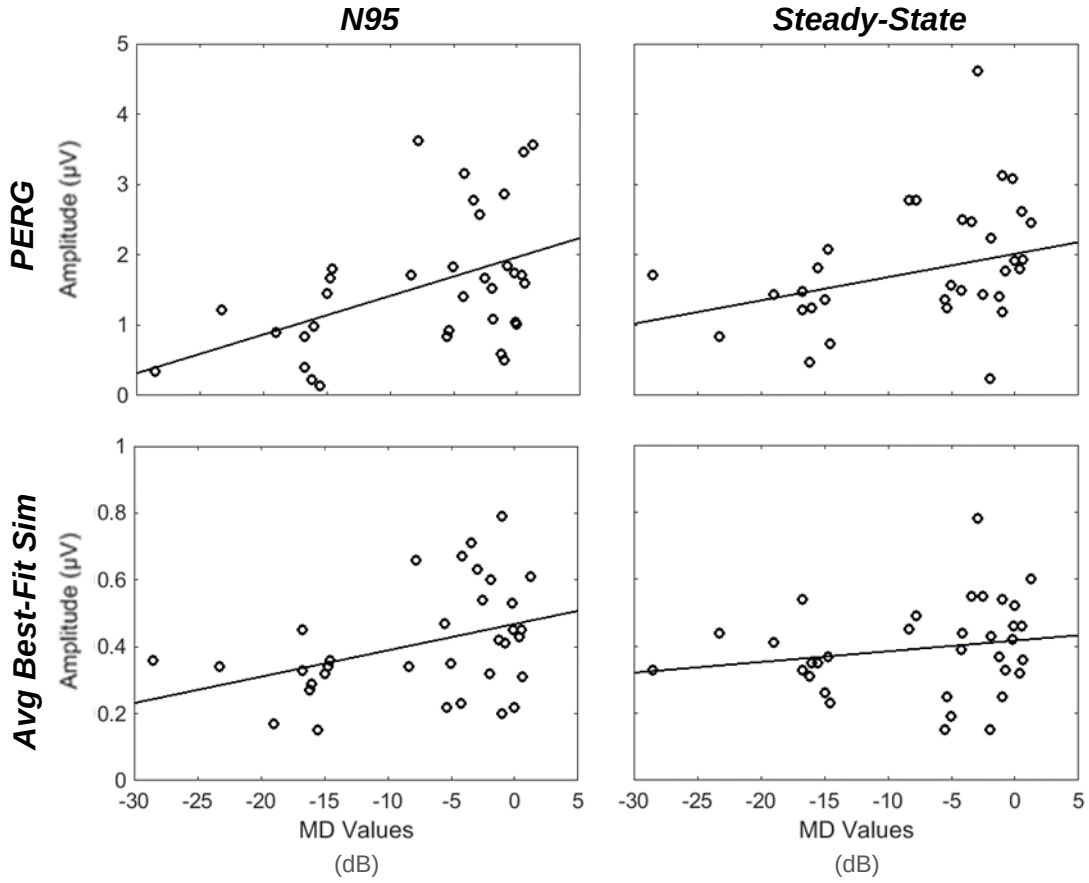

Figure 24. N95 and Steady-state Amplitudes as a Function of MD Values. Both N95 and steady-state response amplitudes are plotted here for both the actual PERG and the averaged best-fit simulation. Each of these measures is shown as a function of mean deviation (MD) values, which can be thought of as a continuous measure of disease severity. Lower values indicate more severe cases of glaucoma. Correlations were conducted for each of these two amplitude measurements, as described in the text. Based on those results, MD values were significantly correlated with each of the PERG amplitudes measures, but not with either of the averaged best-fit amplitude measures.

homogeneity of variance, as detected by Levene's test for Equality of Variances ($F(1,47) = 6.720$, $p = 0.013$).

Summary. As seen in previous literature (Bach & Hoffman, 2008), PERG amplitude tends to be lowered in glaucoma patients relative to control subjects, with steady-state amplitude being more sensitive to this difference than transient amplitude. In the present work, this same trend was generally supported, as steady-state PERGs were of

lower amplitude in patients with severe glaucoma relative to the control population. Although there was no significant difference in transient PERG amplitude found between the control group and any of the categories of glaucoma patients due to the number of tests conducted, it appeared highly likely that N95 would have shown lowered amplitude for patients with severe glaucoma relative to the control group, had a greater number of participants been involved in the study. Mean deviation (MD) values were recorded for each of the glaucoma patients' HVA 10-2, 24-2, or 30-2 assessments. These measurements described the average amount by which each patient's visual field differed from that of the norm for his or her age, with larger MD values representing lower rates of loss of the visual field. Due to glaucoma severity largely being defined based on visual field loss, MD values were used as a continuous measure of disease progression. When N95 and steady-state PERG amplitudes were correlated with these MD values, both correlations successfully showed that amplitude increased with MD value, indicating that the trends of PERG amplitude in the current work followed those seen in previous literature.

In addition to the PERG, averaged best-fit simulations of the PERG from flash ERG responses were created to determine if they could be employed in clinical practice as an alternative to the PERG itself. In one sense, these results mimicked those of the PERG amplitude comparisons in that they showed no difference when amplitudes from the control group were compared to those from mild or moderate glaucoma patients. However, it was found that neither N95 nor steady-state simulations showed a difference in amplitude between individuals in the control sample versus those in the group of patients with severe glaucoma. However, in the case of N95, the result was similar to that

of the PERG in that the difference would have been significant had only that one comparison been assessed (instead of including mild and moderate comparisons as well), so this result may have been different with more participants. Given that no amplitude difference was found for steady-state simulations, though, it appears that the simulation is not as sensitive to disease progression when compared to the actual PERG. This idea was further supported when no significant correlation was found between MD values and amplitudes from N95 and steady-state simulation.

While PERG amplitude has previously been shown to differ between the control population and the glaucomatous population, flash ERG amplitude has been shown to be left largely unaffected by glaucoma (Bach & Hoffman, 2008). This trend was also found in the present work, as there were no amplitude differences found between the control group and any of the groups of patients with glaucoma for any of the flash ERG measures. This pattern of results was of particular importance in the present work, as the PERG simulations were created from flash ERG responses. Given that there were no differences in flash ERG amplitude between the controls and glaucoma patients, however, it can be implied that any differences in simulation amplitude that were found between the control group and the glaucoma group were not due to a confound of lowered flash ERG responses.

Although it appears possible that the simulation can successfully model the PERG response, whether the simulation will be useful as a clinical tool that could successfully be substituted for the PERG remains inconclusive until a larger subject population can be tested. Based on the power analyses mentioned earlier in the Results section of this chapter, it appears that a rather large dataset of 94 or more people would be needed to

detect differences in N95 amplitude between healthy patients and patients with severe glaucoma based on the effect size found here. Therefore, while it seems that the exact model proposed here would not be highly useful in the clinical detection of glaucoma, given that no differences in amplitude were found between control subjects and those with mild or moderate glaucoma, it may still be useful for monitoring the progression of the disease when tested with a larger database as a means of refining the expected norm for the model in each level of severity. Based on the analysis of age effects between the amplitudes from younger adults of Experiment 1 and the older adults from the control group of the present experiment, it does appear to be necessary to account for age (as well as severity level of glaucoma) when creating such norms.

CHAPTER VI

GENERAL DISCUSSION

Experiment 1: Modeling the Contributions of Luminance and Local Spatial Contrast on PERG Response

One of the most critical questions addressed in this first experiment was whether or not it was possible to develop a predictive model that simulates the PERG waveform by using only ERG responses to flash stimuli. For both transient and steady-state conditions, the PERG was successfully modeled for each individual, accounting for the shape and morphology of the entire waveform rather than merely amplitude and implicit time measurements alone (see Figure 16 for examples of these fitted models). When the parameters of these best-fitting models were averaged across individuals, the averaged best-fit for transient models was the sum of the b-wave scaled down to 35% of its original amplitude and d-wave scaled down by 45%. Time-shifting the b-wave before summing with the d-wave was not found to be useful in this condition. In contrast, the parameters of the averaged best-fit for steady-state conditions showed that the b-wave should be scaled down to 25%, and the d-wave scaled down to 30%. Further, the b-wave should be shifted in time to begin 10 ms prior to the d-wave before summing the two waveforms.

Although there are some differences in the precise scaling factors between the transient and steady-state best-fit parameters, the most substantial difference between these two models is the time-shifting required for steady state responses, but not for transient responses. Based on these results, we can infer that there are differences in the

ON and OFF response kinetics as a function of temporal frequency. More specifically, it appears that the ON and OFF responses respond at approximately the same rate when stimulated by the transient PERG, but respond at quite different rates (with the OFF response being delayed relative to the ON response) when stimulated by the steady-state PERG. Interestingly, these results pair well with the origins of the transient versus steady-state PERG response; according to Luo and Frishman (2011), the transient response seems to be comprised of approximately equal amounts of ON- and OFF-pathway activity, whereas the steady-state response is comprised almost entirely of ON-pathway activity. It may be the case that there is an interaction between the proportion of the PERG response that is driven by each pathway and the relative time point at which each pathway's activity is processed within the PERG response. Since it is not currently understood exactly how these two pathways are combining in the PERG response at large, these best-fit model parameters may provide a glimpse into some of the ways that these pathways interact in the case of each of these two temporal frequency ranges.

In addition to these differences between transient and steady-state simulations, there were also differences found between the P50 and N95 components of the transient simulations. The only comparison that yielded a difference in error for the P50 component was that of the 100% uniform flash simulation versus the checked-flash simulation, with the uniform flash stimuli yielding higher degrees of error. This result implies that halving the amount of luminance present in the stimulation did lead to significantly lower rates of error for the P50 range of the simulation. However, when P50 error was assessed for the last three comparisons (50% scaled uniform flash simulation and checked-flash simulation, averaged best fit and individual's best fit, checked-flash

simulation and individual's best fit), no difference was found in any of these cases. Therefore, it may be the case that P50 error is not affected by the spatial arrangement of the stimulus (since no difference was found between the error from 50% scaled uniform flash simulation and that from the checked-flash simulation) and is not reduced by customizing the parameters of the simulation (since the degree of error from the individual best-fit parameters was not lower than that of the averaged best-fit parameters or the checked-flash simulation).

Despite being part of the same transient simulations, N95 error showed the exact opposite pattern of results. First, there was no difference between the N95 error of the 100% uniform flash and that of the checked-flash simulation, but there was a greater degree of N95 error generated from the checked-flash simulation relative to that of the 50% scaled uniform flash simulation. This discrepancy suggests that N95 may be more highly contingent upon stimulus field size rather than the total amount of luminance presented within that stimulus field. Further, a lower degree of N95 error was found for the individual best-fit simulations relative to the averaged best-fit simulations and the checked-flash simulations. Therefore, it appears that N95 error is generally lessened by customizing these best-fit parameters to each individual, mimicking the results of the holistic transient and steady-state simulations.

All of the previous studies that have attempted to simulate the PERG from flash ERG responses have simply used uniform-flash stimuli, and then scaled down these responses to 50% of their original amplitudes before summing (Arden & Vaegan, 1983; Luo & Frishman, 2011; Simpson & Viswanathan, 2007; Viswanathan et al., 2000). The dogma behind this approach is that each uniform flash is the same size as entire PERG

stimulus, but the PERG stimulus is only presenting half of an increment flash and half of a decrement flash at any given time. Therefore, halving the amplitude of each uniform-flash response is meant to yield b- and d-wave amplitudes that are representative of only half of the stimulation actually provided. When 50% uniform-flash d-waves were compared to checked-flash d-waves, there was no difference in amplitude found between the two groups, supporting this method that had been used in previous studies. However, when this same comparison was made amongst the b-waves from each of these response types, it was found that the b-wave amplitudes from the 50% uniform-flash responses were still greater than those from the checked-flash responses.

Given that these patterns of results for both b- and d-wave held in both transient and steady-state recordings, it suggests there may be a non-linear function that characterizes the amplitude of the b-wave relative to the amount of stimulation present. It is also possible that the difference in spatial layout between the uniform-flash stimuli relative to the checked-flash stimuli is having some effect on b-wave amplitude that would not be present if luminance minimums and maximums were altered instead. Even if that is the case, the checked-flash stimuli mimic the precise arrangement of the PERG stimulus, and are therefore the most appropriate stimuli to use in evaluating this assumption accurately. Regardless of whether it is the difference in the amount of luminance present, the difference in spatial layout, or some combination of the two that is producing this discrepancy in b-wave amplitudes, it is important to acknowledge that the portion of the PERG response originating in ON-pathway activity is not adequately represented in the former method of modeling. Previous results must therefore be reconsidered, as it seems that these simulations used flash responses that were not true

representations of the amount of ON- and OFF-pathway activity generated by the increment and decrement halves of the PERG stimulus, respectively. Instead, these models unintentionally used slightly skewed proportions of these two types of pathway activity, with ON-pathway activity being weighted more heavily.

Since these checked-flash stimuli produce responses that seem to more accurately represent the degree of activity from the ON- and OFF-pathways within the PERG response, the question remains as to why the checked-flash model was not as successful as the individualized best-fit models (as determined by a comparison of error). Given that the checked-flash stimulus was an exact representation of what the PERG stimulus would look like if every other check was a neutral gray that did not reverse, it is unlikely that the stimulus erroneously represented the localized increment and decrement responses in the context of the PERG. Therefore, the only explanation this leaves is that presenting the opposite-polarity checked flashes simultaneously (as in the case of an actual PERG stimulus) rather than independently (as in the case of this experiment) leads to a difference in the way that these increment and decrement responses are combined. It may be the case that after these responses combine simultaneously, another contrast-based gain mechanism is altering the final response that is seen in the PERG recording. If this is the case, such a mechanism may even differ between transient and steady-state conditions; several participants' best fits for steady-state stimuli were the checked-flash stimulations, but this was not the case for any participants' best fits under transient conditions.

Experiment 2: Optimizing the PERG Stimulus Based on a Model of Retinal Ganglion Cell Receptive Field Size

As detailed in Chapter I, spatial variation of the PERG stimulus has yielded many different effects on response amplitude across the studies that have assessed this variable. In addition to the novel scaled gratings, the present work utilized one of the most common stimulus choices that has been previously used to assess the potential role of spatial tuning in the PERG response: uniform checkerboards of varying check sizes. Interestingly, this experiment yielded an effect of check size for both the steady-state response and the P50 component of the transient response, but not for the transient response's N95 component. This is directly in contrast with several studies that have shown N95 to be the more likely component to exhibit spatial tuning relative to P50 (Berninger & Schuurmans, 1985; Korth & Rix, 1985; Wu et al., 1992). However, each of these studies only employed two to five participants total, while the present study evaluated spatial tuning curves of 21 participants, providing a more robust representation of the general population relative to these smaller sample sizes. Further, in each of these previous studies, the P50 component still displayed some degree of spatial tuning despite the effect of check size not being quite as drastic as that seen for N95.

When spatial tuning was found in previous literature, the function was typically bandpass in nature (Arden & Vaegan, 1983; Porciatti et al., 1989; Thompson & Drasdo, 1989). This function was seen in the present work's steady-state responses as well, and somewhat in the P50 component of the transient responses (though the P50 spatial tuning curve follows a pattern that is somewhat borderline between a low-pass function and a bandpass function). Since this pattern of results generally characterized both the steady-

state and P50 amplitudes as a function of check size, the question of why these two responses follow roughly the same pattern naturally arises.

As reviewed in Chapter I, macaque monkey data have shown that both the P50 component and steady-state response are largely driven by luminance-based activity, while the N95 component seems to be exclusively driven by spiking activity (Luo & Frishman, 2011). This is puzzling in light of the current results, since spatial tuning in the PERG is generally thought to reflect the properties of the ganglion cells known to drive the PERG response. However, it may be the case that differences in localized luminance responses are causing many of the effects seen from varying check size, given that the resulting PERG waveform is partially dependent upon luminance-based information for both the P50 component and the steady-state response (Luo & Frishman, 2011). This idea is discussed further in a subsequent part of this section.

In the case of the scaled gratings, there was an effect of center spatial frequency for steady-state responses, but not for transient responses. To determine whether uniform checkerboards or scaled gratings should be used to optimize the steady-state response, the stimulus from each category that elicited the highest-amplitude response of that category was identified, and these two response amplitudes were compared. Upon doing so, it was found that most optimized response from uniform checkerboards (0.80 deg checks) yielded a greater amplitude than that of the most optimized response from scaled gratings (6.250 cpd). Therefore, although the goal of employing the scaled stimuli was to optimize the response beyond the capability of the uniform checkerboard, the scaled gratings could not produce as large of a response as could the uniform checkerboards for the one kind of PERG response in which spatial tuning was found.

Although these results indicate that the scaled gratings have failed in their original intent of optimizing the PERG response, the fact that this optimization did not occur in either temporal frequency category may provide further insight into the general nature of the PERG response. Given that these scaled gratings utilized a scaling factor that was based on the change in RGCf size as a function of eccentricity, it appears that scaling individual stimulus elements at the rate of RGCf size change is not the most ideal choice for a PERG stimulus. There are several possible reasons why this may be the case. First, it is possible that the scaling factor used was simply incorrect or, at least, not optimal.

Given the anatomical basis, accountability of the displacement zone at the fovea, and success of the this scaling factor as applied to psychophysical paradigms (Watson, 2014), it is unlikely that the scaling factor itself is erroneous enough to completely alter the results of the present work. It should be noted, however, that the original scaling factor differed slightly by meridian, but that those parameters had to be averaged to create the scaled gratings since the PERG stimulus must be symmetrical to maintain a constant net luminance. Within the eccentricity range used for the current stimulus field sizes, though, the differences across these meridians were quite minimal and are therefore unlikely to substantially change the amplitudes seen here. However, it should also be noted that the actual stimulus field sizes predicted by the Watson data were not equal to the sizes of the individual stimulus elements within the scaled gratings from this experiment. Instead, the rate of change of stimulus field size was the factor used to create these gratings. Although it is unlikely that stimulus elements should be the literal size of the receptive fields they stimulate the PERG stimulus, it is still possible that using only the rate at which these sizes changed acted a limitation in the current work.

If the factor used to scale the gratings in the present work correctly reflected the rate of change of RGCf size as intended, it may still be the case that the scaling factor would not optimize the stimulus response if it was not the most appropriate measure to use for scaling. Since the PERG is known to largely be driven by RGCs, and RGCs are known to exhibit spatial tuning, it has been assumed that the spatial tuning seen in the PERG is the result of collective spatial tuning across the RGCs that are being stimulated. While this may certainly be the case, it is also possible that other cellular activity reflected in the PERG response is either partially or entirely responsible for the response's spatial tuning., and may also help to explain why there has been so much variability seen in past literature that aimed to assess the spatial tuning of the PERG. Even if all of the parameters that would affect RGC responses were controlled for across these studies, there are many other variables (i.e. luminance, precise temporal frequency, etc.) that may differentially affect other cells that contribute to the PERG response.

As previously discussed, spatial tuning was found for steady-state responses and transient P50 responses when uniform checkerboards were viewed, further supporting this possibility. If these earlier processes are heavily influenced by an interaction between size of the local response and its location on the retina, then differences in net response amplitude could easily be misconstrued as originating in the more proximal layers of the retina since such activity drives the PERG response. Since previous mfERG results have shown amplitudes of flash responses to decrease with eccentricity regardless of scaling factor (Rodrigues et al., 2010), it is highly likely that uniform checkerboards would elicit an even more drastic decrease in local luminance response with eccentricity since no scaling factor is employed. Based on the responses in which spatial tuning was observed

for both uniform checkerboards and scaled gratings, it is possible that the stimuli yielding higher response amplitudes may be optimizing the photoreceptor and bipolar-cell responses rather than the ganglion-cell responses. To assess this, it may be beneficial for future work to evaluate the PERG amplitude in a very similar manner to that of the present study, but with a scaling factor that reflects receptive field density of photoreceptors and/or bipolar cells.

In addition to these possibilities, there is also the inherent limitation of edge effects both within the stimulus and at its perimeter. Although the traditional PERG stimulus will contain high-frequency edges throughout the pattern, the edges inside the scaled gratings used here are unusual in that they involve not only horizontal and vertical edges, but diagonal ones as well. Therefore, it may be possible that the edge effects produced at these additional orientations change the processing of the stimulus in unexpected ways that have not been accounted for in this study. Unfortunately, edge effects are generally unavoidable in the case of the PERG response, as PERG standards demand square-wave spatial patterns to produce the largest possible potential (Bach et al., 2013). To assess the influence of spatial scaling without such edge effects interfering, future work could employ PERG stimuli with sine or Gaussian-modulated edges rather than square-wave edges, even though the overall response amplitude will be lowered as a result.

In the case of the outermost stimulus edges, there was a further limitation of windowing effects. Because these scaled gratings were based on a starting center spatial frequency from which all other spatial frequencies were determined as a function of eccentricity and the scaling factor used, the outermost ring of the scaled grating was

limited by the stimulus field size since that had to be equivalent to the size of the checkerboard stimulus. Therefore, the outermost ring of the stimulus was often limited in size relative to what it would need to be to appropriately fulfill the necessary spatial frequency for that ring based on the scaling factor. For this reason, the outermost ring was often a much higher spatial frequency than what was appropriate for that portion of the stimulus, and may have negatively influenced the size of the net response for that reason.

Experiment 3:

Testing the Validity of Modeling the PERG in a Patient Population

Although results from Experiment 1 showed that the PERG could generally be modeled from flash ERG responses in a group of young, healthy adults, it was still possible that these simulations only mimicked the morphology of the PERG and did not truly reflect the same retinal processes. To investigate whether these simulations were actually representative of the retinal processes seen in the PERG, Experiment 3 assessed the efficacy of these simulations in a glaucoma population. Since PERG amplitudes are known to decrease as severity of this disease increases (Bach & Hoffman, 2008), the simulation should be lower in amplitude relative to age-similar controls for the same cases in which the PERG amplitude is relatively lower. It was reasoned that if the simulation was able to produce the same trends as those seen in the PERG, then it was highly likely that the simulation was truly reflecting much of the same retinal activity as that which produced the PERG response.

Before this work could determine whether or not the simulation was deemed successful, the points at which PERG amplitude differed between glaucoma patients and

controls had to first be established. While no differences were found between PERG amplitudes from the control group versus those with mild or moderate glaucoma, some differences were seen between controls and those with severe glaucoma. For transient stimuli, there was no significant difference due to Holm's procedure controlling for error across multiple tests. However, had the control group been compared to only the severe glaucoma patients, N95 amplitude would have been significantly lower in the severe glaucoma sample. Given that the somewhat low number of participants in each of these groups, it is possible that a larger sample size could have shown significant differences for this measure. For steady-state stimuli, PERG amplitudes from patients with severe glaucoma were significantly lower than their healthy counterparts even after Holm's procedure controlled for error across multiple tests. This suggests, then, that the steady-state PERG is a more sensitive measure of glaucomatous changes, as has been suggested in a previous review of similar literature (Bach & Hoffman, 2008).

Although the aforementioned tests did assess amplitude differences based on severity level, the full range of disease progression could not be accounted for since the discrete categorizations of mild, moderate, and severe were used. Therefore, to more fully understand the relationship between PERG amplitude and disease progression, a continuous measure of disease progression was required so that it may be correlated with these amplitudes. Since much of the basis for categorizing glaucoma severity centers around the amount of visual field loss that has resulted from the disease, it seemed necessary to choose a measure that reflected the degree of this loss. Mean deviation (MD) values were therefore selected as the continuous measure of glaucoma severity, as they represent the degree of overall visual field loss in that patient relative to healthy

individuals of the same age range, as determined by the HVA 10-2, 24-2, or 30-2 assessment.

An MD value of 0 represents a visual field that is statistically equivalent to a healthy individual that is of the same age as the patient. Negative values indicate greater visual field loss than the patient's healthy counterparts, and positive values indicate a lower degree of visual field loss relative to that norm. Therefore, greater severity levels of glaucoma tend to align well with lower MD values. Since PERG amplitudes only differed between controls and glaucoma patients in the case of steady-state responses, and potentially in the case of transient N95 responses, these were the only two measures of amplitude that were correlated with MD values. Both N95 amplitude and steady-state amplitude were correlated with the MD values of the glaucoma patient sample, indicating that these measures of PERG amplitude decreased as disease severity increased.

After assessing the patterns of PERG amplitude differences between the control group and the glaucoma patients, the amplitudes from averaged best-fit simulations were evaluated to determine if they yielded the same trends. Since these simulations were meant to reflect the true PERG response as accurately as possible, a different set of averaged best-fit parameters was used for each category (control, mild, moderate, severe), though the parameters did not vary greatly across these categories. When amplitudes from these simulations were compared between the control group and each category of glaucoma patients, no differences were found. Since these amplitudes did tend to decrease somewhat as severity increased (albeit not at levels of significance), it may once again be the case the differences would have been seen in a larger sample of patients. However, since neither N95 nor steady-state simulation amplitudes were

correlated with MD values, these simulations do not appear to be as sensitive to glaucomatous changes as compared to the actual PERG response.

Since there were no differences found in flash amplitude between the control group and any category of glaucoma patients (as expected), it is unlikely that confounds in the flash ERG responses altered the success of the resulting simulations. Since no differences in these flash ERG amplitudes were found, this naturally leaves the question of why the simulations were not as successful as the actual PERG response in detecting amplitude differences between the control population and the glaucoma patients. The two most likely sources of differences in retinal processing between the PERG response and the simulation created from flash ERG responses are those of the spatial context of the PERG stimulus and the simultaneous presentation of increment and decrement stimuli.

Based on the limited degree of success of the checked-flash simulations from Experiment 1 (Chapter II), however, it is unlikely that the lack of spatial context of the stimulus dramatically altered the results of the present experiment. Therefore, the most likely explanation behind the discrepancy between PERG response amplitude and simulation amplitude is that increment and decrement stimuli are presented simultaneously within the PERG stimulus, but separately in the case of flash ERG stimuli. If this simultaneous presentation is indeed necessary to evoke the retinal processes that are present in the PERG response, then it may be the case that there is a gain mechanism being employed that is not accounted for when responses elicited by separately-presented flash stimuli are combined.

Since both this experiment and Experiment 1 only achieved limited success with modeling the PERG from flash ERG responses, future work may consider determining a

common set of modeling parameters across a large sample of healthy adults. It may be necessary, however, to segment the appropriate parameters by age range. By determining a definitive set of modeling parameters within only the control population, the model would solely be meant to represent the standard PERG. Therefore, when these parameters are applied to patients with glaucoma, they should produce a simulation that will show deviations from the standard PERG since the parameters would not be customized to this particular clinical group. Additionally, future work may also be able to improve this model by using flash ERG responses from stimuli presented in a Ganzfeld dome to PERG responses presented in a full-field context. A custom designed, large-field PERG stimulus display would need to be developed to make full-field PERG recordings possible.

General Conclusions

Each of the three experiments discussed above intended to address assumptions that underlie the dogma of the PERG response. Although the specific implications of each experiment's results are discussed in the preceding segments of this chapter, the origins of the various PERG components can be further clarified by assessing their similarities and differences across the results of these three experiments. In both Experiments 1 and 2, there were several substantial similarities between the steady-state PERG and the P50 component of the transient PERG. In the case of Experiment 1, checked-flash simulations yielded better fits than uniform-flash simulations, but yielded the same goodness of fit as uniform-flash simulations that had been scaled down to 50% of their original amplitudes. However, N95 did not show these same patterns. In the case of Experiment 2, spatial tuning was found in uniform checkerboards for P50 and steady-state PERG amplitudes, but not in the case of N95.

Based on the analyses of PERG origins conducted by Luo and Frishman (2011), a key similarity between P50 and steady-state PERG responses is that of a partial origin of earlier retinal processes that respond to changes in luminance. In contrast, N95 was shown to be almost entirely composed of later retinal processes that respond to changes in contrast. Therefore, it may be that these similarities seen between P50 and steady-state PERG responses in Experiments 1 and 2 are due to the portions of these responses that are luminance-based. If this is the case, then it implies that both the amount of luminance presented in the stimulus or accounted for in algebraic manipulations of the response (as in Experiment 1) and the spatial tuning that can be seen in response to uniform checkerboard stimuli of varying check sizes (as in Experiment 2) are primarily affecting the photoreceptor and bipolar cell contributions to the response.

Since these cells are the primary contributors to luminance-based responses, then it follows that the aforementioned scenarios in which P50 and steady-state PERGs yield similar results are likely to be driven by these photoreceptor and bipolar cell layers rather than the ganglion cell layer. Therefore, although the holistic PERG response may largely be driven by ganglion cell activity, the roles of photoreceptors and/or bipolar cells should not be entirely discounted in assessing differences between individual response components, particularly in cases where an alternative to the traditional PERG is being employed.

Because these luminance-based influences have different effects on different components of the PERG, it may be possible to adapt future studies to account for which component or components are being assessed. For instance, future modeling may control for variables based on waveform component rather than just temporal frequency so that

differences in luminance- versus contrast-based contributions can be modeled differently. In the case of future studies to further optimize the PERG response through spatial scaling, it may be useful to scale the stimulus elements based on parameters based on changes in photoreceptor density rather than ganglion cell receptive fields, such as is done for multifocal ERG (mfERG) stimuli. Given that there is already a standard for the mfERG stimulus (Sutter & Tran, 1992), it may be possible to use the localized increment and decrement responses elicited from this stimulus to model the PERG that would be produced from splitting each hexagon within the array into a bipartite field.

This grouping of P50 and steady-state PERG responses did not seem to hold in PERG responses within glaucoma patients, however (as seen in Experiment 3). Instead, it seemed that N95 and steady-state amplitudes were more closely aligned in the trends they showed when amplitudes from the control group were compared to those from glaucoma patients. These results reaffirm the idea that the luminance-based components of the PERG response were not driving this amplitude difference, which should instead be related to the contrast-based components of the PERG response since it is caused by the dysfunction of the ganglion cell layer. This idea is further supported by the finding that while PERG amplitude was lowered for patients with glaucoma relative to the control group, flash ERG amplitude was unaffected by the disease.

In regards to the role of ON- versus OFF-pathway activity within the PERG, the weighting of the ON response appears to be much more influential to the resulting PERG response relative to the weighting of the OFF response based on the results of scaling these two responses in Experiment 1. This was found to be true in both transient and steady-state conditions. However, that same experiment showed that the response kinetics

of the ON and OFF pathways may differ when ON and OFF responses are being combined in the transient PERG response versus the steady-state PERG response. For both Experiments 1 and 3, all averaged best-fit parameters showed that goodness of fit increased when the b-wave started after the d-wave before summing in the case of the transient simulations, and before the d-wave in the case of the steady-state simulations. Since these trends were found for both of these experiments, it can be reasoned that this relationship between ON- and OFF-pathway response kinetics and temporal frequency is not drastically affected by glaucoma.

These three experiments collectively show that the PERG does not represent a perfect cancellation of linear retinal activity in either healthy or glaucomatous states, and that its spatial tuning is not likely to be highly reflective of spatial tuning properties from the ganglion cell populations that drive its response. Despite the many recent advancements made in understanding the origins of the PERG, the present work points to several elements of the PERG response that have yet to be fully explained. For instance, it is still unclear what exactly prevents the PERG from being modeled perfectly with the combination of flash ERG responses, and the degree to which that perfected model may be clinically useful in the assessment of glaucoma patients. Further, it remains to be determined what exactly drives the spatial tuning of the PERG, and if the PERG stimulus can be optimized to that mechanism so as to produce a larger response. Although these questions remain largely unanswered, the most imperative message of the current work is that the current assumptions behind the PERG are likely to be far too simple and should therefore continue to be tested and questioned.

REFERENCES

Arden, G. B., & Vaegan. (1982). Differences between the focal and pattern electroretinogram in man. *Journal of Physiology - London, 327*(JUN), P67-P68.

Arden, G. B., & Vaegan. (1983). Electroretinograms evoked in man by local uniform or patterned stimulation. *The Journal of Physiology, 341*(1), 85-104.

Armington, J. C., & Brigell, M. (1981). Effects of stimulus location and pattern upon the visually evoked cortical potential and the electroretinogram. *International Journal of Neuroscience, 14*(3-4), 169-178.

Armington, J. C., Corwin, T. R., & Marsetta, R. (1971). Simulatenously recorded retinal and cortical responses to patterned stimuli. *Journal of the Optical Society of America, 61*(11), 1514-1521.

Armstrong, R. A. (2011). Visual symptoms in Parkinson's disease. *Parkinsons Disease, 2011*. doi: 10.4061/2011/908306

Bach, M., Brigell, M. G., Hawlina, M., Holder, G. E., Johnson, M. A., McCulloch, D. L., . . . Viswanathan, S. (2013). ISCEV standard for clinical pattern electroretinography (PERG): 2012 update. *Doc Ophthalmol, 126*(1), 1-7.

Bach, M., & Hoffman, M. B. (2008). Update on the pattern electroretinogram in glaucoma. *Optometry and Vision Science, 85*(6), 386-395.

Bach, M., & Holder, G. E. (1996). Check size tuning of the pattern electroretinogram: a reappraisal. *Documenta Ophthalmologica, 92*(3), 193.

Bach, M., & Schumacher, M. (2002). The influence of ambient room lighting on the pattern electroretinogram (PERG). *Documenta Ophthalmologica, 105*(3), 281-289.

Baker, C. L., Hess, R. R., Olsen, B. T., & Zrenner, E. (1988). Current source density analysis of linear and non-linear components of the primate electroretinogram. *J Physiol, 407*, 155-176.

Ben-Shlomo, G., Bach, M., & Orfi, R. (2007). Temporal and spatial frequencies interact in the contrast transfer function of the pattern electroretinogram. *Vision Research, 47*(15), 1992-1999.

Ben-Shlomo, G., Bakalash, S., Lambrou, G. N., Latour, E., Dawson, W. W., Schwartz, M., & Ofri, R. (2005). Pattern electroretinography in a rat model of ocular hypertension: functional evidence for early detection of inner retinal damage. *Experimental Eye Research, 81*(3), 340-349.

Berardi, N., Domenici, L., Gravina, A., & Maffei, L. (1990). Pattern ERG in rats following section of the optic nerve. *Experimental Brain Research, 79*(3), 539-546.

Berninger, T., & Schuurmans, R. P. (1985). Spatial tuning of the pattern ERG across temporal frequency. *Documenta Ophthalmologica: Advances in Ophthalmology, 61*(1), 17-25.

Blondeau, J. L., Lafond, G., & Brunette, J. R. (1987). Pattern electroretinogram and optic nerve section in pigeons. *Current Eye Research, 6*(6), 747-756.

Bode, S. F., Jehle, T., & Bach, M. (2011). Pattern electroretinogram in glaucoma suspects: new findings from a longitudinal study. *Invest Ophthalmol Vis Sci, 52*(7), 4300-4306.

Brannan, J. R., Bodis-Wollner, I., & Storch, R. L. (1992). Evidence for two distinct nonlinear components in the human pattern ERG. *Vision Research, 32*(1), 11-17.

Brigell, M. G., Peachey, N. S., & Seiple, W. H. (1987). Pattern electroretinogram threshold does not show contrast adaptation. *Invest Ophthalmol Vis Sci, 28*(9), 1614-1616.

Bubl, E., Kern, E., Ebert, D., Bach, M., & Tebartz van Elst, L. (2010). Seeing gray when feeling blue? Depression can be measured in the eye of the diseased. *Biological Psychiatry, 68*(2), 205-208.

Bush, R. A., & Sieving, P. A. (1994). A proximal retinal component in the primate photopic ERG a-wave. *Investigative Ophthalmology & Visual Science, 35*(2), 635-645.

Cellini, M., Toschi, P. G., Strobbe, E., Balducci, N., & Campos, E. C. (2012). Frequency doubling technology, optical coherence technology and pattern electroretinogram in ocular hypertension. *BMC Ophthalmol, 12*, 33.

Chichilinsky, E. J., & Kalmar, R. S. (2002). Functional asymmetries in ON and OFF ganglion cells of primate retina. *The Journal of Neuroscience, 22*(7), 2737-2747.

Chou, T. H., Park, K. K., Luo, X., & Porciatti, V. (2013). Retrograde signaling in the optic nerve is necessary for electrical responsiveness of retinal ganglion cells. *Invest Ophthalmol Vis Sci, 54*(2), 1236-1243.

Chou, T. H., & Porciatti, V. (2012). The bioelectric field of the pattern electroretinogram in the mouse. *Investigative Ophthalmology & Visual Science, 53*(13), 8086-8092.

Cook, C., & Foster, P. (2012). Epidemiology of glaucoma: what's new? *Canadian Journal of Ophthalmology, 47*, 223-226.

Curcio, C. A., & Allen, K. A. (1990). Topography of ganglion cells in human retina. *CNE Journal of Comparative Neurology, 300*(1), 5-25.

Dawson, W. W., Trick, G. L., & Litzkow, C. A. (1979). Improved electrode for electroretinography. *Investigative Ophthalmology & Visual Science, 18*(9), 988-991.

Drasdo, N., Millican, C. L., Katholi, C. R., & Curcio, C. A. (2007). The length of Henle fibers in the human retina and a model of ganglion receptive field density in the visual field. *Vision Research, 47*(22), 2901-2911.

Enroth-Cugell, C., & Robson, J. G. (1966). The contrast sensitivity of retinal ganglion cells of the cat. *The Journal of Physiology, 187*, 517-522.

Evers, H. U., & Gouras, P. (1986). Three cone mechanisms in the primate electroretinogram: Two with, one without off-center bipolar responses. *Vision Research, 26*(2), 245-254.

Falsini, B., Marangoni, D., Salgarello, T., Stifano, G., Montrone, L., Campagna, F., . . . Colotto, A. (2008). Structure-function relationship in ocular hypertension and glaucoma: interindividual and interocular analysis by OCT and pattern ERG. *Graefe's Archive for Clinical and Experimental Ophthalmology, 246*(8), 1153-1162.

Falsini, B., & Porciatti, V. (1996). The temporal frequency response function of pattern ERG and VEP: changes in optic neuritis. *Electroencephalography and Clinical Neurophysiology, 100*(5), 428-435.

Fiorentini, A., Maffei, L., Pirchio, M., Spinelli, D., & Porciatti, V. (1981). The ERG in response to alternating gratings in patients with diseases of the peripheral visual pathway. *Invest Ophthalmol & Vis Sci, 21*(3), 490-493.

Foster, P., Buhrmann, R., Quigley, H. A., & Johnson, G. J. (2002). *86*(2), 238-242.

Garcia-Martin, E., Rodriguez-Mena, D., Satue, M., Almarcegui, C., Dolz, I., Alarcia, R., . . . Pablo, L. E. (2014). Electrophysiology and optical coherence tomography to evaluate Parkinson disease severity. *Invest Ophthalmol Vis Sci, 55*(2), 696-705.

Giuffre, I., Falsini, B., Gari, M. A., & Balestrazzi, E. (2013). Pattern electroretinogram assessment during ibopamine test in ocular hypertension. *Eur J Ophthalmol, 23*(6), 819-822.

Graham, S. I., Wong, V. A., Drance, S. M., & Mikelberg, F. S. (1994). Pattern electroretinograms from hemifields in normal subjects and patients with glaucoma. *Invest Ophthlamol Vis Sci, 35*(9), 3347-3356.

Guy, J., Feuer, W. J., Porciatti, V., Schiffman, J., Abukhalil, F., Vandenbroucke, R., . . . Lam, B. L. (2014). Retinal ganglion cell dysfunction in asymptomatic G11778A: Leber hereditary optic neuropathy. *Invest Ophthalmol Vis Sci, 55*(2), 841-848.

Harrison, J. M., O'Connor, P. S., Young, R. S., Kincaid, M., & Bentley, R. (1987). The pattern ERG in man following surgical resection of the optic nerve. *Investigative Ophthalmology & Visual Science, 28*(3), 492-499.

Heine, M., & Meigen, T. (2004). The dependency of simultaneously recorded retinal and cortical potentials on temporal frequency. *Documenta Ophthalmologica, 108*(1), 1-8.

Hess, R. F., & Baker, C. L. (1984). Human pattern-evoked electroretinogram. *Journal of Neurophysiology, 51*(5), 939-951.

Hood, D. C., & Birch, D. G. (1995). Phototransduction in human cones measured using the a-wave of the ERG. *Vision Research, 35*(20), 2801-2810.

Jafarzadehpour, E., Radinmehr, F., Pakravan, M., Mirzajani, A., & Yazdani, S. (2013). Pattern electroretinography in glaucoma suspects and early primary open angle glaucoma. *J Ophthalmic Vis Res, 8*(3), 199-206.

Janknecht, P., Wesendahl, T., Feltgen, N., Otto, T., & Bach, M. (2001). Steady-state electroretinograms and pattern electroretinograms in pigs. *Graefe's Archive for Clinical and Experimental Ophthalmology, 239*(2), 133-137.

Junghardt, A., Wildberger, H., Robert, Y., & Torok, B. (1993). Pattern electroretinogram and visual evoked potential amplitudes are influenced by different stimulus field sizes and scotomata. *Documenta Ophthalmologica: Advances in Ophthalmology, 83*(2), 139-149.

Katsumi, O., Tetsuka, S., Mehta, M. C., Tetsuka, H., & Hirose, T. (1993). Effect of hemifield stimulation on simultaneous steady-state pattern reversal electroretinogram and visual evoked response. *Ophthalmic Research, 25*(2), 119-127.

Kirkham, T. H., & Coupland, S. G. (1983). Pattern ERGs and check size - absence of spatial-frequency tuning. *Current Eye Research, 2*(8), 511-521.

Korth, M. (1983). Pattern-evoked responses and luminance-evoked responses in the human electroretinogram. *The Journal of Physiology*(337), 451-469.

Korth, M., & Rix, R. (1984). Effect of stimulus intensity and contrast on the pattern ERG. *Ophthalmic Research, 16*(1-2), 60-66.

Korth, M., & Rix, R. (1985). Changes in spatial selectivity of pattern-ERG components with stimulus contrast. *Graefe's Archive for Clinical and Experimental Ophthalmology, 223*(1), 23-28.

Leguire, L. E., & Rogers, G. L. (1985). Pattern electroretinogram: use of noncorneal skin electrodes. *Vision Research, 25*(6), 867-870.

Luo, X., & Frishman, L. J. (2011). Retinal pathway origins of the pattern electroretinogram (PERG). *Investigative Ophthalmology and Visual Science, 52*(12), 8571-8584.

Maffei, L., & Fiorentini, A. (1981). Electroretinographic responses to alternating gratings before and after section of the optic nerve. *Science, 211*(4485), 953-955.

Marmor, M. F., Fulton, A. B., Holder, G. E., Miyake, Y., Brigell, M., & Bach, M. (2009). ISCEV Standard for full-field clinical electroretinography (2008 update). *Doc Ophthalmol, 118*, 69-77.

McCulloch, D. L., Garcia-Filion, P., Fink, C., Chaplin, C. A., & Borchert, M. S. (2010). Clinical electrophysiology and visual outcome in optic nerve hypoplasia. *The British Journal of Ophthalmology, 94*(8), 1017-1023.

McCulloch, D. L., Garcia-Filion, P., van Boemel, G. B., & Borchert, M. S. (2007). Retinal function in infants with optic nerve hypoplasia: electroretinograms to large patterns and photopic flash. *Eye, 21*(6), 712-720.

Miura, G., Wang, M. H., Ivers, K. M., & Frishman, L. J. (2009). Retinal pathway origins of the pattern ERG of the mouse. *Experimental Eye Research, 89*(1), 49-62.

Odom, J. V., Maida, T. M., & Dawson, W. W. (1982). Pattern evoked retinal response (PERR) in human: effects of spatial frequency, temporal frequency, luminance and defocus. *Current Eye Research, 2*(2), 1982-1983.

Pangeni, G., Lammer, R., Tornow, R. P., Horn, F. K., & Kremers, J. (2012). On- and off-response ERGs elicited by sawtooth stimuli in normal subjects and glaucoma patients. *Documenta Ophthalmoligica, 124*, 237-248.

Peachey, N. S., & Seiple, W. H. (1987). Contrast sensitivity of the human pattern electroretinogram. *Investigative Ophthalmology & Visual Science, 28*(1), 151-157.

Poloschek, C. M., & Bach, M. (2009). The mfERG response topography with scaled stimuli: effect of the stretch factor. *Doc Ophthalmol, 119*, 51-58. doi: 10.1007/s10633-009-9169-6

Porciatti, V., Bosse, B., Parekh, P. K., Shif, O. A., Feuer, W. J., & Ventura, L. M. (2013). Adaptation of the steady-state PERG in early glaucoma. *J Glaucoma*.

Porciatti, V., Falsini, B., Fadda, A., Neroni, M., Minnella, A., & Scalia, G. (1989). Changes in spatial tuning of the pattern electroretinogram with age. *Metabolic, Pediatric, and Systemic Ophthalmology, 12*(1-3), 74-75.

Porciatti, V., Saleh, M., & Nagaraju, M. (2007). The pattern electroretinogram as a tool to monitor progressive retinal ganglion cell dysfunction in the DBA/2J mouse model of glaucoma. *Invest Ophthalmol Vis Sci, 48*(2), 745-751.

Porciatti, V., & Sartucci, F. (1996). Retinal and cortical evoked responses to chromatic contrast stimuli. *Brain, 119*(3), 723-740.

Porciatti, V., Sorokac, N., & Buchser, W. (2005). Habituation of retinal ganglion cell activity in response to steady state pattern visual stimuli in normal subjects. *Investigative Ophthalmology & Visual Science, 46*(4), 1296-1302.

Porciatti, V., & Ventura, L. M. (2009). Physiologic significance of steady-state pattern electroretinogram losses in glaucoma: clues from simulation of abnormalities in normal subjects. *Journal of Glaucoma, 18*(7), 535-542.

Preiser, D., Lagreze, W. A., Bach, M., & Poloschek, C. M. (2013). Photopic negative response versus pattern electroretinogram in early glaucoma. *Invest Ophthalmol Vis Sci, 54*(2), 1182-1191.

Quigley, H. A., & Broman, A. T. (2006). The number of people with glaucoma worldwide in 2010. *British Journal of Ophthlamology, 90*, 262-267.

Rimmer, S., & Katz, B. (1989). The pattern electroretinogram: technical aspects and clinical significance. *Journal of Clinical Neurophysiology: Official Publication of the American Electroencephalographic Society, 6*(1), 85-99.

Robson, J. G., Saszik, S. M., Ahmed, J., & Frishman, L. J. (2003). Rod and cone contributions to the a-wave of the electroretinogram of the macaque. *Journal of Physiology, 547*(2), 509-530.

Rodrigues, A. R., da Silva Filho, M., Silveira, L. C. L., & Kremers, J. (2010). Spatial distributions of on- and off-responses determined with the multifocal ERG. *Doc Ophthalmol, 120*, 145-158. doi: 10.1007/s10633-009-9205-6

Rodriguez-Mena, D., Almarcegui, C., Dolz, I., Herrero, R., Bambo, M. P., Fernandez, J., . . . Garcia-Martin, E. (2013). Electropysiologic evaluation of the visual pathway in patients with multiple sclerosis. *J Clin Neurophysiol, 30*(4), 376-381.

Siegel, M. J., Marx, M. S., Bodis-Wollner, I., & Podos, S. M. (1986). The effect of refractive error on pattern electroretinograms in primates. *Current Eye Research, 5*(3), 183-187.

Sieving, P. A., Murayama, K., & Naarendorp, F. (1994). Push-pull model of the primate photopic electroretinogram: A role for hyperpolarizing neurons in shaping the b-wave. *Visual Neuroscience, 11*, 519-532.

Simpson, M. C., & Viswanathan, S. (2007). Comparison of uniform field and pattern electroretinograms of humans. *Journal of Modern Optics, 54*(9), 1281-1288.

Sokol, S., Jones, K., & Nadler, D. (1983). Comparison of the spatial response properties of the human retina and cortex as measured by simultaneously recorded pattern ERGs and VEPs. *Vision Research, 23*(7), 723-727.

Stockton, R. A., & Slaughter, M. M. (1989). B-wave of the electroretinogram: A reflection of ON bipolar cell activity. *The Journal of General Physiology, 93*(1), 101-122.

Sutter, E. E., & Tran, D. (1992). The field topography of ERG components in man - I. The photopic luminance response. *Vision Res, 32*(3), 433 - 446.

Tafreshi, A., Racette, L., Weinreb, R. N., Sample, P. A., Zangwill, L. M., Medeiros, F. A., & Bowd, C. (2010). Pattern electroretinogram and psychophysical tests of visual function for discriminating between healthy and glaucoma eyes. *American Journal of Ophthalmology, 149*(3), 488-495.

Talla, V., Yang, C., Shaw, G., Porciatti, V., Koilkonda, R. D., & Guy, J. (2013). Noninvasive assessments of optic nerve neurodegeneration in transgenic mice with isolated optic neuritis. *Invest Ophthalmol Vis Sci, 54*(7), 4440-4450.

Tetsuka, S., Katsumi, O., Mehta, M., Tetsuka, H., & Hirose, T. (1992). Effect of stimulus contrast on simultaneous steady-state pattern reversal electroretinogram and visual evoked response. *Ophthalmic Res, 24*(2), 110-118.

Thompson, D., & Drasdo, N. (1989). The effect of stimulus contrast on the latency and amplitude of the pattern electroretinogram. *Vision Research, 29*(2), 309-313.

Tobimatsu, S., Celesia, G. G., Cone, S., & Gujrati, M. (1989). Electroretinograms to checkerboard pattern reversal in cats: Physiological characteristics and effect of retrograde degeneration of ganglion cells. *Electroencephalogr Ciln Neurophysiol, 73*(4), 341-352.

Ueno, S., Kondo, M., Niwa, Y., Terasaki, H., & Miyake, Y. (2004). Luminance dependence of neural components that underlies the primate photopic electroretinogram. *Investigative Ophthalmology & Visual Science, 45*(3), 1033-1040.

Ueno, S., Kondo, M., Ueno, M., Miyata, K., Terasaki, H., & Miyake, Y. (2006). Contribution of retinal neurons to d-wave of primate photopic electroretinograms. *Vision Research, 46*, 658-664.

Uva, M. G., Di Pietro, M., Longo, A., Lauretta, K., Reibaldi, M., & Reibaldi, A. (2013). Pattern ERG and RNFL thickness in hypertensive eyes with normal blue-yellow visual field. *Graefes Arch Clin Exp Ophthalmol, 251*(3), 839-845.

Vaegan, Anderton, P. J., & Millar, T. J. (2000). Multifocal, pattern and full field electroretinograms in cats with unilateral optic nerve section. *Documenta Ophthalmologica, 100*, 207-229.

Vaegan, & Arden, G. B. (1987). Effect of pattern luminance profile on the pattern ERG in man and pigeon. *Vision Res, 27*(6), 883-892.

Ventura, L. M., Golubev, I., Feuer, W. J., & Porciatti, V. (2010). The PERG in diabetic glaucoma suspects with no evidence of retinopathy. *J Glaucoma, 19*(4), 243-247.

Ventura, L. M., Golubev, I., Feuer, W. J., & Porciatti, V. (2013). Pattern electroretinogram progression in glaucoma suspects. *J Glaucoma, 22*(3), 219-225.

Viswanathan, S., Frishman, L. J., & Robson, J. G. (2000). The uniform field and pattern ERG in macaques with experimental glaucoma: removal of spiking activity. *Invest Ophthalmol Vis Sci, 41*(9), 2797-2810.

Viswanathan, S., Frishman, L. J., Robson, J. G., Harweth, R. S., & Smith, E. L. (1999). The photopic negative response of the macaque electroretinogram: reduction by experimental glaucoma. *Investigative Ophthalmology & Visual Science, 40*(6), 1124-1136.

Vukmanic, E., Godwin, K., Shi, P., Hughes, A., & DeMarco, P., Jr. (2014). Full-field electroretinogram response to increment and decrement stimuli. *Doc Ophthalmol, 129*(2), 85-95. doi: 10.1007/s10633-014-9455-9

Watson, A. B. (2014). A formula for human retinal ganglion cell receptive field density as a function of visual field location. *Journal of Vision, 14*(7), 1-17.

Wu, S., Armington, J. C., & Reeves, A. (1992). Electroretinograms (ERGs) and visual-evoked potentials (VEPs) elicited by pattern displacement. *Visual Neuroscience, 8*(2), 127-136.

Zapf, H. R., & Bach, M. (1999). The contrast characteristic of the pattern electroretinogram depends on temporal frequency. *Graefes Arch Clin Exp Ophthalmol, 237*(2), 93-99.

CURRICULUM VITA

Kate A. Godwin
Department of Psychological and Brain Sciences
University of Louisville
Life Sciences Building, Room 317
Louisville, KY 40292
Phone: (502) 852-0790
Email: kate.godwin@louisville.edu

Education:

2013 – Present **University of Louisville, Ph.D. Candidate**
Major Area: Experimental Psychology

2011 – 2013 **M.S. Experimental Psychology**
University of Louisville

2007 - 2011 **B.S. Psychology**
Berry College

Research Experience:

University of Louisville, Department of Psychological and Brain Sciences, Louisville, KY
Graduate Research Assistant, July 2011 - Present

Colorado State University, Psychology Department, Fort Collins, CO
Research Experience for Undergraduates: Summer Program on Mind and Brain, June 2010 – August 2010

Berry College, Psychology Department, Mt. Berry, GA
George Scholar Student Researcher, August 2009 - May 2011

Teaching Experience:

University of Louisville, Instructor
PSYC 331, Sensation and Perception, August 2015 – December 2015

University of Louisville, Guest Lecturer for Dr. Melinda Leonard
PSYC 201, Honors Introduction to Psychology
"Developing through the Lifespan," February 11, 2014

University of Louisville, Teaching Assistant
PSYC 302, Experimental Psychology, January 2014 – May 2014
PSYC 302, Experimental Psychology, August 2013 – December 2013

PSYC 201, Introduction to Psychology, January 2013 – May 2013
PSYC 301, Quantitative Methods in Psychology, August 2012 – December 2012

University of Louisville, Graduate Teaching Assistant Academy, August 2013 - May 2014

Grants / Awards:

University of Louisville, Graduate Student Council Spring Graduate Student Research Grant, March 2016

University of Louisville, Arts and Sciences Graduate Student Union Spring Research Funds, February 2016

University of Louisville, Intramural Research and Creative Activities Grant, June 2014

University of Louisville, Arts and Sciences Graduate Student Union Spring Research Funds, February 2014

University of Louisville, Graduate School Fellowship
(2 years), July 2011 – June 2012, second year to be used July 2015 – June 2016

National Science Foundation, Research Experience for Undergraduates,
June 2010 – August 2010

Berry College, George Scholar Research Grant, August 2009 – May 2011

Berry College, Academic Scholarship, August 2007 – May 2011

Professional Service:

School of Interdisciplinary and Graduate Studies Student Ambassador, August 2014 – May 2015

Student Representative for Department of Psychological and Brain Sciences, July 2014 – June 2015

Founder of and Mentor for First-Year Mentoring Program in Experimental Psychology, July 2013 – June 2015

Graduate Student Council Departmental Representative, July 2012 – June 2013

Professional Memberships:

Association for Research in Vision and Ophthalmology, February 2012 – Present

Association for Psychological Science, January 2011 – January 2012

Psi Chi, April 2009 - Present

Publications and Papers:

Godwin, K. & DeMarco, P. Simulating the human pattern electroretinogram using flash stimuli. *Manuscript in preparation.*

Vukmanic, E., **Godwin, K.,** Shi, P., Hughes, A., & DeMarco, P., Jr. (2014). Full-field electroretinogram response to increment and decrement stimuli. *Documenta Ophthalmologica*, 129(2), 85-95.

Poster Presentations:

Godwin, K.A. & DeMarco, P.J. (2015, May). *Simulating the human pattern electroretinogram using flash stimuli.* Poster presented at the 2015 Annual Meeting of the Association for Research in Vision and Ophthalmology, Denver, CO.

Godwin, K.A. & DeMarco, P.J. (2013, May). *Change in flash electroretinogram morphology from scotopic to photopic conditions*. Poster presented at the 2013 Annual Meeting of the Association for Research in Vision and Ophthalmology, Seattle, WA.

Godwin, K.A. & DeMarco, P.J. (2013, April). *Effects of stimulus variation on the pattern electroretinogram*. Poster presented at the 23rd Annual Neuroscience Day hosted by the Louisville Chapter of Society for Neuroscience, Louisville, KY.

Shi, P., **Godwin, K.A.**, & DeMarco, P.J. (2012, May). *Temporal interactions between the b-wave and d-wave of the human electroretinogram.* Poster presented at the 2012 Annual Meeting of the Association for Research in Vision and Ophthalmology, Fort Lauderdale, FL.

Godwin, K.A., Hughes, A., & Haney, M. (2011, May). *Using spatial contrast sensitivity to assess form perception in autism*. Poster presented at the 23rd Annual Convention of the Association for Psychological Sciences, Washington, D.C.

Douda, N. D., Volbrecht, V. J., **Godwin, K. A.,** Miller, A. D., & Nerger, J. L. (2010). *Scotopically equated stimuli versus photopically equated stimuli in unique hue judgments.* Poster presented at the 2010 Fall Vision Meeting, Rochester, NY.